Universität Hamburg
DER FORSCHUNG | DER LEHRE | DER BILDUNG

Exploring the community assembly of non-vascular vegetation based on a process-based modeling approach

Dissertation

with the aim of achieving a doctoral degree at the Faculty of Mathematics,
Informatics and Natural Sciences
Department of Biology
at Universität Hamburg

Submitted by

Yunyao Ma

From Jiangxi, China

Hamburg, 2024

Yunyao Ma

aus Jiangxi, China

Universität Hamburg

Fakultät für Mathematik, Informatik und Naturwissenschaften

Fachbereich Biologie

Institut für Pflanzenwissenschaften und Mikrobiologie

Ohnhorststraße 18

22609 Hamburg

Datum der Disputation: 15.05.2024

der/die Erstgutachter/in: Prof. Dr. Philipp Porada

der/die Zweitgutachter/in: Prof. Dr. Maaike Y. Bader

Zusammensetzung der Prüfungskommission:

Prof. Dr. Philipp Porada

Prof. Dr. Maaike Y. Bader

Prof. Dr. Christian Beer

Prof. Dr. Kai Jensen

Information on published chapters

Chapter 2:

Exploring environmental and physiological drivers of the annual carbon budget of biocrusts from various climatic zones with a mechanistic data-driven model.
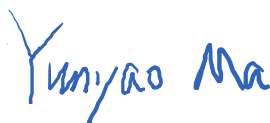
Authors: **Yunyao Ma**, Bettina Weber, Alexandra Kratz, José Raggio, Claudia Colesie, Maik Veste, Maaike Y. Bader, and Philipp Porada

.

Author contributions:

Yunyao Ma and Philipp Porada designed the study; Yunyao Ma did all data processing and ran the model; Yunyao Ma did the data analysis and interpretation with the support of Philipp Porada, Claudia Colesie, Bettina Weber, and Maaike Y. Bader; Bettina Weber, Alexandra Kratz, Maik Veste, and José Raggio provided the observational data. Yunyao Ma wrote the initial manuscript; and all authors revised the manuscript.

Signature: _____   _____

Yunyao Ma   Prof. Dr. Philipp Porada (first advisor)

Chapter 3

Quantifying the effect of competition on the functional assembly of bryophyte and lichen communities: A process-based model analysis

Authors: **Yunyao Ma**, Maaike Y. Bader, Imke Petersen, Philipp Porada

Author contributions:

Yunyao Ma and Philipp Porada designed the study; Yunyao Ma collected the species relative abundance data in the field with the help of Imke Petersen; Imke Petersen conducted other experiments and collected the data. Yunyao Ma performed all data analysis and model simulations. Yunyao Ma, Maaike Y. Bader, and Philipp Porada contributed to the data interpretation and discussions. Yunyao Ma wrote the initial manuscript. All authors revised the manuscript.

Signature: _____

Yunyao Ma   Prof. Dr. Philipp Porada (first advisor)

Table of Contents

Chapter 1 - General introduction

1.1 The characteristics of non-vascular vegetation

Non-vascular vegetation, referred to hereafter as NVV, encompasses diverse groups of photosynthetic organisms, including lichens (symbiotic associations between fungus and algae or cyanobacteria) and bryophytes (mosses, liverworts, and hornworts). NVV have different characteristics from vascular plants (i.e., trees and grasses). The first distinct characteristic is that NVV lack a vascular system including xylem and phloem (Whitton, 2013). The lack of such features means that NVV do not require multi-layer bark. Thereby, NVV is typically very tiny and grow close to the ground. Furthermore, NVV do not have specialized true leaves and roots. Instead, they possess an undifferentiated green body, known as a thallus (e.g. lichens), leaf-like structures, called phyllids (leafy bryophytes; Schofield, 2024), and root-like structures, called rhizoids (mosses) or rhizines (some lichens; Jones & Dolan, 2012; Syers & Iskandar, 1973). Similar to vascular plants, NVV can undergo photosynthesis in their green tissues. However, unlike vascular plants that absorb soil water via roots, the rhizoids/rhizines mostly serve to firmly anchor the vegetation to the growth substrate (Jones & Dolan, 2012). Moreover, NVV have no stomata and related mechanisms found in vascular plants to actively regulate water exchange between the organism and the atmosphere. Instead, NVV are poikilohydric, meaning the water status is totally dependent on and can equilibrate rapidly with the surrounding atmospheric humidity (Hanson & Rice, 2014). NVV passively acquire water through rainfall or non-rainfall (i.e., dew and water vapor) sources, relying on the water potential gradient between the organism and the atmosphere. Furthermore, in dry air, these poikilohydric vegetation exhibit tolerance to some desiccation, which is achieved by remaining metabolically inactive during dry periods and resuming their metabolic activities upon rewetting (Lange et al., 2001). Further, the organisms tend to be fully hydrated in humid environments, which limits the CO_2 diffusion through the thallus (Lange et al., 1996).

NVV are distributed globally, spanning from arid deserts to rainforests and arctic tundra (Chen et al., 2020; Lakatos et al., 2006; Schmitz et al., 2020; Shaw et al., 2005). Additionally, they can grow across diverse elevations, ranging from sea level

to high altitudes, and on nearly all surfaces, including rocks, walls, soil surfaces and also on leaves and bark as epiphytes (Turner & Pharo, 2005; Wolf, 1994). NVV (i.e., lichen, moss, algae, cyanobacteria) can also grow together on or within the topsoil layer and form biological soil crusts (biocrusts; Belnap et al., 2003). Biocrusts, documented to cover around 12% of the land surface (Rodriguez-Caballero et al., 2018), are prevalent across all biomes and constitute a major vegetation community in global drylands where vascular plants are limited (Belnap et al., 2016; Samolov et al., 2020).

As globally distributed vegetation, NVV play a crucial role in providing essential ecological functions across different environments. For instance, biocrusts are reported to be the major moderator to soil organic carbon, nitrogen content and microbial community in desert ecosystems (Chamizo et al., 2012; Li et al., 2016). Hence, NVV have always been utilized for land degradation control and ecological restoration in arid and semi-arid environments (Li et al., 2021; Xiao et al., 2015). Furthermore, cyanobacteria associated with mosses and lichens facilitate biotic nitrogen fixation, thereby enhancing the fertility of nutrient-poor soils (Rousk et al., 2017). Additionally, NVV epiphytes influence global hydrological cycling via the interception of fog and rainfall (Porada et al., 2018), and NVV communities on rock enhance the weathering rate, which indicates their role as a modulator of atmospheric CO_2 concentration (Porada et al., 2016; Wang et al., 2021).

1.2 Non-vascular community assembly

Acknowledging the important role that NVV play in global ecosystem functioning is crucial to gaining a better understanding of community assembly processes, such as environmental filtering and biotic interactions (Spasojevic & Suding, 2012), which are yet understudied for NVV. These processes shape the community structure in terms of the diversity and composition, which may have a large impact on the functioning of the ecosystem (Schulze & Mooney, 1994; Tilman et al., 2014; Vitousek & Hooper, 1994). For example, the high-diversity mixtures of vegetation demonstrate higher soil nitrogen concentration compared to monoculture communities (Ewel et al., 1991); the relative abundance of NVV species with high maximum water holding capacity might affect the ecosystem water cycling. Moreover, acquiring more knowledge of the mechanisms of the community assembly is essential for exploring the adaptation of

ecosystem functions provided by NVV to future environmental changes, and enhancing the theoretical basis for conservation purposes. Furthermore, the species richness pattern of NVV, such as mosses, diverges from the general latitudinal gradient observed in most vascular plants where diversity typically increases with decreasing latitude, as confirmed by Geffert et al. (2013). Understanding community assembly may provide new insights into the mechanisms contributing to this distinct species richness pattern between NVV and vascular plants, thereby improving our ability to predict changes in richness patterns under climate change.

Community assembly is typically assessed using various measures employed to quantify the community diversity and composition (e.g., Spasojevic & Suding, 2012). One may count the total number and relative abundance of species in a community as a measure of species diversity and composition. However, although species diversity and composition remain an essential measure, functional diversity and functional composition tend to be considered as the most effective means of understanding ecosystem functions (Botta-Dukát, 2005). Functional diversity and composition are characterized by the range, distribution and relative abundance of the functional traits (physiological, morphological or structural attributes) of organisms comprising a community (Díaz et al., 2007). One common way to assess the functional composition is by calculating the community-weighted mean values of functional traits form all organisms in a community. Functional diversity is often expressed as the variety of plant functional strategies, expressed as the presence of different trait values within a multidimensional trait space (Conti & Díaz, 2013; Reu et al., 2011).

Recently, trait-based ecology has proposed that the community structure is shaped by how the interaction between abiotic and biotic factors on functional traits (Kraft, Adler, et al., 2015). As observed in the economics spectrum for NVV, some key traits form trade-offs due to constrained resource availability imposed by the environment (Oke & Turetsky, 2020; Wang et al., 2017). For instance, bryophytes may invest more biomass in metabolic components, indicating higher concentration of nitrogen and phosphorus, albeit at the cost of structural traits (e.g., shoot mass per area; Wang et al., 2017). Thereby, organisms possess distinct combinations of functional traits and trade-offs that dictate their performance in certain processes (i.e., maintenance,

growth and reproduction) and in response to the environment, particularly climatic and biotic factors (Nock et al., 2016; Violle et al., 2007). In other words, these climatic and biotic factors filter for organisms with specific traits and trade-offs that can perform well (Schwinning & Ehleringer, 2001). For example, freezing environments lead to a convergence toward low water content to achieve maximum net photosynthesis in biocrusts (Colesie et al., 2014). Therefore, climatic and biotic filtering are two fundamental community assembly processes, shaping both functional diversity and composition, which has been a heated topic over the years (Kraft, Adler, et al., 2015).

Yet, despite many studies exploring the responses of NVV and its functional traits to abiotic drivers (e.g., Färber et al., 2014; Lange et al., 2005; Roos et al., 2019), the observations in these studies are typically confined to one study area or gradients of elevation or vertical canopy height. Rarely have studies aggregated observations across diverse climatic zones into a consistent framework to explore the roles of multiple abiotic drivers for NVV growth and communities. Furthermore, while the impacts and underlying mechanisms of temporal variations in abiotic factors (e.g., temperature), particularly seasonal and inter-annual variations, on the vascular plant communities have been extensively studied (e.g., Holmgren et al., 2013; Piao et al., 2008), this area remains relatively understudied for non-vascular communities. Hence, there is still a substantial need for further research to fully understand the relationships between non-vascular communities and abiotic factors. Moreover, to my knowledge, even less research has been done on the contribution of biotic interactions (i.e., competition) to NVV community assembly.

1.3 The abiotic and biotic factors in community assembly

1.3.1 Climatic factors

Abiotic factors, such as climatic factors, exert strong control on the community assembly by modulating the carbon balance (difference between the gross photosynthesis and respiration, e.g., Coe et al., 2012). In order to survive in the community, organisms must be able to maintain a positive carbon balance in the long term.

It is widely accepted that light intensity plays an essential role in the carbon balance

of NVV as it is a source for photosynthetic electron-transfer reaction. The net photosynthesis rate generally increases with rising light intensity albeit to a certain threshold, meaning further increments beyond the point in light intensity may lead to a saturation of photosynthesis with no subsequent improvement in carbon balance observed (Lange et al., 1998).

In addition to light, atmospheric moisture serves as a key determinant influencing the carbon balance of NVV since it acts as water input for NVV. The carbon balance might be affected by the magnitude of water input (Coe et al., 2012; Metcalfe & Ahlstrand, 2019). Under dry conditions, organisms remain less metabolically active or even inactive, yielding diminished carbon balance (Coe et al., 2014; Veste et al., 2008). Similarly, in humid environments, the high resistance to CO_2 diffusion through the thallus due to water films hinders photosynthesis (Cowan et al., 1992), leading to a negative impact on the carbon balance. Therefore, maintaining an optimal water content (OWC) is crucial for achieving peak net photosynthesis. Moreover, different moisture sources, such as rainfall, dewfall and fog, may exert varying impacts on the carbon balance of NVV (Baldauf et al., 2021). For instance, dewfall has been observed to primarily enhance the photosynthesis and facilitates carbon assimilation in drylands, whereas fog mainly stimulated respiration, thereby exerting a negative effect on the carbon balance (Chamizo et al., 2021). Besides the magnitude and type, the frequency of rainfall throughout a year has also large impact on the survival of NVV (Baldauf et al., 2018; Reed et al., 2012), as it determines the frequency of wet-dry cycles experienced by NVV during the year and, consequently, resulting in variations in the annual carbon balance.

Further, CO_2 concentration is a key factor for carbon balance since it is also a source for photosynthesis, and photosynthesis can enhance with an increasing CO_2 concentration (Lange, 2002; Lange et al., 1999). Additionally, elevated CO_2 concentration has the potential to alleviate the depressed net photosynthesis rates observed at supersaturated status (i.e., water contents is greater than optimum water content, see Green et al, 1994; Lange et al., 1999).

Temperature plays a crucial role in the carbon balance of NVV, affecting both photosynthesis and respiration. As temperature rises, respiration rates increase (Rastorfer & Higinbotham, 1968), while net photosynthesis reaches its maximum at

an optimum temperature dictated by the physiological properties of the organism and its local climate (Colesie et al., 2014; Grote et al., 2010).

Nevertheless, despite numerous empirical studies reporting the importance of these climatic factors for carbon balance of NVV, research remains limited on the relative importance of these factors, particularly across diverse climates.

1.3.2 Physiological properties

The response of the carbon balance to a climatic condition might be regulated by physiological parameters of NVV, as it was observed that the carbon balance response to varying rainfall event sizes differed among species collected during different seasons, which is attributed to the varying physiological status of species in different seasons (Coe et al., 2012). Thereby, the physiological properties might also explain the community assembly under certain climatic conditions by affecting the carbon balance of organisms.

The critical physiological parameters impacting carbon balance through their impact on photosynthesis and respiration has been explored: the content of enzyme Rubisco, for instance, can largely regulate photosynthesis rates in light-saturated conditions (Stitt & Schulze, 1994). An increase in Rubisco concentration might enhance photosynthesis rates, as imposed by the kinetic properties of Rubisco. Furthermore, light absorption rate is a key parameter for light-response photosynthesis as it indicates the amount of input light used by organisms for photosynthesis, whereas the water content compensation points of CO_2 assimilation (minimum water content requirement for positive net CO_2 assimilation) and the OWC control the response of photosynthesis rates to water conditions (Green et al., 2011). Additionally, the variations in temperature optima for gross photosynthesis among different organisms reflect their differences in photosynthesis rates in response to temperature (Perera-Castro et al., 2020). Aside from these parameters related to photosynthesis, respiration is also regulated by various parameters. The temperature dependence of respiration rate has been widely described by biologists using Q_{10} function (e.g., Tjoelker et al., 2001), which includes two parameters, temperature-dependent Q_{10} value and reference maintenance respiration rate (respiration rate at the reference temperature). Therefore, these two parameters might regulate the respiration rate and thus carbon balance largely.

However, it is important to note that the physiological parameters can be strongly species dependent, which might lead to the different carbon balance and survival of species under a same climatic condition. For instance, Lange et al (1999) found the non-depressed net photosynthesis of certain species in response to high water content, in contrast to the others.

Despite the strong sensitivity of the carbon balance of NVV to various physiological parameters, the relative importance of them across different climatic zones remains largely unknown. Gaining insight into the relative importance of climatic factors and physiological parameters, especially across diverse climatic zones, provides a better understanding of the key drivers of carbon balance under different climatic conditions. This knowledge may advance our understanding of the relationship between NVV community assembly and climatic factors, thereby enhancing our ability to predict community assembly.

1.3.3 Biotic interaction

Next to abiotic factors, biotic interaction such as inter-specific competition is also a process that can influence community assembly (Chesson, 2000). There is a body of evidence for the impacts of competition on the functional diversity and composition of forest and herbaceous plant communities (e.g., Gross et al., 2015; Kunstler et al., 2012; Silvertown & Dale, 1991; Xu et al., 2021). However, the role of competition in the NVV community is poorly understood.

The hypothesis explaining how competition shapes community assembly has been the subject of debate for years. Intuitively, ecologically different species are often hypothesized to have less intensive competition than species with similar ecological strategies, since they may use different resources (competition-relatedness hypothesis, MacArthur & Levins, 1967). The ecological similarities and differences among coexisting species can be quantified based on functional traits related to resource acquisition, defense ability, and regeneration rate (Kraft & Ackerly, 2010). Hence, the more similar the traits of two species, the more similar their ecological strategies become, which ultimately leads to a more intense competition between them.

However, other studies challenge the competition-relatedness hypothesis. For instance, Cahill et al (2008) found weak relationships between competition strength

and relatedness in vascular plant communities. Various studies suggested that the competition might be driven by variations of hierarchical competitive abilities of different species (competition hierarchy hypothesis), including bryophyte communities (Mälson & Rydin, 2009). The competitive advantage in the competitive hierarchy is strongly related to functional traits as trait variation may reflect fitness differences (Gross et al., 2015; Herben & Goldberg, 2014). For instance, taller species can be superior to the shorter ones in the competitive hierarchy, since taller ones have a higher ability to capture light, resulting in strong competition and even competitive exclusion of the shorter species. Therefore, competition based on competition hierarchy hypothesis leads to an opposite outcome to the competition-relatedness hypothesis: the greater the disparity in trait values determining the competitive ability of two species, the more intense the competition will be, and this may often lead to the exclusion of the inferior competitor in the absence of niche differentiation (Chesson, 2000).

One common way for exploring the impact of the competition process on the functional composition and diversity (i.e., trait distributions) of non-vascular communities is to investigate how trait values respond to competition within a multidimensional trait space. It is important to note that the concept of trait combinations in multidimensional trait space differs from the coexistence theory based on species level, which includes niche partitioning and hierarchical competition among species (Chesson, 2000). However, the competition process can be effectively implemented by drawing inspiration from the competition hierarchy hypothesis. That is, expressing competition implicitly by representing competitive ability as a function of functional traits. This approach not only achieves the goal of studying the responses of functional traits to competition but also substantially decreases the complexity of estimating the pairwise competition within a community.

1.4 Dynamic global vegetation models

The study of the roles of abiotic and biotic factors in plant communities is usually carried out using experiments combined with statistical methods or statistic modeling approaches. Dynamic global vegetation model (DGVM), a numerical, mechanistic, process-based model, allows for a deeper mechanistic understanding of community

assembly processes and is more suitable for extrapolation and prediction.

DGVMs were initially designed for understanding how climate and vegetation interact to affect the dynamics of terrestrial ecosystems (Prentice et al., 2007). DGVMs have since been widely applied to address problems regarding the dynamics of carbon, water and energy budget at regional to global scales in response to environmental changes, since the models provide realistic representation of numerous biogeochemical and biogeophysical processes of vegetation (Bonan, 2015; Cramer et al., 2001). Further, DGVM is a powerful approach for predicting ecosystem structure and functioning dynamics influenced by past, present and future climates, and for gaining insights into their underlying drivers (Tao & Zhang, 2010; Thuiller et al., 2006). Although a very useful tool, the approach used to represent the enormous plant functional diversity in most of DGVMs has been criticized for many issues (Harrison et al., 2021).

In most of the DGVMs, the global vegetation is categorized into a small number of plant functional types (PFTs) based on the morphological and physiological features and bioclimatic limits of the vegetation (Kattge et al., 2011). Each PFT is represented by a predefined set of parameter values, typically chosen as the averages from a wide spectrum of trait values of species within the same PFT. These parameters of PFTs remain constant throughout simulations governing the ecophysiological responses to physical and biotic factors. However, the subjectively chosen PFTs prior to simulations potentially impact the accuracy of predictions, such as the vegetation cover and water cycling in Sahara region (Groner et al., 2018). Further, the coarse representation of trait diversity by several PFTs may not be sufficient to represent the full diversity in the field as the ecology community has observed that the variation within PFTs is larger than between PFTs for many traits (Kattge et al., 2011). Thus, the limited number of parameterized PFTs with static PFT-specific parameters might lead to inaccuracies in model predictions (Groenendijk et al., 2011; Verheijen et al., 2013).

To improve the accuracy of predicting the climate-vegetation interaction, advanced DGVMs have been moved from fixed-PFT scheme towards a more flexible trait-based approach that includes increased trait diversity in the model, such as aDGVM (Scheiter et al., 2013) or JeDi-DGVM (Pavlick et al., 2013). The advanced DGVMs

attempt to represent the full diversity by considering a large number of physiological and morphological types or strategies, each characterized by a unique set of traits. Unlike the subjective selection of PFTs, the advanced DGVM allows for the potential existence of all species in all places. Communities are assembled based on the simulated performance and dynamics of individual species under specific environmental conditions, all of which are subject to constrains imposed by trait trade-offs (negative association between two or more traits). As more explicit physiological and ecological processes such as reproduction and competition are incorporated, advanced models can also achieve a more accurate simulation of the dynamics and performance of individual species. Hence, eco-evolutionary DGVMs (Berzaghi et al., 2020) have the potential to simulate the community assembly and contribute to an improved understanding of the interplay between terrestrial ecosystems and climate, ultimately helping more accurately predict changes in ecosystem structure and functioning in responses to climate change.

However, the NVV are always ignored in advanced DGVMs. LiBry model is a process-based DGVM that was developed specifically for NVV by accounting for NVV-specific properties such as the poikilohydry and the dependence of CO_2 diffusivity on water content (Porada et al., 2013). Similar to other advanced DGVMs, this model simulates the full diversity potential of each simulated NVV community (or a location) by randomly generating a broad spectrum of physiological and morphological strategies. Each strategy is distinguished by its unique set of functional traits (e.g., albedo, height, maximum molar carboxylation rate (Vcmax_M), reference maintenance respiration rate etc.). The model emulates natural selection within each community/location by simulating the dynamic responses of a range of biophysical and biochemical processes of these strategies to various climatic factors. These processes encompass water, energy and carbon balance. The carbon balance of each strategy subsequently influences its expansion in cover area, which is subject to a reduction due to disturbances in the simulations. Furthermore, an implicit competitive interaction process is integrated into the model. This ecological process regulates the cover area of each strategy by changing the allocation of available space for expansion. The existence of strategies in the community/location is determined at the end of simulations by assessing whether strategies can maintain a

positive cover area. Therefore, the LiBry model is able to simulate the explicit assembly of NVV communities, shedding light on the underlying mechanisms of the community assembly.

1.5 Thesis outline

The primary aim of the thesis is to deepen our understanding of community assembly in non-vascular vegetation, specifically the roles of abiotic and biotic factors in shaping community assembly. To this end, I applied the process-based dynamic vegetation model LiBry at multiple local study sites across diverse climatic zones. In Chapter 2, the importance of individual climatic factors and physiological parameters in community assembly are assessed by quantifying the annual carbon balance, a key metric for the growth and survival of organisms, across various climatic zones. To this end, I performed several sensitivity analyses of the LiBry model without competition. I consider the following research questions:

(a) What is the relative importance of different climatic factors and physiological parameters for the carbon balance of biocrusts in contrasting climates?

(b) What role does seasonal acclimation of the physiological parameters play in carbon balance estimation?

Chapter 3 explores the impact of competition on the assembly of lichen and bryophyte communities in temperate regions. To this end, I performed a series of simulations employing diverse trait-based competition schemes under varying levels of competitive intensities. I pose the guiding research question:

What role does competition play in the emergence of the functional composition of lichen and bryophyte communities?

In the end, I will conclude with a synthesis to summarize and generally discuss the roles of abiotic and biotic factors in non-vascular community assembly. Additionally, I will discuss potential implications and provide directions for future research.

Chapter 2 - Exploring environmental and physiological drivers of the annual carbon budget of biocrusts from various climatic zones with a mechanistic data-driven model

Published in Biogeosciences

Yunyao Ma, Bettina Weber, Alexandra Kratz, José Raggio, Claudia Colesie, Maik Veste, Maaike Y.Bader, and Philipp Porada

Abstract.

Biocrusts are a worldwide phenomenon, contributing substantially to ecosystem functioning. Their growth and survival depend on multiple environmental factors, including climatic ones, and the relations of these factors to physiological processes. Responses of biocrusts to individual environmental factors have been examined in a large number of field and laboratory experiments. These observational data, however, rarely have been assembled into a comprehensive, consistent framework that allows quantitative exploration of the roles of multiple environmental factors and physiological properties for the performance of biocrusts, in particular across climatic regions. Here we used a data-driven mechanistic modeling framework to simulate the carbon balance of biocrusts, a key measure of their growth and survival. We thereby assessed the relative importance of physiological and environmental factors for the carbon balance at six study sites that differ in climatic conditions. Moreover, we examined the role of seasonal acclimation of physiological properties using our framework, since the effects of this process on the carbon balance of biocrusts are poorly constrained so far. We found substantial effects of air temperature, CO_2 concentration, and physiological parameters that are related to respiration on biocrust carbon balance, which differ, however, in their patterns across regions. The ambient CO_2 concentration is the most important factor for biocrusts from drylands while air temperature has the strongest impact at alpine and temperate sites. Metabolic respiration cost plays a more important role than optimum temperature for gross photosynthesis at the alpine site; this is not the case, however, in drylands and temperate regions. Moreover, we estimated a small annual carbon gain of 1.5 g m^{-2} yr^{-1} by lichen-dominated biocrust and 1.9 g m^{-2} yr^{-1} by moss-dominated biocrust at a dryland site,

while the biocrusts lost a large amount of carbon at some of the temperate sites (e.g., -92.1 for lichen- and -74.7 g m^{-2} yr^{-1} for moss-dominated biocrust). These strongly negative values contradict the observed survival of the organisms at the sites and may be caused by the uncertainty in environmental conditions and physiological parameters, which we assessed in a sensitivity analysis. Another potential explanation for this result may be the lack of acclimation in the modeling approach since the carbon balance can increase substantially when testing for seasonally varying parameters in the sensitivity analysis. We conclude that the uncertainties in air temperature, CO_2 concentration, respiration-related physiological parameters, and the absence of seasonal acclimation in the model for humid temperate and alpine regions may be a relevant source of error and should be taken into account in future approaches that aim at estimating the long-term biocrust carbon balance based on ecophysiological data.

1. Introduction

Non-vascular photoautotrophs, such as lichens, mosses, eukaryotic algae and cyanobacteria, together with heterotrophic microorganisms, form biological soil crusts (biocrusts) which occur in various environments across the globe and provide a wide range of important ecosystem functions, such as build-up of soil organic carbon and nutrients (Belnap et al., 2016; Chamizo et al., 2012; Dümig et al., 2014; Ferrenberg et al., 2018). Due to the importance of biocrusts in ecosystem functioning, their growth and survival have been extensively studied, through different methodological approaches. An established measure to quantify the growth of biocrusts is their long-term carbon balance (hereafter, C balance), which corresponds to the (accumulated) net carbon flux across the system boundaries including all relevant carbon gains and losses.

In order to ensure survival, any species needs to achieve a positive C balance in the long-term, while negative values may occur for short periods. Acknowledging the importance of C balance, an increasing number of studies have investigated the long-term C balance of individual non-vascular organisms as well as biocrust communities, and their environmental drivers. An annual carbon budget of 21.49 g C m^{-2} based on measured field data was reported in the study of Lange (2003b) on the crustose lichen *Lecanora muralis* growing on a rock surface in a temperate climate of

southern Germany. Furthermore, Büdel et al. (2018) estimated an annual C balance of 1.7 g C m^{-2} based on measurements on cyanobacteria-dominated biocrust in an Australian dry savannah ecosystem. Several other studies obtained long-term, large-scale values of the C balance by scaling up short-term, local measurements of CO_2 exchange rate under natural field conditions (Lange et al., 1994; Zotz et al., 2003). For an estimation of the global C balance of cryptogamic covers, which include biocrusts, conversion factors based on the maximum photosynthesis rate have been suggested as a best-guess solution (Elbert et al., 2012). However, there are some drawbacks to these approaches for acquiring a C balance at both organism and community scale. First, the measurement of the long-term continuous CO_2 exchange rate of an individual organism or biocrust community has technical limitations and is highly time- and resource-consuming. Second, upscaling via extrapolation may result in bias in annual C balance estimation if the length and the frequency of sampling cannot capture the full variability of CO_2 exchange throughout the year (Bader et al., 2010). Moreover, using empirical approaches alone, it is difficult to understand the underlying mechanisms of how climatic conditions affect individual physiological processes, and consequently which role these processes play in the observed changes in C balance and growth at the individual as well as community level. Such approaches are thus subject to large uncertainty when used for projections of C balance under climate change.

Most studies on the relationships between C balance and environmental factors for biocrusts are based on laboratory experiments (e.g. Coe et al., 2012b; Cowan et al., 1992; Lange et al., 1998) or direct field measurements in situ over short periods of time (e.g. Brostoff et al., 2005; Lange et al., 1994). From this work cited above, it has been recognized that the C balance of biocrusts is strongly influenced by factors such as water supply, temperature, radiation, and CO_2 concentration and the complex relations of these factors to physiological processes such as photosynthesis and respiration. While the highest values of productivity under field conditions are achieved when the environmental factors are in the range that is optimal for the specific biocrust, it has been found that biocrusts are also able to achieve metabolic activity and thus, potential productivity, under sub-optimal conditions of temperature and light (Colesie et al., 2016; Raggio et al., 2017, 2014). It is largely unknown, however,

which relative importance each of these environmental factors and physiological parameters has for the long-term C balance of biocrusts under natural field conditions, and if the importance of factors/parameters shows a spatial and temporal pattern. In addition, seasonal acclimation of photosynthetic and respiratory properties of species to intra-annually varying climate factors found by several studies (e.g. Gauslaa et al., 2006; Lange and Green, 2005; Wagner et al., 2014) may substantially affect biocrust C balance, thus leading to further complexity in the spatio-temporal relations between C balance and environmental factors/physiological parameters. One of the few experimental studies investigating biocrust acclimation potential to changing temperatures has found threshold temperatures for the survival of lichen species (Colesie et al., 2018) but the overall extent of the impact is poorly understood.

Here, we applied a mechanistic data-driven model to (a) complement empirical estimates of the annual C balance of biocrusts and (b) to address the knowledge gaps concerning the relative importance of different environmental factors and physiological parameters for the C balance in contrasting climates, thereby accounting for the role of seasonal acclimation. The advantage of this modeling approach is that it can predict at high temporal resolution the dynamic C balance of biocrust organisms for given locations by simulating the physiological processes driven by environmental factors. The model allows for a deeper mechanistic understanding of the C balance of biocrusts through factorial experiments and sensitivity analyses regarding physiological parameters and individual environmental factors, which would be impractical to realize in field or laboratory experiments. To complement our analyses using the data-driven model, a process-based dynamic non-vascular vegetation model, called LiBry, was employed as a supporting tool (Porada et al., 2013).

2. Material and Methods

We simulated the C balance of biocrusts from six climatically different study sites in a semi-empirical way using a data-driven model. The model simulates photosynthetic rate based on the Farquhar photosynthesis model developed by Farquhar and von Caemmerer (1982) and respiration rate based on a Q10 relationship. The C balance is computed as the difference of photosynthesis and respiration accumulated over a given time period. In the model, both photosynthesis and respiration depend on surface temperature, relative water saturation, and the activity of the biocrust, which are

all simulated in a coupled way via the surface energy balance as a function of climate input data. Photosynthesis additionally depends on ambient CO_2 concentration.

To calibrate the model, we first determined soil and land surface properties that are required for the coupled energy and water balance in the model through fitting simulated to measured surface temperature patterns. Then, we parameterized the physiological properties of the organisms using measured relationships between net photosynthesis and light intensity, water content, and temperature. Finally, we validated the model with regard to the water content or activity patterns of biocrusts and compared the modelled CO_2 assimilation rate to measured values. The data sets used for calibration and validation of the model as well as basic climate conditions of each site are described in Table 1. Sites were listed in ascending order of total annual precipitation based on measured data.

2.1 Study sites

In our study we considered six sites, namely two dryland sites at Almeria (Spain) and Soebatsfontein (South Africa; hereafter D1 and D2); three temperate sites at Gössenheim (Germany), Öland (Sweden), and Linde (Germany; Hereafter T1, T2, and T3); and one alpine site at Hochtor (Austria; Hereafter A1) (Table 1). These sites were chosen based on data availability for C balance estimation, and because they cover a broad range of climatic conditions. The field and laboratory measurements conducted at all sites were following a similar protocol, which allows comparing the simulation results among sites. The necessary empirical data for C balance estimation regarding climatic conditions, species physiological characteristics, and status especially in terms of moisture such as water content or activity, have been monitored in a relatively small number of experiments, so far, and the six study sites chosen here to provide a good opportunity to utilize these data for an extended modeling approach. In this context, activity measurements are more suitable than soil moisture records since they are direct, non-invasive and they do not show deviations in the temporal patterns at high resolution, which may occur with soil moisture time series.

Sites D1 and D2 are characterized by an arid climate with mean annual precipitation of less than 250 mm, but a wet winter season (Büdel et al., 2014; Haarmeyer et al., 2010). Sites T1, T2, and T3 have a temperate climate. The mean precipitation in these three sites is around 550 mm (Büdel et al., 2014; Diez et al., 2019). Site A1 is

located in a humid alpine region with a mean annual precipitation between 1750 and 2000 mm, of which more than 70% are snowfall; the A1 site is covered by snow for at least 200 days per year (Büdel et al., 2014). More detailed site descriptions are provided in the corresponding studies cited above.

2.2 Observational Data

2.2.1 Climatic variables

The proposed data-driven model for estimating the annual C balance of dominant biocrust types at each site was forced by hourly microclimatic variables. The forcing data sets of the data-driven model include photosynthetically active radiation (PAR), long-wave radiation (near-infrared), relative air humidity, air temperature, wind speed, rainfall, and snowfall. All the microclimatic variables were measured on-site by climate stations with a temporal resolution of 10 min (5 min in A1 and D1; data available at http://www.biota-africa.org; Raggio et al., 2017; M. Veste, unpublished data), except for long-wave radiation and snowfall, which were taken from ERA5 dataset (https://www.ecmwf.int/en/forecasts/datasets/reanalysis-datasets/era5). Although directly measured surface temperature data are available for all sites, we use ERA5-based down-welling long-wave radiation instead to simulate surface temperature on biocrusts. This is necessary since, in our model, calculations of photosynthesis and respiration require not only surface temperature, but also depend on water saturation of biocrusts (affecting activity). However, we do not have water saturation data available at most sites. Therefore, we instead simulate the dynamic water saturation of biocrusts based on climate, via processes such as evaporation, rainfall, and dew. The calculation of evaporation and dew automatically includes the computation of a surface temperature that emerges from solving the surface energy balance, thereby including down-welling long-wave radiation. Since the simulated surface temperature that is connected to simulated water saturation slightly deviates from the observed surface temperature (see Fig. 2.1 and S2.1), we do not directly use the observed surface temperature as input in the modeling approach, to avoid inconsistencies. Then all these microclimate data were aggregated to data with hourly temporal resolution.

2.2.2 Dynamic biocrust variables

Besides the surface temperature, biocrust activity was either monitored directly (binary: active or not active) using a continuous chlorophyll fluorescence monitoring system (Raggio et al., 2014, 2017), or indirectly via the electrical conductivity of the substrate (BWP, Umweltanalytische Produkte GmbH, Cottbus, Germany; Weber et al., 2016; M. Veste, unpublished data). For site D2, the biocrust water content was calculated instead of activity based on electrical conductivity. Due to snow covering the measuring instruments, data of site A1 only covers the time from August to October. Samples from both lichen- and also moss-dominated biocrusts were measured at all sites, except for site T3 where four BWPs were mostly located in moss-dominated biocrusts. At site D2, additionally cyanolichen- and cyanobacteria-dominated biocrusts were monitored. The measured surface temperature, water content, and activity data at all sites were then aggregated to data with a temporal resolution of one hour.

As explained in Sect. 2.2.1, we did not directly use the observed surface temperature and activity (or water content) as forcing data for the model, but estimated the time-series of surface temperature and water saturation data at all sites based on a simulation of the energy and water balance. The activity of the organisms was then approximated via the empirical equations describing the link between water saturation and metabolic activity (see Porada et al., 2013). Furthermore, ambient CO_2 concentration was assumed to be constant at 400 ppm. The CO_2 concentration at the soil surface may be higher than 400 ppm due to the flux of respired CO_2 from the soil. Since our study sites are on open ground, we do not assume substantial accumulation of CO_2 in the near-surface boundary layer. We discuss the effect of uncertainties in CO_2 concentration below in Sect. 4.2.

For validation of C balance, we used data of the on-site CO_2-exchange rate of different biocrust types (lichen- and moss- and also cyano-dominated biocrusts removed from surplus soil; the latter composed of cyanolichen and cyanobacteria) that were measured by a portable gas exchange system at several time intervals from November 4th to 8th at site D2 (Tamm et al., 2018). For the other sites, additional field measurements of CO_2-exchange were not available.

2.2.3 Photosynthesis response and water storage

For all sites, CO_2 exchange measurements under controlled conditions in the labora-tory or in the field (site T3) were conducted using a mobile gas exchange system GFS 3000 (Walz GmbH, Effeltrich, Germany) with an infrared-gas analyzer to explore the physiological characteristics of samples of different biocrust types (same as those measured for validation; main species see Table 1; Diez et al., 2019; Raggio et al., 2018; Tamm et al., 2018). Before measurements, the soil underneath these biocrust samples was removed up to the amount necessary to preserve the physical structure of the biocrusts. And the samples were subjected to reactivation for at least two days (D2) or three days (T1, T2, D1, A1). At T1, T2, A1 and D1, for instance, samples were kept at 12°C under 12 h dark and 12 h light (100 µmol m^{-2} s^{-1}) conditions for three days and wetted once a day. Net photosynthesis was measured at different ranges of light intensity, water content, and temperature. Light response curves, for instance, were determined at optimum water saturation and 15 °C, water response curves were measured at 400 µmol m^{-2} s^{-1} and 15 °C at sites D1, T1, T2, and A1 (Raggio et al., 2018). Moreover, the maximum water storage capacity (MWC) of the samples was quantified in the laboratory for samples from sites D1, T1, T2, and A1 (Raggio et al., 2018), whereas the MWC at site D2 was approximated as the maximum value when measuring water response curves (Tamm et al., 2018; Weber et al., 2012). MWC at site T3 was estimated as the value of the same genus measured in Ham-burg, Germany (*Cladonia portentosa* and *Polytrichum formosum*, Petersen et al., in prep.). MWC was acquired since it is one of the essential parameters of the model to convert the specific water content in mm to relative water saturation required by the model used here.

Table 2.1: Properties of the study sites and data which are available (+ sign) for calibration and validation of the data-driven model.

Site	Alme-ria, Spain	Soebats-fontein, South Africa	Gössen-heim, Bavaria, Ger-many	Öland, Sweden	Linde, Bran-denburg, Ger-many	Hochtor, Austria

Code		D1	D2	T1	T2	T3	A1
Climate		arid	arid	Temperate	Temperate	Temperate	Alpine
Measured annual rainfall [mm]		110	141	424	441	449	744
Dominant species at the site		*Psora decipiens, Didymodon rigidulus*	*Psora decipiens, Psora crenata, Ceratodon purpureus, Collema coccophorum*	*Psora decipiens, Trichostomun crispulum*	*Psora decipiens, Tortella tortuosa*	*Cladonia furcata, Polytrichum piliferum*	*Psora decipiens, Tortella rigens*
Data for Calibration	Laboratory CO_2 exchange response curves	Light, water, temperature	Light, water, temperature	Light, water, temperature	Light, water, temperature	Light, temperature	Light, water, temperature
	Surface temperature	+	+	+	+	+	+
Data for Val-	Water content	-	+	-	-	-	-
	Activity	+	-	+	+	+	+

idation	CO₂ ex-change on site	-	+	-	-	-	-
References		Raggio et al., 2018	Tamm et al., 2018; Weber et al., 2012	Raggio et al., 2018	Raggio et al., 2018	Veste, unpublished data; Diez et al. 2019	Raggio et al., 2018

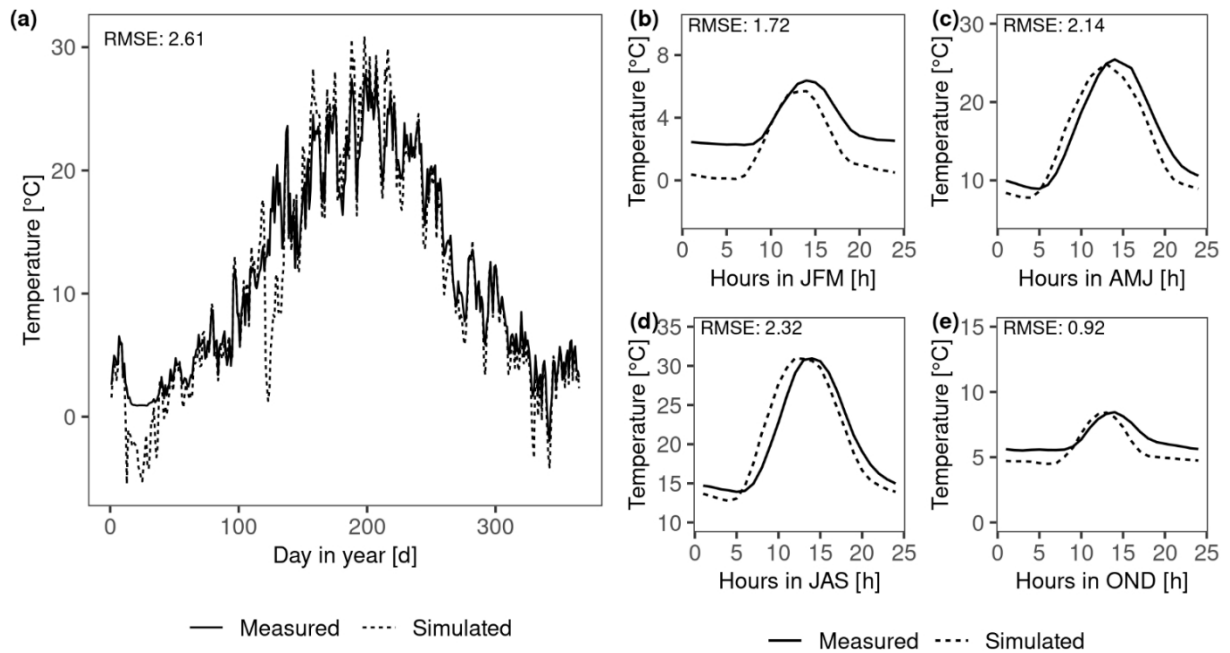## 2.3 Parameterization of the data-driven model

2.3.1 Abiotic surface properties

Several abiotic parameters of the data-driven model describing soil and land surface properties, such as roughness length or soil thermal conductivity, were required to simulate the energy and water balance. These parameters were obtained by fitting the daily and diurnal surface temperature patterns of lichen-dominated biocrust at all sites except for site T3. At site T3, we compared the surface temperature patterns of simulated moss-dominated biocrusts to data collected by sensors in four locations.

The set of parameters that corresponded to minimum differences between simulated and measured values (visual assessment) was used in the data-driven model. The calibration results of surface temperature and the photosynthesis response curves at site T2 are shown in Fig. 2.1 and Fig. 2.2, respectively. The results of dominant species at other sites are shown in Fig. S2.1 and S2.2.

The daily surface temperature was simulated accurately (the maximum value of root mean square error (RMSE) at all sites is 3.78) except for site T3 where the temperature during cold seasons was underestimated, and at site D1 the peak temperature within a day in hot seasons was underestimated (Fig. S2.1). The peak in surface temperature occurred too early by around 1-2 hours at site D1, A1, T1 and T2, but the magnitude of the peak corresponded well to the measured data (Fig. 2.1 and S2.1). Therefore, in general, the fitting of the surface temperature patterns was satisfactory.

The mismatches may result from the measured climate variables such as PAR or air temperature at 2 m being inconsistent with the measured surface temperature (detailed descriptions are in Supplement) and bias in the calibrated soil properties such as soil thermal conductivity since it may affect the surface temperature difference between morning and evening. A sensitivity analysis of soil thermal conductivity to C balance is shown in the Supplement.


Figure 2.1: Calibration results of abiotic parameters of the data-driven model by fitting the daily (a) and diurnal (b-e) patterns of surface temperature at site T2. (b) to (e) represent the patterns of average hourly surface temperature from January to March (JFM), April to June (AMJ), July to September (JAS), and October to December (OND), respectively.

2.3.2 Biocrust physiological properties

Furthermore, several parameters required by the Farquhar photosynthesis scheme and the respiration scheme were directly measured or calculated from gas exchange data sets, such as MWC of the thallus, optimum water content, the optimum temperature for gross photosynthesis, metabolic respiration cost, and the $Q10$ value of respiration. Since the ambient temperature range that was applied in the laboratory for samples from all sites except D2 was too small to capture the optimum temperature of photosynthesis reliably, we approximated the optimum temperature from the measured data set as the average surface temperature during active periods. In addition, the optimum temperature was also constrained by fitting the Farquhar equations to

photosynthesis curves, as related to environmental factors light, water content, and temperature. Such fitting method was also used to obtain some other photosynthesis-related parameters of organisms, such as molar carboxylation and oxygenation rate of RuBisCO (Vcmax, Vomax), respiration cost of RuBisCO enzyme (Rub_ratio), and minimum saturation for activation (Sat_act0).
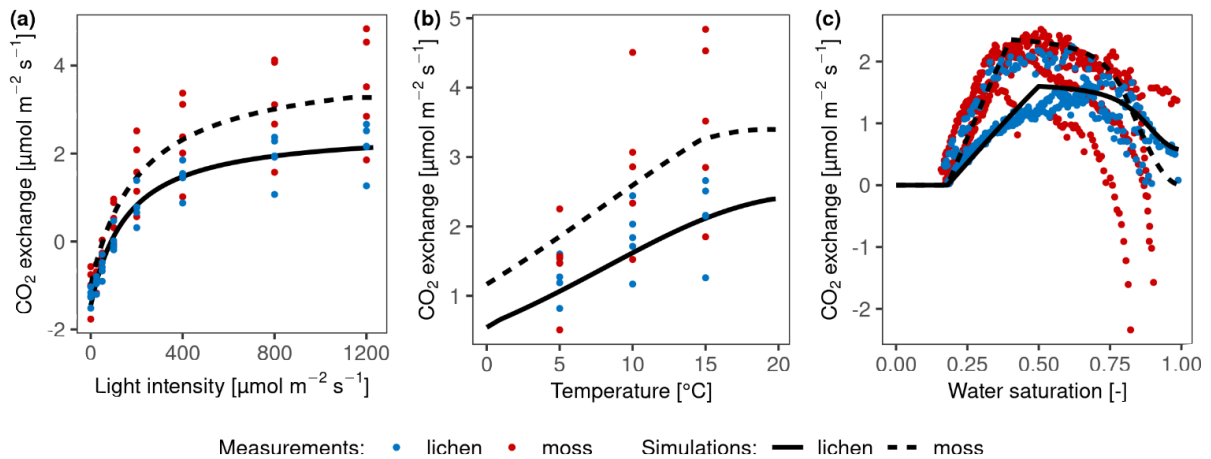
Figure 2.2: Calibration of photosynthesis parameters of the model by fitting photosynthesis response curves of moss- and lichen-dominated biocrust samples to measurements at site T2. (a): net photosynthesis rate in response to light at optimum water content and 15 °C. (b): net photosynthesis rate in response to temperature at 1200 µmol m^{-2} s^{-1} light and optimal water content. (c): net photosynthesis rate in response to relative water saturation at 400 µmol m^{-2} s^{-1} light and 15 °C.

Since the measured values between replicates showed large variation, in particular the water and temperature-dependent data, as illustrated by the coloured points in Fig. 2.2, we fitted the curves to the average values of all replicates. The calibration results showed that visually and overall, the photosynthetic curves could be parameterized to fit the measurements well, given that different samples were used for measuring responses to different driving factors, and considering the methodological differences between light and water response curve measurements. However, the water responses were least well-fitted, especially at high water contents. The measured net photosynthesis response rate was negative in some cases at high water saturation, but it is not possible to reproduce this negative net photosynthesis rates with our adapted Farquhar photosynthetic model for the light and CO_2 conditions of the laboratory setup. Under these conditions, gross photosynthesis is larger than respiration and thus CO_2 is required to diffuse from the atmosphere into the thallus, not out of it.

Even under low diffusivity, caused by high water saturation, there will be no net diffusion of CO_2 from the thallus into the ambient air assuming that inward and outward flows of CO_2 share the same pathway and that diffusion of CO_2 between atmosphere and thallus is in steady-state with the flux (respiration minus gross photosynthesis). For details please see the Supplement. Furthermore, matching the simulated temperature-response of net photosynthesis to the measured data under cool conditions turned out to be difficult for samples from site T1 and A1 (Fig. S2.2). There were too few data points in the measured temperature response data set to constrain the optimum temperature and temperature relation (see Fig. 2.2), but the fitting turned out well because the simulated optimum temperature for net photosynthesis at site T1 was coincidentally close to the value of 17 °C reported by Colesie et al. for this site. (2014; see Fig. S2.2).

2.4 Validation of the data-driven model

The water saturation and activity estimated by the data-driven model were validated by comparing with the daily and diurnal patterns of measured activity (5 sites, not at site D2) and water content data (only at D2). Furthermore, the C balance estimated by the data-driven model was validated by comparison to the in situ measured net CO_2 exchange rate of moss, lichen, and cyanocrust-dominated biocrusts. These data were sampled at site D2 by removing the soil respiration rate, predicted by means of a fitted regression (Weber et al., 2012). Since data on water saturation were available, measured PAR, surface temperature, and water content were used to simulate the C balance using the data-driven model, in contrast to the setup described above. The activity, however, was calculated in the same way as described in the setup. Moreover, the parameters of the model were the same as the calibrated ones of the corresponding biocrust types.

2.5 Sensitivity analysis

To investigate the role of environmental factors, physiological properties, and also seasonal acclimation for the simulated annual C balance of biocrusts, we conducted three sensitivity analyses using our data-driven model. With this setup, we intend to put into context the effects of environmental conditions and the uncertainty associated with the physiological properties that were used to parameterize the model. We

additionally explore the impact of seasonally acclimatized physiological properties on carbon assimilation at site T1, since variation between seasons represents additional uncertainty in the estimation of the C balance.

2.5.1 Effects of environmental factors

To investigate the role that environmental factors, namely air temperature (T_air), light intensity (Light), ambient CO_2 concentration (CO_2), and different types of water sources play in regulating the C balance of biocrusts, sensitivity analyses were conducted for lichen-dominated biocrusts from all study sites. The different types of water sources include rainfall (Rain) and non-rainfall water inputs such as dew and water vapor, which are determined by relative air humidity (R_hum). All the environmental factors were reduced and increased by half (+/- 50%), except for T_air and R_hum. The T_air differences varied by 5 K and R_hum by 20%. Moreover, relative humidity was constrained between 0 and 100% when the varied relative humidity exceeded this range.

The annual C balance for each modified environmental factors was then normalized following Eq. (1), and normalized again among different environmental factors within each climatic zone for comparing the relative importance of environmental factors:

$$Normalized\,C\,balance = \frac{C_{ij} - C_j}{|C_j|} \tag{1}$$

where C_{ij} is the C balance of factor j under operation i, and C_j is the original C balance of factor j.

A positive normalized C balance demonstrates an increase in annual C balance when certain environmental factors change, and a larger magnitude of the normalized C balance number demonstrates a larger effect of this environmental factor compared to a factor with a smaller value.

2.5.2 Effect of physiological parameters

The sensitivity analysis of physiological parameters was conducted for lichen-dominated biocrust at all study sites. The original parameter values were obtained by calibration to measured net photosynthesis response curves. We then varied the values of the following physiological parameters by a consistent range for all sites: metabolic respiration cost per surface area (Resp_main), Q_{10} value of respiration (q10), the op-

timum temperature for gross photosynthesis (Topt), respiration cost of RuBisCO enzyme (Rub_ratio), and light absorption fraction in cells (ExtL), minimum saturation for activation (Sat_act0), and minimum saturation for full activation (Sat_act1). Specifically, we increased or decreased Resp_main, ExtL, q10, Sat_act0 by 30%, Rub_ratio and Sat_act1 by 20%, and Topt by 5 K. These parameters are chosen since they are closely related to the response of photosynthesis and respiration to water, light, and temperature. These ranges of different parameters were determined based on the observed bounds of the photosynthetic response curves of all replicates (see calibration results with varied parameters at all sites in Fig. S2.5-S2.10), which have large deviations between each other at most sites as shown in Fig. 2.2 and Fig. S2.2. The effects of the varied physiological parameters on the C balance were then normalized using the same normalization method as for the environmental factors (in Sect. 2.5.1) for comparison among parameters and climatic zones.

2.5.3 Effect of seasonal acclimation

Another sensitivity analysis was performed for site T1 to investigate the impact of seasonally acclimatized physiological properties on the C balance. We analysed the lichen- and moss-dominated biocrusts at site T1 as an example, because the measured time-series of activity showed that in temperate sites such as T1, the organisms were active most of the time, and thus the C balance would be more sensitive to seasonally varying properties.

In the analysis, rather than keeping all calibrated parameters fixed throughout the simulation period of the data-driven model, the physiological parameters metabolic respiration cost per surface area (Resp_main), light absorption fraction in cells (ExtL), and the ratio of Jmax to Vcmax (jvratio) were set to another set of values in the winter months in order to adapt to the climatic conditions, since biocrusts at sites T1 were collected in summer months. These new, "dynamic" parameters were applied in an additional simulation and the resulting C balance was compared to the original simulation based on the "fixed" parameters. The dynamic parameters were chosen and varied based on the literature: Respiration of lichens was found to acclimate to seasonal changes in temperature (Lange and Green, 2005). Moreover, under low light, organisms showed shade-adapted physiological characteristics with low PAR compensation and saturation points (LCP and LSP; Green and Lange, 1991).

These properties can be expressed by certain parameters of the data-driven model. For instance, the respiration rate is determined by the parameter Resp_main; LCP and LSP can be affected by changing the slope of the photosynthesis-light relations through the parameter ExtL; LCP and LSP can also be modified via the parameter jvratio as it influences the value of light use efficiency at unsaturated light.

Accordingly, in an hourly simulation during September and December, January, and February, the parameter Resp_main was reduced to half to lighten the respiratory cost for the samples collected at site T1. The size of ExtL was doubled to increase the slope of photosynthesis-light relations. In addition, the parameter jvratio was doubled as well to enhance the light use efficiency.

2.6   LiBry Model

LiBry is a process-based dynamic global vegetation model (DGVM) specific to non-vascular vegetation. The model mimics environmental filtering in the real world by simulating many different functional strategies and selecting those which maintain a positive C balance under the respective climatic conditions. The strategies are characterized by a combination of 11 physiological and morphological parameters. More information about the model is briefly described in the Supplement, and a full detailed description can be found in Porada et al. (2013, 2019).

For this study, the LiBry model was run for 300 years with repeated microclimate forcing data of one year from the six study sites, calibrated abiotic parameters same as the data-driven model, and initially generated 1000 strategies. C balance and dynamics of the surface cover of the strategies were simulated until a steady state was reached, so that the final successful strategies were those where long-term biomass values were positive. Moreover, at the end of the simulation, the average values of functional traits were estimated by weighting all surviving strategies based on their relative cover. The (hypothetical) strategy characterized by these average values is called average strategy. The strategy with the largest cover area is called dominant strategy.

Furthermore, we compared the physiological parameters of the average strategy and the selected dominant strategies to the ones of organisms in the field by means of their respective photosynthesis response curves. This comparison can verify the C balance estimated by the data-driven model from a reversed perspective as LiBry

model is based on the same processes as the data-driven model, but the strategies were freely selected by the LiBry model based on their C balance, without prescribing values based on site level observations.

3. Results

3.1 Data-driven model

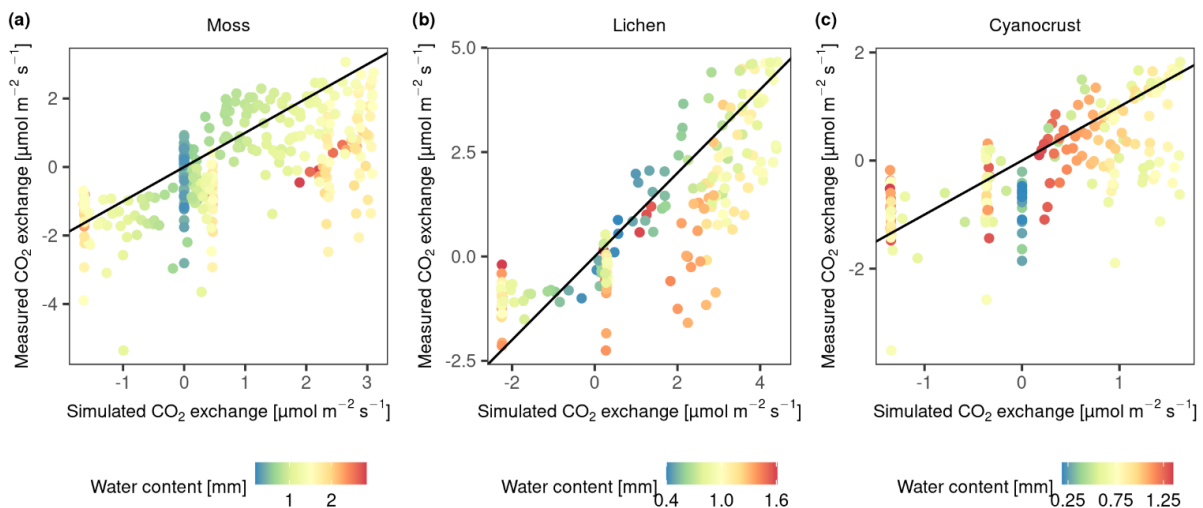#### 3.1.1 Validation of the data-driven model
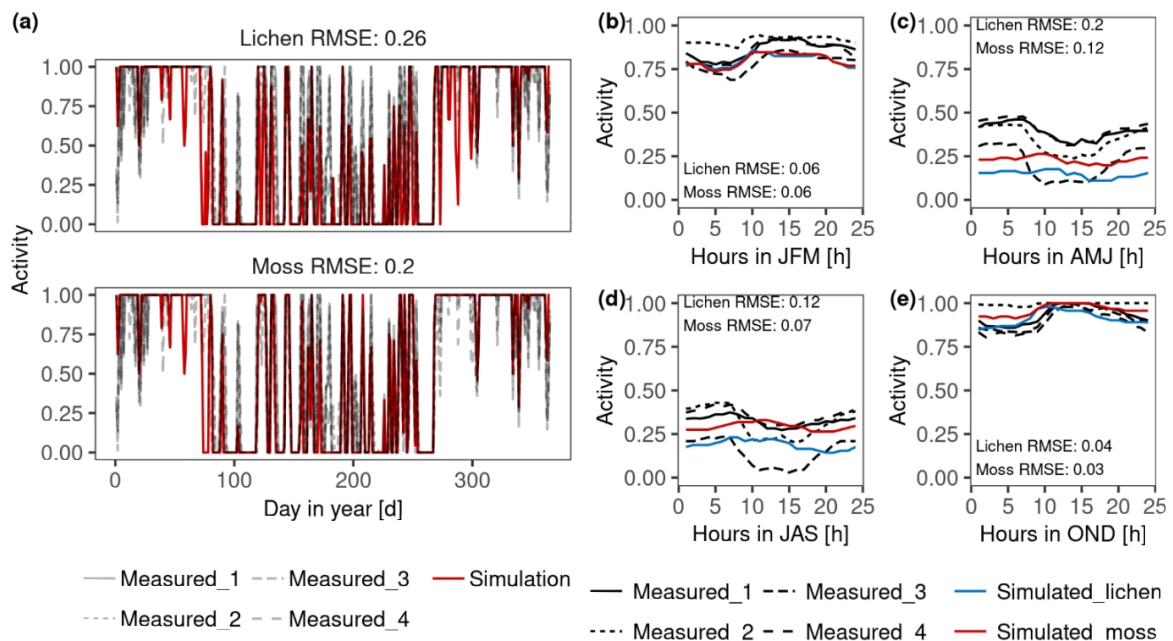
Figure 2.3: Validation of the estimated daily (a) and diurnal (b-e) patterns of activity of lichen- and moss-dominated biocrusts at site T3. The simulated patterns of activity were compared to measured data by four sensors at different locations. (b) to (e) represent the patterns of average hourly activity from January to March (JFM), April to June (AMJ), July to September (JAS), and October to December (OND), respectively.

In general, the simulated daily and diurnal patterns of activity (water content at site D2) fit the measurements reasonably well in magnitude (Fig. 2.3 and Fig. S2.3). However, our fitting resulted in a more dampened diurnal activity pattern simulated by the model, and the activity at night and in the morning was underestimated during several seasons at sites D1, T1, T2 and A1. In addition, both the daily and diurnal activity during April and June at site T1 were underestimated. Furthermore, water content was overestimated for moss-dominated biocrust, especially when there was a large amount of water input at D2, although the patterns corresponded well to the

measured data for all three biocrust types (Fig. S2.3). This overestimation may have resulted from the bias in measured MWC of samples used for constraining the water content in the model.

The comparison of simulated and on-site measured CO_2 exchange rates of three biocrust types (moss, lichen, and cyanocrust composed of cyanolichens and cyanobacteria) at site D2 showed mismatches, especially when water saturation was at both ends of the gradient (Fig. 2.4). The CO_2 exchange rate at high water content was overestimated compared to the measurements. Moreover, there were large variations in measurements of respiration and CO_2 exchange rate as water content was low and thus simulated CO_2 exchange rate was zero. Excluding the values at both ends of water content (0.58 and 1.74 mm for moss; 0.22 and 0.68 mm for lichen; 0.65 and 1.24 mm for cyanocrust), the accuracy of the model predictions was improved (root mean square error (RMSE) decreased from 1.44 to 1.36 for moss, 1.27 to 0.65 for lichen, and 0.79 to 0.77 for cyanocrust). Furthermore, the simulations were similar to measurements in magnitude. Therefore, despite the large variation, we are confident about the general validity of the model.

Figure 2.4: Validation of the photosynthesis and respiration scheme of the data-driven model through comparison of modelled and measured CO_2 exchange rate of moss, lichen, and cyanocrust given the measured water content, surface temperature, PAR, and calculated activity. Observational data were collected in November in 2013 at site D2. The 1:1 line is shown in black.

3.1.2 Estimated C balance by data-driven model

The simulated annual C balance of each collected biocrust type at each site is listed in Table. 2. The annual C balance of lichen- and moss-dominated biocrusts at dryland D1 showed a small positive value. Moreover, the moss-dominated biocrust at dryland D2 gained small amount of carbon while lichen-dominated biocrust and a cyanocrust additionally measured at site D2 showed a small net release of carbon in the model.

**Table 2.2**: Simulated annual carbon budgets of each biocrust type at all sites.

	Lichen g C m^{-2} yr^{-1}	Moss g C m^{-2} yr^{-1}	Cyanocrust g C m^{-2} yr^{-1}
D1 (Almeria)	1.5	1.9	
D2 (Soebatsfontein)	-1.7	3.1	-8.3
T1 (Gössenheim)	-42.8	-39.4	
T2 (Öland)	-92.1	-74.7	
T3 (Linde)	9.4	18.7	
A1 (Hochtor)	-17.9	-6.8	

Furthermore, according to these data-driven model simulations, despite the C balance of two biocrust types being positive at site T3, a large amount of carbon was lost at the sites T1 and T2 in temperate humid regions. These results imply that according to the data-driven model, the biocrusts would not survive in the long-term at most of the temperate humid research sites. At the alpine site A1, both lichen- and moss-dominated biocrust lost carbon in a year with long periods of ice cover.

3.2 Dominant strategies selected by the LiBry Model

In general, the photosynthesis response curves of dominant and average strategies selected by the LiBry model did not fit well to the measurements, especially at temperate site T2 (Fig. 2.5; the results for the other sites with negative C balance are shown in Fig. S2.4). Specifically, the selected physiological traits which determine water and light acquisition of the dominant and average strategies in LiBry differed

from those of the collected samples at all sites. Compared to the measured samples, the LiBry strategies showed markedly higher efficiency at low light intensity and faster activation. By design, the LiBry model selected strategies with a positive C balance in the long-term run, and thus the mismatches are consistent with the fact that the data-driven model simulated negative C balances.
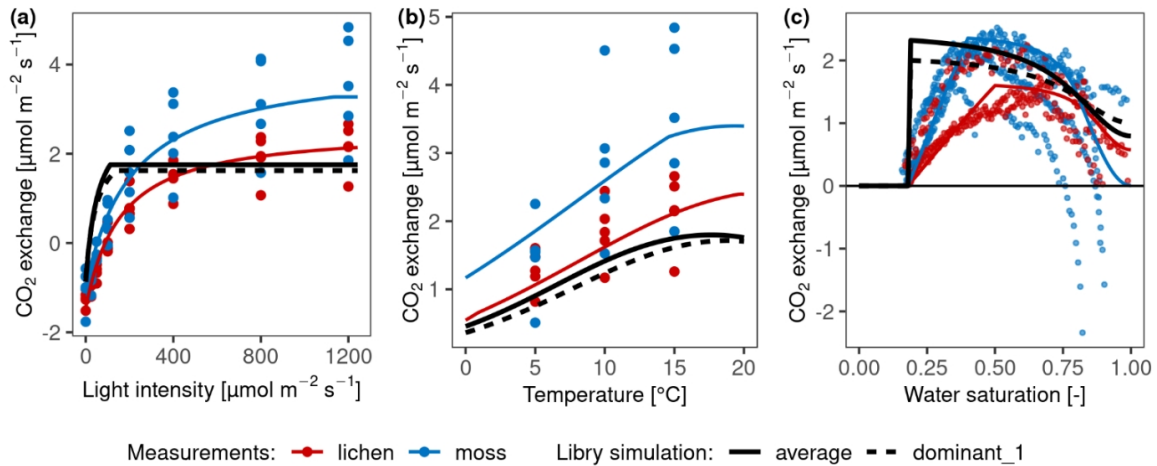

Figure 2.5: Comparison of net photosynthesis response of measured samples with simulated selected dominant and average strategies of LiBry at site T2. (a): light response curve; (b): temperature response curve; (c): water response relation. The colored points represent the measured CO_2 exchange rates of moss and lichen, and the coloured lines correspond to the data-driven model. The black lines show the photosynthesis response of the dominant strategy selected by the LiBry model (dashed) and the average strategy (solid). The parameter values of the average strategy correspond to the average of all surviving strategies.

3.3 Driving factors of variation of the C balance

3.3.1 Environmental factors

The environmental factors light intensity, CO_2 concentration, air temperature, and various water sources, had different effects on the C balance of lichens in different climate zones (Fig. 2.6). For all sites within a given climate zone, the effects of different environmental factors on C balance were overall similar but showed an apparent larger variation at the temperate site T3 in contrast to the other two temperate sites, and at site D2 compared to D1 (Fig. 2.6a). This may be due to physiological differences of the investigated biocrust species between these sites and consequently variations in the responses of net photosynthesis rate to temperature, water, and light between them (Fig. 2.2 and S2.2).

Furthermore, the spatial patterns of the relative importance of different environmental factors show that the factors which have the strongest effects differ between climatic regions (Fig. 2.6b).
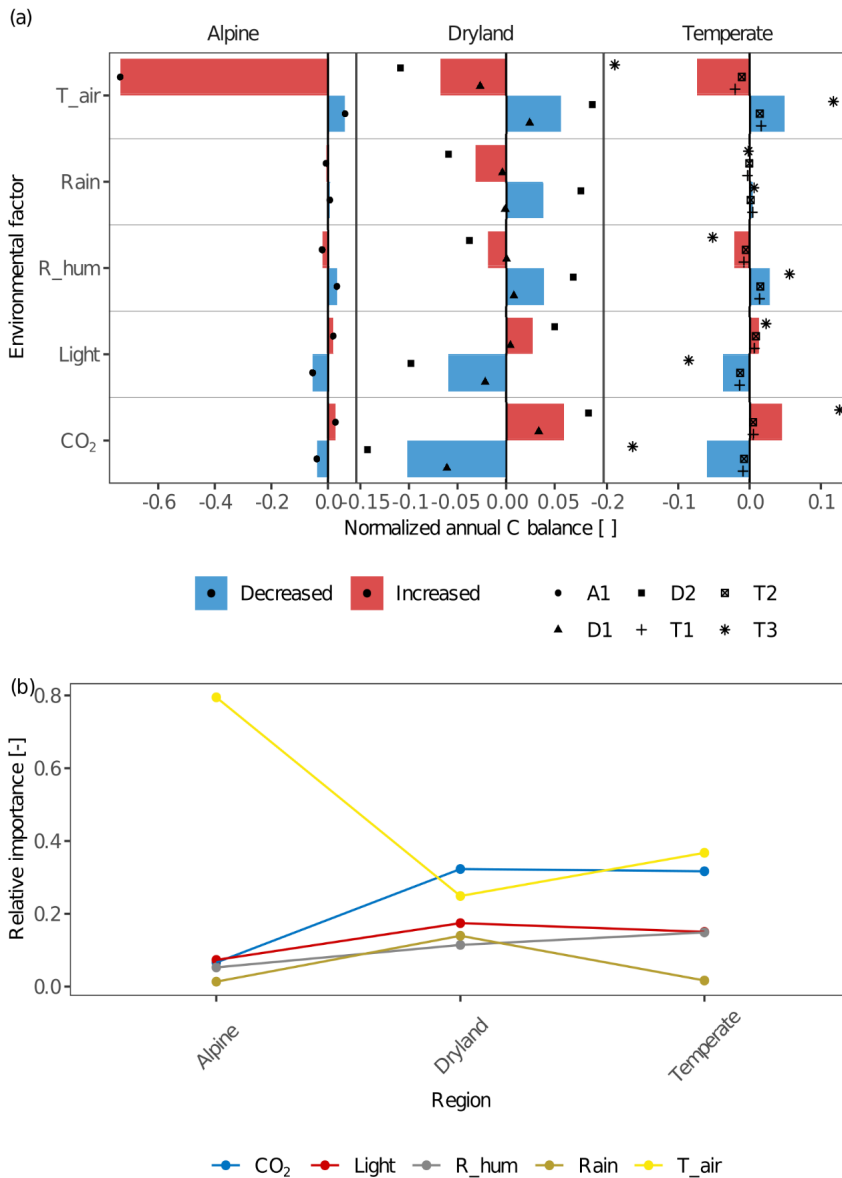
Figure 2.6: (a) The effects of environmental factors - CO_2 concentration (CO_2), relative air humidity (R_hum), rainfall amount (Rain), air temperature (T_air) and light intensity (Light) on the annual C balance of lichens in different climate regions. The altered annual C balance resulting from increasing or decreasing environmental factors is normalized by the C balance under original environmental conditions. The colored columns indicate the average value of the normalized C balance at sites with similar climate conditions. Various styles of black points indicate different sites. Positive normalized C balance implies that the annual C balance increases with varying environmental factors and more carbon was accumulated in a year at the site, and vice versa. A larger

normalized C balance reflects that the C balance is more sensitive to the altering environmental factor, and thus the environmental factor has a larger effect on C balance. (b) Relative importance of each environmental factor compared to other factors across the climatic regions. Larger relative importance implies a more important effect the factor has on the C balance compared to other factors in the given climatic region, and vice versa.

In general, air temperature and CO_2 concentration were the most important drivers for C balance of biocrust organisms between climate zones. Light intensity and relative humidity played a relevant role in impacting the C balance as well. Rainfall amount had lower relative importance at all sites except dryland D2, where the effect of rainfall on C balance was similar to other factors (Fig. 2.6a). Therefore, rainfall amount showed a maximum in relative importance in drylands, compared to other regions. In general, the effect of the other water source, relative air humidity, was moderate but notable at all climate zones, and is slightly larger in temperate region in comparison to other climate zones. Furthermore, the humidity had a slightly larger impact on C balance in comparison to rainfall amount at all temperate and alpine sites (e.g., change amplitude was 0.007 for rainfall and 0.021 for humidity at T1). In drylands, however, the impacts of water sources on C balance varied between sites. The results showed that relative humidity had a slightly larger impact than rainfall amount at D1 while smaller at D2 (the change in amplitude at D2 was 0.108 for humidity and 0.137 for rainfall).

The ambient CO_2 concentration was an essential factor for the C balance at all sites especially in drylands, resulting in positive effects on C balance with increasing CO_2. Furthermore, light intensity had a marked impact on the C budget at all sites, and it was relatively more important in drylands and temperate regions than the alpine site. At all sites, the normalized C balance increased with enhanced light intensity and vice versa (e.g., normalized C balance at T2 are -0.013 and 0.008 for half and doubled light intensity). Air temperature had a large impact on C balance at all sites. Especially at the alpine site A1, C balance decreased strongly as air temperature raised by 5 K (normalized C balance of -0.735), and at all sites, the direction of the effect remained constant, namely, warming decreased the C balance and vice versa.

3.3.2 Physiological parameters

We found that physiology plays an important role in all regions. In particular, the respiration-related parameters such as q10, Resp_main, and Topt have a notably higher impact on C balance estimation (Fig. 2.7). Furthermore, the relative importance of several physiological parameters showed similar patterns across climatic zones: in all regions, q10 is the most essential parameter, Sat_act0 and Sat_act1 play little roles in affecting C balance. Other parameters showed slightly different patterns among regions. Metabolic respiration cost (Resp_main), for instance, plays a more important role than optimum temperature for gross photosynthesis (Topt) at the alpine site, while the optimum temperature is more essential in drylands and temperate regions (Fig. 2.7b).
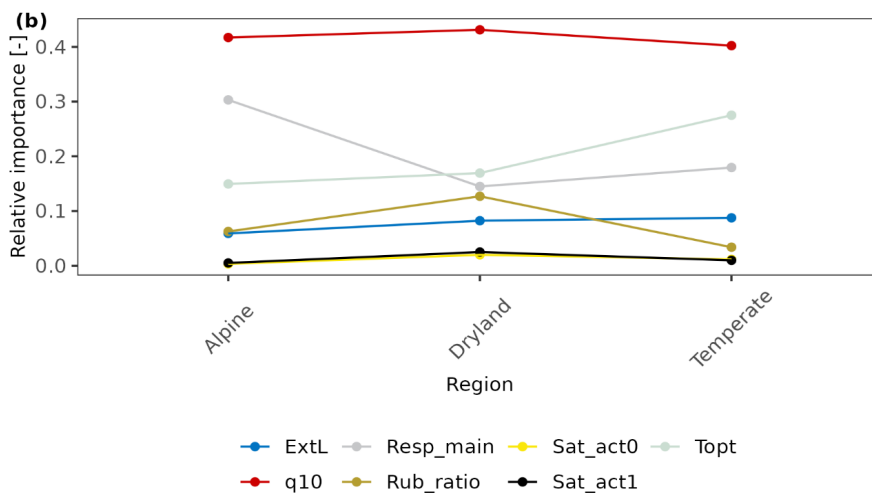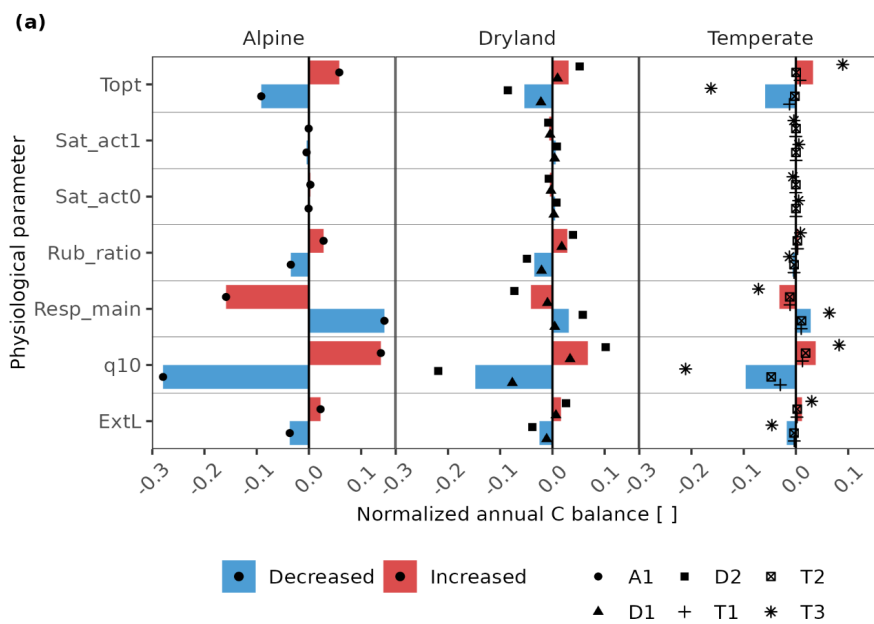
Figure 2.7: (a) The effects of physiological parameters – metabolic respiration cost per surface area (Resp_main), Q_{10} value of respiration (q10), the optimum temperature for gross photosynthesis (Topt), respiration cost of RuBisCO enzyme (Rub_ratio), and light absorption fraction in cells (ExtL), minimum saturation for activation (Sat_act0), and minimum saturation for full activation (Sat_act1) – on the annual C balance of lichen-dominated biocrusts in different climate regions. The parameters decreased or increased by a consistent range for all sites based on the measured deviation in photosynthesis response curves of replicates. The altered annual C balance resulting from increasing or decreasing parameters is normalized by the original C balance. The coloured columns indicate the average value of the normalized C balance at sites with similar climate conditions. Various styles of black points indicate different sites. (b) Relative importance of each physiological parameter compared to other parameters across the climatic regions. Larger relative importance implies a more important effect the parameter has on the C balance compared to other parameters in the given climatic region, and vice versa.

However, even though physiology parameters play an important role in all regions, the C balance at T1, T2 and A1 did not become positive when the physiological parameters were varied reasonably, that is the parameters were varied to relatively cover the deviation of response curves of replicates. Furthermore, the change in C balance value is much smaller in drylands compared to other regions (as shown in Fig. S2.11 in the Supplement).

3.3.3 Acclimation of physiological properties

The sensitivity analysis for acclimation showed a marked increase in annual productivity of lichen- and moss-dominated biocrusts at site T1 (Fig. 2.8) when the seasonal acclimation of several physiological parameters was included in the model (from -42.8 to -15.5 g C m^{-2} yr^{-1} and from -39.4 to -4.2 g C m^{-2} yr^{-1}).
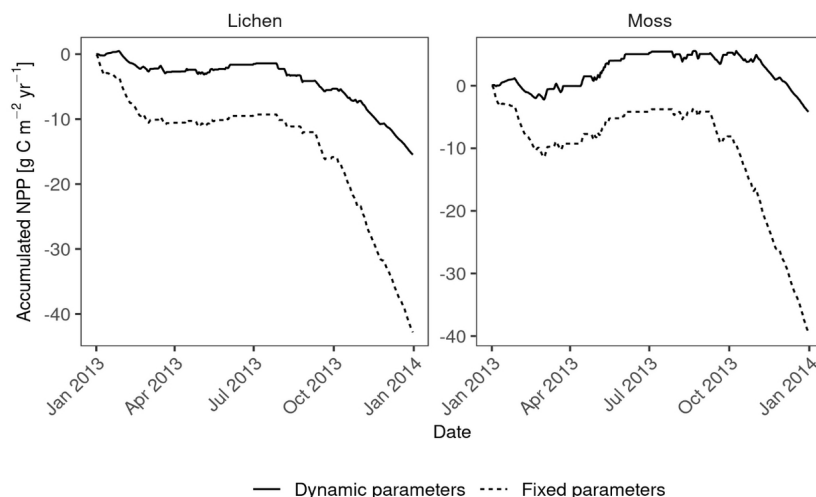
Figure 2.8: Comparison of accumulated annual C balance between two simulations in the sensitivity analysis of seasonal acclimation of physiological properties. In the simulation "fixed parameters", all parameters that have been calibrated or measured remained constant throughout the simulation year. For the simulation "dynamic parameters" at site T1, parameter metabolic respiration cost per surface area (Resp_main) was reduced by half, light absorption fraction in cells (ExtL) was doubled but restricted to one, the ratio of Jmax to Vcmax (jvratio) was increased by two times from September to February to adapt to the winter climates. For the other months, the "fixed" values were used.

4. Discussion

4.1 Simulated C balance of data-driven model

The data-driven model aims to provide observation-based estimates of the carbon fluxes of non-vascular photoautotrophs which may serve as approximation for the C balance of vegetation in biocrust-dominated ecosystems. At the two dryland sites, the moss-dominated biocrusts were estimated to be carbon sinks on an annual basis, and lichen-dominated biocrust can also be a carbon sink at one of the dryland sites. As shown in the results, mosses accumulated 1.9 and 3.1 g C m^{-2} yr^{-1} at site D1 and D2, respectively, and lichens accumulated 1.5 g C m^{-2} yr^{-1} at site D1.

The estimated C balance at the two dryland sites is consistent with the magnitude of the annual C balance of different biocrust types reported by various studies in arid habitats. Feng et al. (2014) recorded that the biocrusts composed of lichens, mosses, and cyanobacteria of the Mu Us Desert in China took up 3.46 to 6.05 g C m^{-2} yr^{-1}. Brostoff et al. (2005) estimated a larger carbon gain by lichen biocrust of 11.7 g C m^{-2} yr^{-1} in the Mojave Desert, USA. For cyanobacteria, an annual carbon uptake of 0.02 to 2.3 g C m^{-2} was reported for deserts (Jeffries et al., 1993). The estimated C balance values in drylands fluctuate relatively largely, but the magnitude is consistent with the simulated results by the data-driven model at D1 and D2.

For biocrust lichens growing on rock surface without soil attached underneath in a temperate grassland, Lange (2003b) measured an annual carbon gain of 21.49 g C m^{-2}. Additionally, several studies estimated the carbon budget in humid tundra habitats. An amount of ~12–70 g C m^{-2} yr^{-1} carbon was fixed by moss-dominated biocrust, for instance (Schuur et al., 2007). The magnitude of these values corresponds to the estimation of the C balance at T3. However, the estimated annual carbon losses of

lichens and mosses by the data-driven model in temperate regions T1 and T2 should actually lead to the death of these organisms, which is not consistent with their dominant abundance in the field and is much lower than published by previous studies.

The mismatches of trait values between strategies predicted via selection by the Li-Bry model for the sites and the collected species with regard to their net photosynthesis response curves indicate that the physiological parameter values that would be necessary to maintain a positive C balance in LiBry are not compatible with those of the sampled biocrusts. This is in line with the results of the data-driven model, which also simulates a negative C balance and is based on the same physiological processes as LiBry. This also applies to the lack of seasonal acclimation in both modeling approaches, since the strategies in LiBry are assumed to have constant functional properties throughout the simulation.

4.2 Uncertainties of long-term C balance simulated by the data-driven model.

The data-driven model simulated relatively reasonable C balance values in drylands but unrealistic, negative values at temperate sites T1 and T2. Since the same or similar gas exchange methodology has been used for all sites, differences in the simulated C balance among these regions likely result from variation in the species-specific interactions between climate and physiological processes, including seasonal variation in physiological properties due to acclimation.

As the results (Fig. 2.6) show, CO_2 concentration is an essential factor for the annual C balance of biocrusts, especially at dryland and some temperate sites. Therefore, uncertainty in the CO_2-value prescribed in the model may be a source of error. The CO_2 concentration at the surface boundary might exceed the value of 400 ppm that was prescribed in the model because of CO_2 diffusion from the soil, which may lead to an underestimated C balance (Fig. 2.6a). However, with enhanced CO_2 concentration in the sensitivity analysis (600 ppm) at site T1, for instance, the estimated C balance increased only slightly, and is still strongly negative (-37.0 g C m^{-2} yr^{-1} for lichen and -30.2 g C m^{-2} yr^{-1} for moss). Hence, the lower CO_2 concentration can partially contribute to the strongly negative C balance at T1 and T2, but is not a major factor. Furthermore, the negative C balance at temperate and alpine sites may result from the uncertainties in physiology, which were also observed between replicates (see Fig. 2.2 and Fig. S2.2). An overestimation of dark respiration rates of the photoau-

totrophs in the biocrust may result from including a small amount of heterotrophic respiration. The overestimated respiration rate then leads to an overestimation of the parameter metabolic respiration cost per surface area (Resp_main) and might also cause an underestimated Q_{10} value (q10) calculated from the respiration rates. The uncertainties of these two parameters reduce the estimated C balance largely (Fig. 2.7). Additionally, the optimum temperature (Topt), which is also the reference temperature for calculating the respiration rate, cannot be well constrained by the limited measured temperature response data set. Thus, Topt may be underestimated. The larger difference in surface temperature to Topt results in a larger respiration rate, and lower gross photosynthesis, which leads to a lower C balance.

Although the uncertainty in individual physiological parameters may not lead to the markedly negative C balance estimates, as indicated by still negative values upon variation of these parameters (Fig. S2.11), additive effects of all parameters combined with long-term unfavourable environmental conditions may cause a large amount of carbon lost over a year. The optimal conditions are rare within a year, which was also described by Lange (2003b). Thus, the overestimated respiration rate leads to a lower carbon gain during the relatively optimal conditions, which may not be sufficient to compensate for exaggerated C losses under long-term harsh conditions, such as autumn and winter at site T1, for instance. For this reason, the simulated C balance of mosses and lichens in temperate humid regions was mostly negative.

In addition to the uncertainty in the values of physiological parameters, seasonal acclimation of these physiological traits to the current climatic conditions may play an important role in regulating the C balance at humid sites where the organisms are active throughout the year, such as site T1 (Fig. 2.8). It was observed, for instance, that the respiration of lichens shows acclimation to seasonal changes in temperature, and the maximum CO_2 exchange rate of the organisms remains steady throughout the year (Lange and Green, 2005). Gauslaa (2006) found a higher chlorophyll a/b ratio in forest lichens with increasing light. Moreover, depression in quantum efficiency in summer under extremely dry conditions has been observed (Vivas et al., 2017). These varied physiological properties of organisms within a year may result in different photosynthesis and respiration rates, and thus different C balances in comparison

to the ones that cannot acclimate to the seasonal climate. The missing seasonal acclimation of physiological traits may explain why the data-driven model estimated a negative C balance for biocrusts in humid regions.

Another limitation of the modeling approach may be the lack of separate responses of respiration and photosynthesis to metabolic activity. Both photosynthetic activity and respiration reach their maximum in the model once the water saturation reaches the optimum value for net photosynthesis (Wopt_np). In some cases, however, respiration rate may reach the maximum value only at a higher saturation than Wopt_np (Lange, 1980), indicating that the model may overestimate respiration in the long-term.

In comparison to the unrealistic C balance numbers at T1 and T2, we estimated more reasonable values in drylands and at T3. However, we do not make a definitive statement about whether or not the model predicts an accurate C balance in drylands. since the measured climate data and photosynthesis response curves that were used for calibrating land surface properties and various physiological parameters represent only samples of the large physiological and climatic variation. A higher accuracy would be more likely to be expected in drylands as these regions have a more uniform climate throughout the year than temperate regions that show substantial seasonality. Additionally, variation in light conditions is slightly more relevant for the simulated C balance than variation in moisture (see Fig. 2.6) because the organisms are able to become inactive, meaning that the dry season in drylands does not have a decisive effect on the C balance, while low light in winter in temperate climate does since organisms have to be active then. Furthermore, the longer total inactive period in drylands could reduce the bias in the magnitude of the simulated C balance caused by incorrectly estimated physiological parameter values. We estimated a smaller absolute change in annual C balance in drylands with varied physiological parameters in the sensitivity analysis (for instance, the C balance of lichens changed by 34.6 g C m^{-2} yr^{-1} for parameter Topt at T1, while it changed only by 1.5 g C m^{-2} yr^{-1} at D1).

Furthermore, the estimated C balance may be inaccurate due to the potential bias in estimated relative water saturation, which partly depends on prescribed MWC obtained by measurements. However, the outcome of the sensitivity analysis of MWC at

T1 revealed that the annual carbon estimation is robust to the uncertainties with regard to the prescribed MWC (details in the Supplement). Another factor that potentially affects the accuracy of C balance estimates is interannual climatic variability. While the model estimated unrealistic C balance values of lichen-dominated biocrusts at T1 and T2 for current conditions, the C balance may have been different in other years. Therefore, the simulation of annual C balance based on multi-year climate data is worthy of future study to understand the long-term C balance better. Moreover, the estimated negative C balance of certain lichen and moss species may not be generalizable and representative for the overall situation in the field due to the large variation in physiological adaptation strategies to climate. There could be other organisms that form cryptogamic covers, for instance, that show a different degree of depression in net photosynthesis at high water content (Lange et al., 1995), and thus have more reasonable C balance values.

4.3 Potential factors influencing the C balance

Despite diverse climatic conditions, we found similarities regarding the dominant environmental factors and physiological parameters controlling the C balance. Thereby, CO_2 and air temperature were the two most important environmental factors at all sites. Relative air humidity, partly precipitation, and light intensity were also relevant for the estimation of the C balance. In terms of physiological parameters, the respiration-related parameters were the most important drivers, while parameters that affect Vcmax and thus the light-independent CO_2 assimilation rate were relevant, too.

The relative importance of these factors/parameters varied slightly among climatic regions. Regarding the comparison between environmental factors, we cannot rule out that the magnitudes of changes in environmental factors that we applied in the sensitivity analysis were not balanced, which may have led to an overestimation of the relative importance of certain factors, such as air temperature, for instance, compared to the others. The spatial patterns across climate regions of a given environmental factor, however, are not affected by this, which means that differences between climatic regions for a given factor are most likely robust. Hence, air temperature is more relevant at the alpine site and relative air humidity has a higher impact in temperate than in other regions, rainfall and CO_2 are likely to have the largest effect on C balance in drylands. Even though the data-driven model failed to estimate reasonable C

balance at some sites, the comparison of the relative importance of the environmental factors across climatic regions may be valid since the measurement procedure is consistent. Moreover, the patterns of relative importance remain similar when excluding the sites with strongly negative C balance (T1, T2, and A1; as shown in the Fig. S2.12 in the Supplement). Nevertheless, we only studied the sensitivity of the C balance of biocrusts dominated by the lichen *Psora decipiens* and *Cladonia furcata* (at T3), and there are variations between lichens of different growth forms and between biocrust types. For example, cyanolichens increase in abundance with increasing rainfall, but trebouxioid lichens have their physiological optimum in drier conditions (Phinney et al., 2021). Moreover, the impact of precipitation on isidiate lichens is weaker than that of temperature (Phinney et al., 2021).

4.3.1 Environmental factors

Our results suggest that warming can result in a large amount of carbon loss at all sites, with a particular large effect in the alpine region. The consistent effects of warming on C balance of biocrusts are found in various field studies (e.g., Darrouzet-Nardi et al., 2015; Ladrón de Guevara et al., 2014; Li et al., 2021; Maestre et al., 2013). This can be explained by the overall less optimal water and temperature conditions associated with warming. The simulated increasing respiratory costs with warming overcompensate gains in gross photosynthesis.

Ambient CO_2 concentration affects the gross photosynthesis rate to a large extent in the model. Although the intra-annual change in air CO_2 concentration may be small in the field compared to other environmental factors, the increase of CO_2 in the atmosphere in recent decades (IPCC 2021) may alter the long-term C balance substantially. However, this beneficial effect of elevated CO_2 on photosynthesis and C balance may be reduced in reality due to future limitation of growth by nitrogen (Coe et al., 2012a), which is not considered in the model, or also due to shortened activity periods resulting from warmer and drier future climatic conditions.

Light intensity has the third largest effect on C balance, slightly larger than moisture. Light is one of the essential factors for photosynthesis as simulated by our model, and it is a limiting factor of photosynthetic carbon assimilation, in particular in winter at temperate and alpine sites (the mean value of radiation maxima in January is 244

µmol m^{-2} s^{-1} at T1 and 245 µmol m^{-2} s^{-1} at the alpine site). Hence, increasing light intensity can promote carbon accumulation.

Factors that determine water supply are rainfall and non-rainfall inputs such as dew and water vapor that are related to relative humidity. The relative importance of different moisture factors in mediating C balance varies in the model. Relative humidity plays a more important role in mediating the C balance than rainfall amount. This may be due to the timing of dew or water vapor uptake, which is greatest before sunrise (Chamizo et al., 2021; Ouyang et al., 2017) and prolongs the activated periods in the early morning when the organisms start assimilating carbon (Veste and Littmann, 2006). This may result in a markedly increased annual C balance in the model. Rainfall amount was not a key factor affecting the simulated biocrust performance at one of the arid sites, which is consistent with another study (Baldauf et al., 2021). At the other dryland site (D2), however, this was not the case. Moreover, we found that the effect of the amount of rainfall is small in humid temperate and alpine regions as well. The differing effects of rainfall on the C balance depend on the change in relative water saturation that follows from rainfall event sizes and patterns throughout the year (Reed et al., 2012). In some cases, decreased rainfall leading to lower water saturation of biocrusts may facilitate photosynthetic carbon gain via increasing the CO_2 diffusivity from the atmosphere into the chloroplast (Lange et al., 1997). Nevertheless, reducing water saturation below a certain value can cause a decline in the duration of activity (Proctor, 2001; Veste et al., 2008) which thus reduces carbon accumulation. Thus, there may be a rain threshold below which decreasing rain may start having a negative effect on biocrust C balances. The threshold is likely species-specific as it is associated with the water-holding capacity of the organism. Our simulation results thus highlight the need for the combined application of field experiments and data-driven modeling to improve our understanding of differential responses to variation in precipitation.

4.3.2 Physiological parameters

The parameter q10 is a key parameter that substantially affects respiration. Resp_main is the dark respiration rate at a reference temperature that is linked in the model to Vcmax, the maximum rate of carboxylation of RuBisCO in the Calvin Cycle of photosynthesis (Walker et al., 2014). Topt is a parameter that controls gross photo-

synthesis as well as respiration as it is also the reference temperature for calculating respiration rates. Rub_ratio can affect Vcmax and hence the maximum CO_2 assimilation rate, while ExtL regulates the light using efficiency under limited light conditions. Sat_act0 and Sat_act1 are two parameters that determine the range of water saturation for initial activation and full metabolic activity. They have the smallest effects on the C balance of lichen-dominated biocrusts at all sites.

Our modeling results give insights into the relative effects of individual physiological parameters on annual C balance across different climatic zones. However, the impacts of physiology on biocrust C balance are complex since they always arise from combinations of these physiological parameters. Thereby, different parameter combinations that correspond to different relative impacts on the C balance may lead to the same response curves. Hence, we cannot directly link individual physiological parameters to the underlying mechanisms since we do not have enough data to distinguish multiple possible parameter combinations from each other, in case they produce the same response curves.

4.4   Validation of the data-driven model

The validation results of the model showed an overall good fit of daily and diurnal patterns of water content and activity (Fig. 2.3 and S2.3), and C balance at D2 (shown in Fig. 2.4) given the uncertainties in the data used to parameterize and evaluate the model. This indicates that the data-driven model may be a reliable tool for C balance estimation, provided that a sufficient amount of suitable forcing data is available.

A potential explanation for the general underestimation of activity at night and morning during several periods in a year is the larger prescribed MWC and Sat_act0of organisms in the model compared to those of the samples from the activity measurements. Consequently, simulated saturation was lower, but minimal saturation for being active was higher than the samples. Thus, the activity may have been underestimated at small water inputs such as dew and water vapor, which occur mainly during the night and in the morning hours (Fig. S2.13). Moreover, underestimated activity in April and June at site T1 (Fig. S2.3 F(b)) may have resulted from a gap in rainfall measurements during this period. Not only rainfall amount but also timing and frequency of rainfall events are essential for the physiological responses of biocrust

communities (Belnap et al., 2004; Coe et al., 2012b; Reed et al., 2012). Therefore, although the measured annual total amount of rainfall is reasonable (424 mm at site T1), the missing rainfall during a series of days in summer at site T1 would lead us to incorrectly predict that the biocrusts remain inactive on these days.

Moreover, the mismatch between modelled and observed CO_2 assimilation rates at low or high water contents at site D2 (Fig. 2.4) may have partly resulted from the calibration procedure. In the calibration the simulated CO_2 exchange rates were higher than measurements when the saturation exceeded the optimum saturation and hardly showed any negative values at high saturation (Fig. S2.2 f). In turn, the simulated CO_2 exchange rates of biocrusts with an extremely low water content were zero while the measurements showed negative values (see Fig. S2.2 f), pointing at a certain degree of metabolic activity in natural conditions. Furthermore, the samples used for validation were different from the ones for calibration, which can also lead to inaccuracies.

Additionally, the ability of the model to capture seasonality variations of C balance, which have been shown by other studies (Büdel et al., 2018; Lange, 2003a; Zhao et al., 2016), could not be evaluated here since the monitoring of C balance in the field and collection of samples used for photosynthesis performance measurements were conducted only during October and early November.

5. Conclusions

Our data-driven model provides possibilities to predict the long-term C balance of biocrusts in the field across various climate zones, and it enables us to analyse mechanisms that drive the C balance, despite marked uncertainties in the parametrization. We simulated reasonable C balance values in drylands but unrealistic ones at temperate sites with substantial seasonality. Uncertainties in environmental factors and respiration rate are likely to be the source of error for the C balance estimation since (1) all environmental factors that were examined in our study may act as relevant drivers for the C balance of biocrusts and (2) respiration-related parameters had the largest impacts compared to other physiological parameters, such as water relations or parameters solely related to Vcmax. CO_2 and air temperature showed the strongest effects among environmental factors and at the alpine site, the air temperature was most relevant. Compared to environmental factors, the relative

impacts of physiological parameters are rather equal across climate regions. The optimum temperature may be slightly more relevant in temperate regions, while metabolic respiration cost is most important at the alpine site. Due to the importance of respiration-related physiological parameters, more studies to improve their accuracy are warranted in the future application of C balance modeling approaches.

Our study suggests that a better, more detailed understanding of the seasonal variation of physiological traits is necessary, as the more realistic estimations in drylands compared to temperate sites could be due to the weaker climate seasonality. The model needs to be calibrated with a larger number of samples collected and measured in various seasons to take the acclimation of physiological properties into account. Additionally, the integration of acclimation of physiological traits in process-based models may improve their accuracy in C balance estimation.

6. Supporting information

6.1 Supporting figures
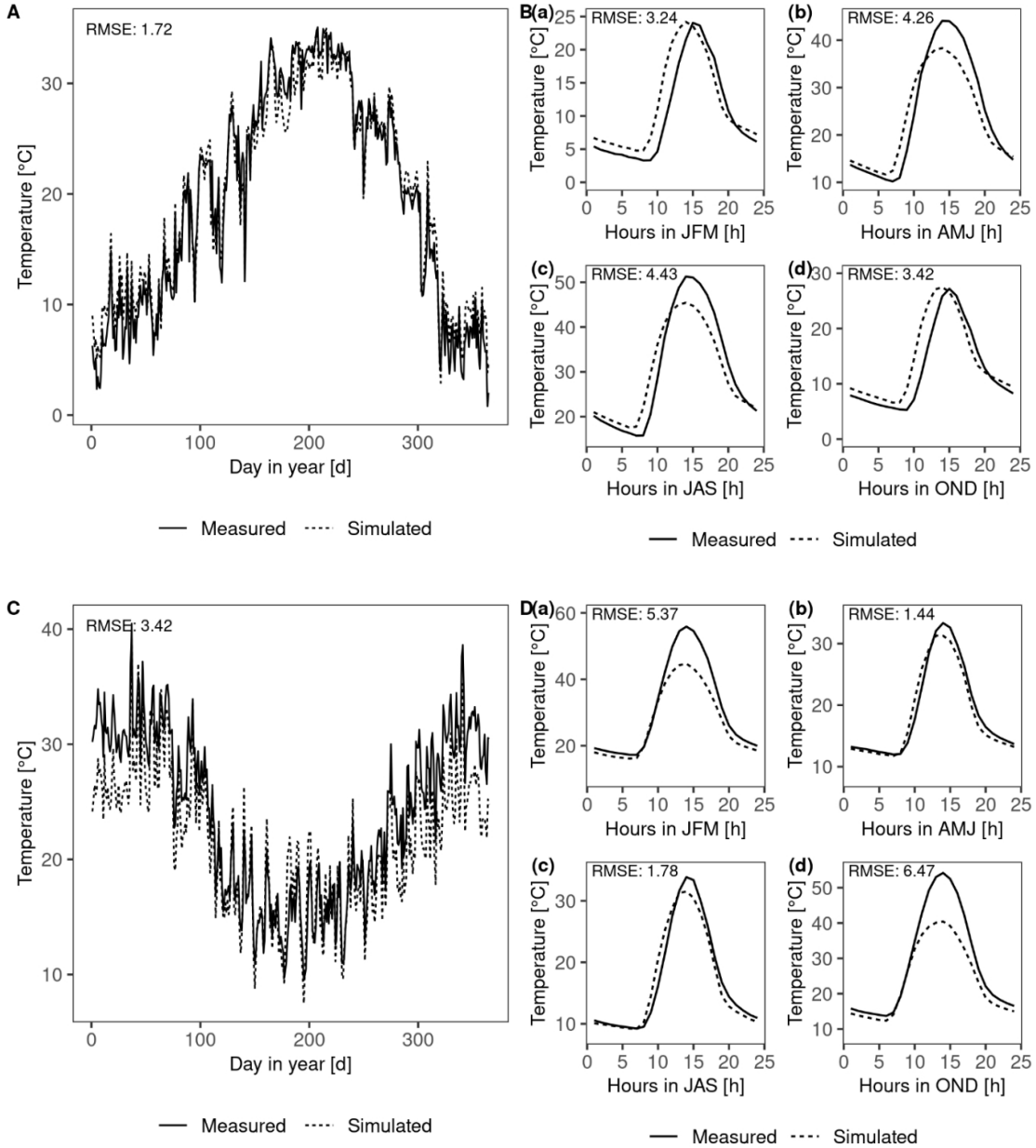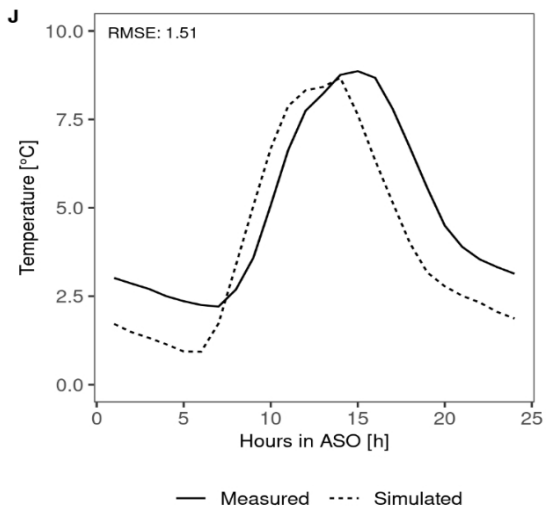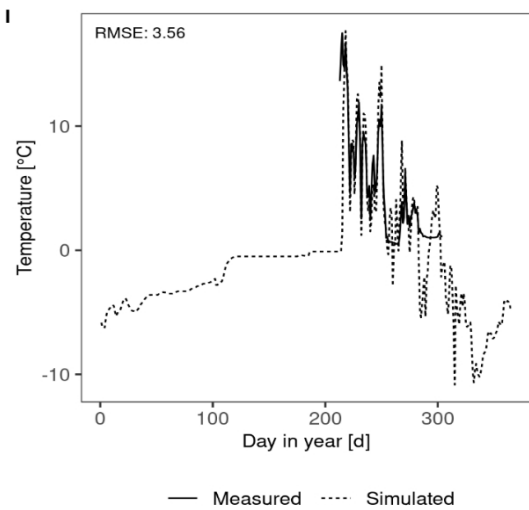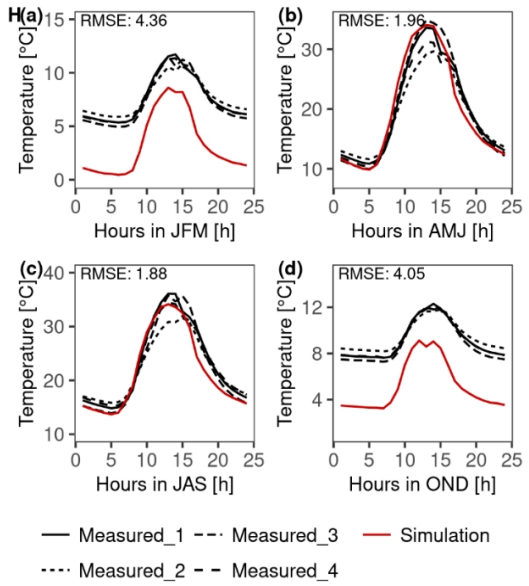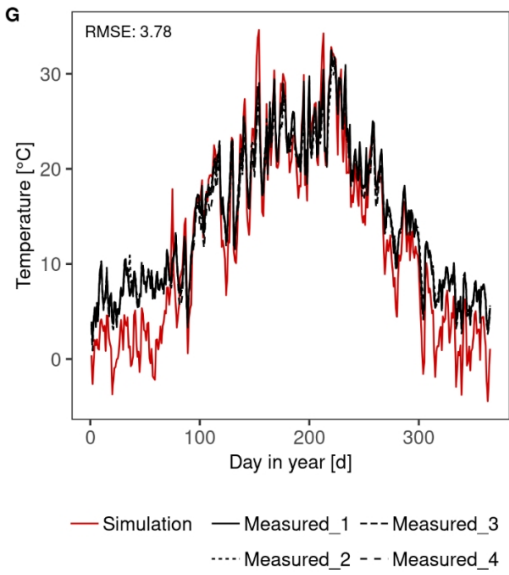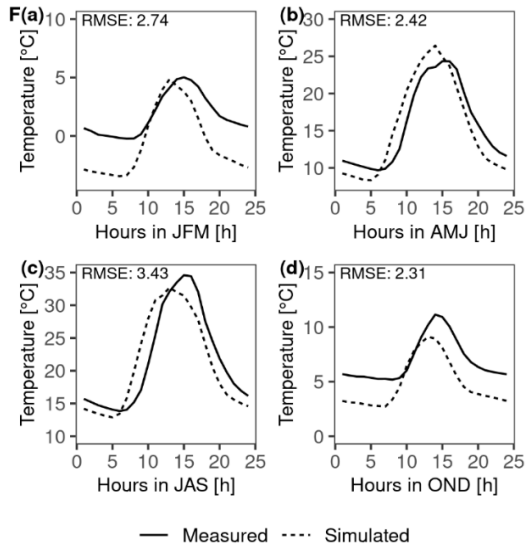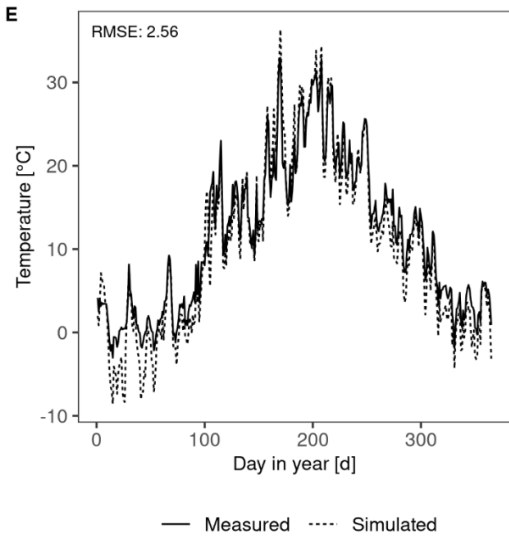
Figure S2.1: Calibration of abiotic parameters for the data-driven model via comparing the seasonal (left panel) and diurnal (right panel) surface temperature of lichen-dominated biocrusts at sites D1 (A, B), D2 (C, D), T1 (E, F), and A1 (I, J); at site T3 (G, H) the simulated patterns of moss-dominated biocrusts was compared to measured temperature data by four sensors at different locations. In the right panel describing the diurnal patterns (B, D, F, H), the (a), (b), (c) and (d) indicate the comparison of patterns of hourly average data in January, February and March (JFM); April, May and June (AMJ); July, August and September (JAS); October, November and December (OND), respectively. At site A1 (J), the average data was during August, September and October (ASO).
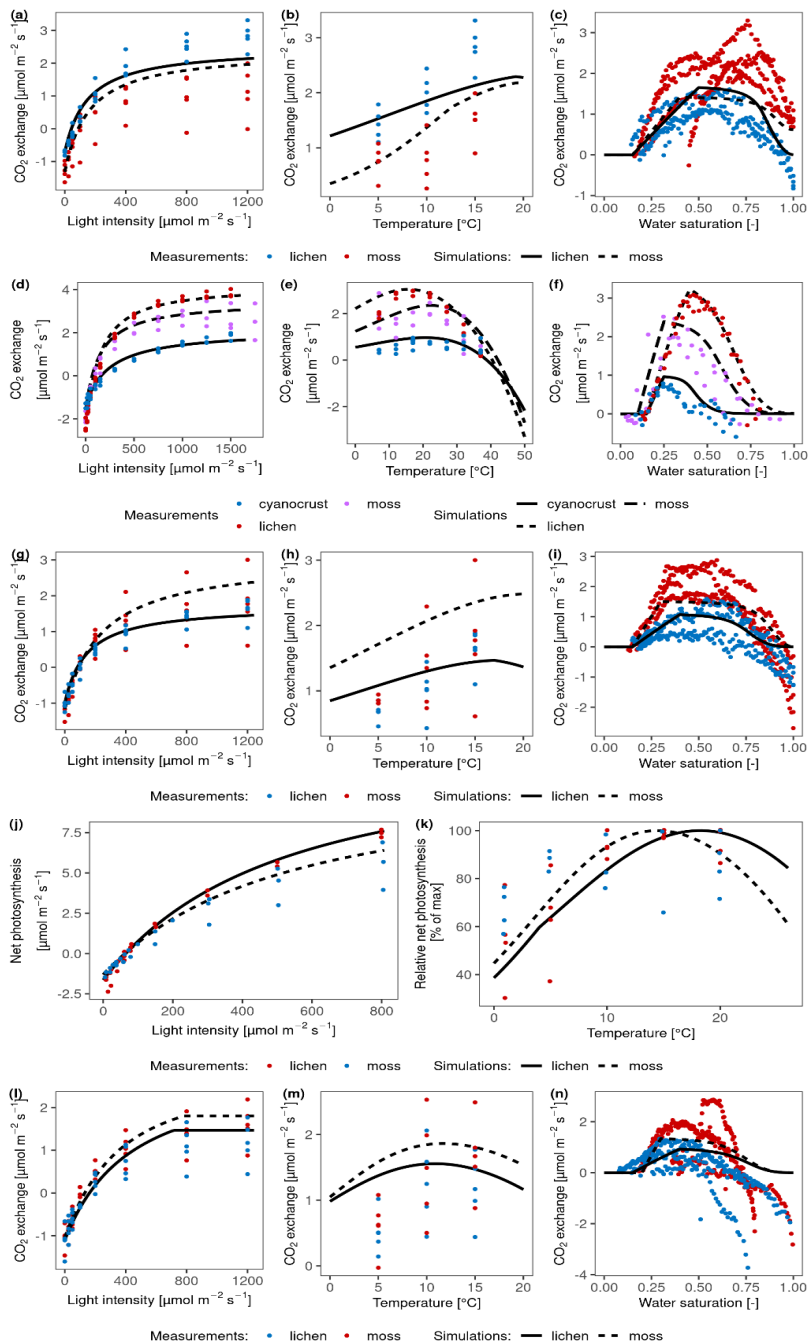
Figure S2.2: Calibration results of physiological traits for the data-driven model at site D1 (a, b, c), D2 (d, e, f), T1 (g, h, i), T3 (j, k) and A1 (l, m, n), via fitting the photosynthetic response curves to some environmental factors. (a, d, g, j, l): net photosynthesis rate in response to light at optimum water content (OWC) and 15°C at D1, T1 and A1; OWC and 22 °C at D2; water saturation for 30% and 15°C at T3. (b, e, h, k, m): net photosynthesis rate in response to temperature at 1200 µmol m^{-2} s^{-1} light and OWC at D1, T1 and A1; 500 µmol m^{-2} s^{-1} light and OWC at D2; 1500 µmol m^{-2} s^{-1} light and water saturation for 30% at T3. (c, f, i, n): net photosynthesis rate in response to relative water saturation at 400 µmol m^{-2} s^{-1} light and 15°C at D1, T2 and A1; 500 µmol m^{-2} s^{-1} light and 22 °C at D2.
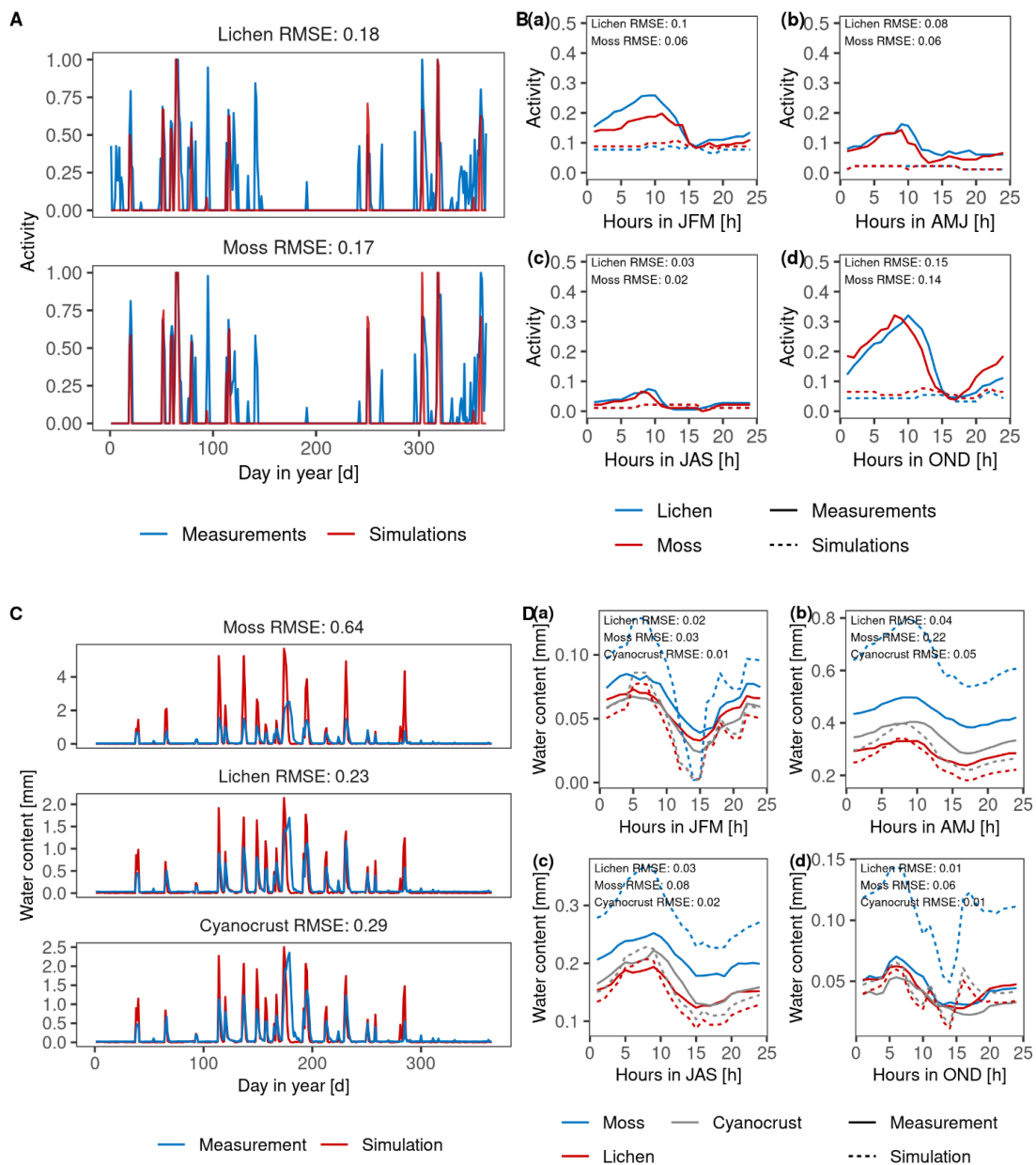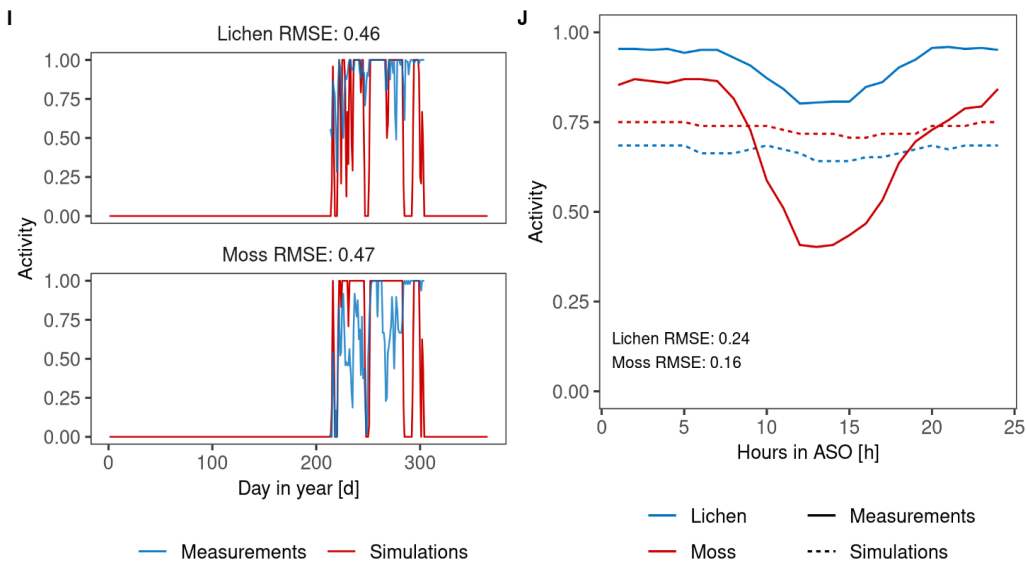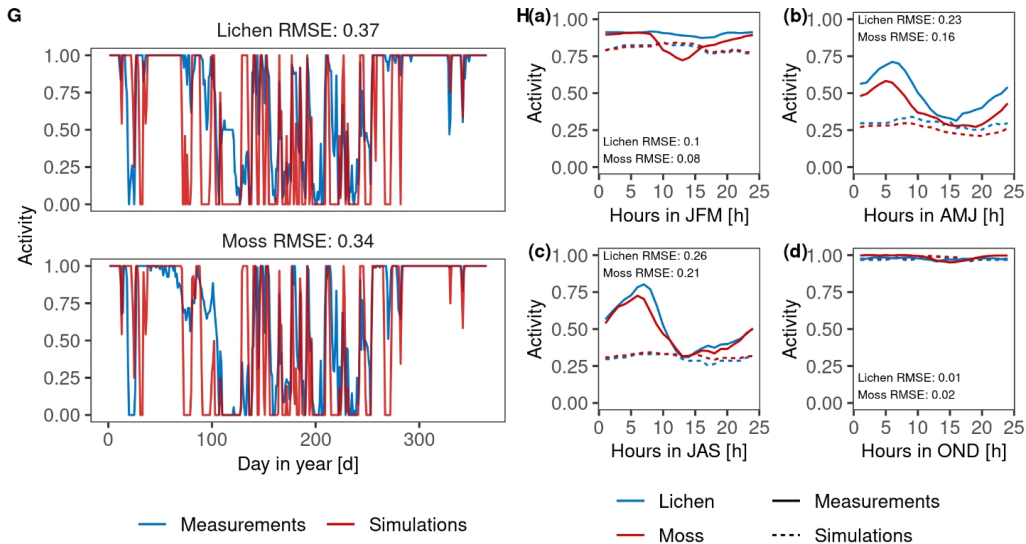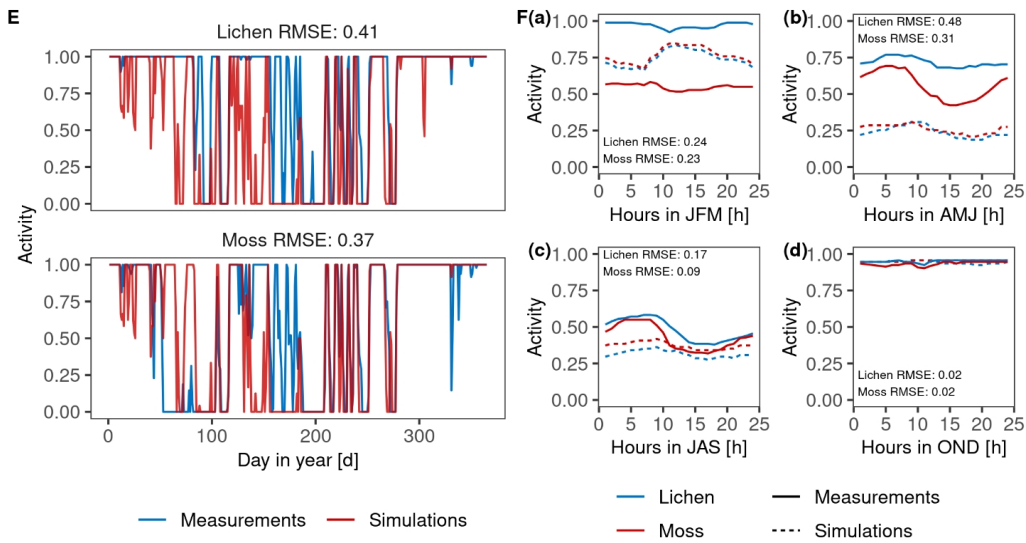
Figure S2.3: Validation of the water and energy balance in the data-driven model via comparing the seasonal (left panel) and diurnal (right panel) water content at site D2 (C, D) or activity patterns of lichen- and moss-dominated biocrusts at sites D1 (A, B), T1 (E, F), T2 (G, H) and A1 (I, J). In the right panel describing the diurnal patterns (B, D, F, H), the (a), (b), (c) and (d) indicate the comparison of the hourly average data in January, February and March (JFM); April, May and June (AMJ); July, August and September (JAS); October, November and December (OND), respectively. At site A1 (J), the average data was during August, September and October (ASO).
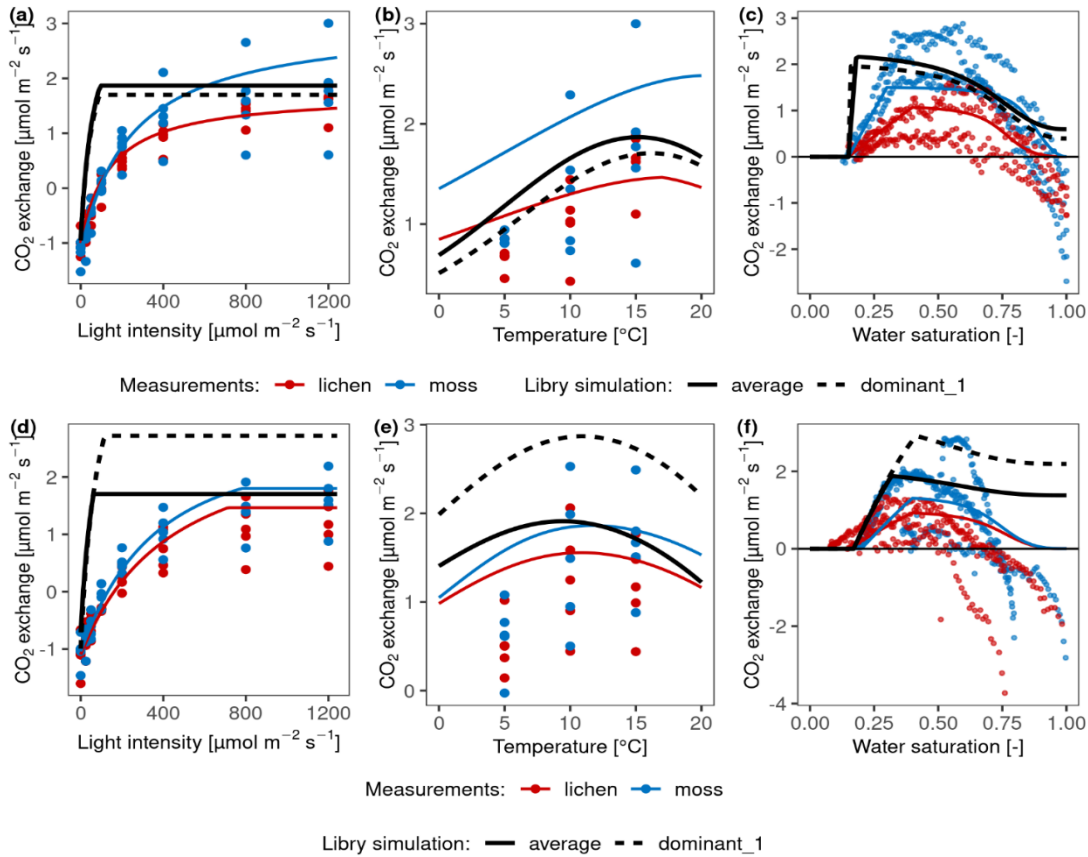
Figure S2.4: Comparison of photosynthetic performance of dominant strategies selected by LiBry model and the measured data as well as the fitted response curves by data-driven model at site T1 (a, b, c) and A1 (d, e, f). (a, d): photosynthesis relation in response to light intensity; (b, e): photosynthesis relation in response to temperature; (c, f): photosynthesis relation in response to water saturation. The colored points and lines represent the measured and simulated by data-driven model CO_2 exchange rates of moss and lichens. The black lines show the simulated photosynthetic relations of the most dominant strategies with positive C balance selected by LiBry model and the average strategy calculated by LiBry model. The parameter values for the average strategy are the average of the corresponding parameters for all selected surviving strategies.
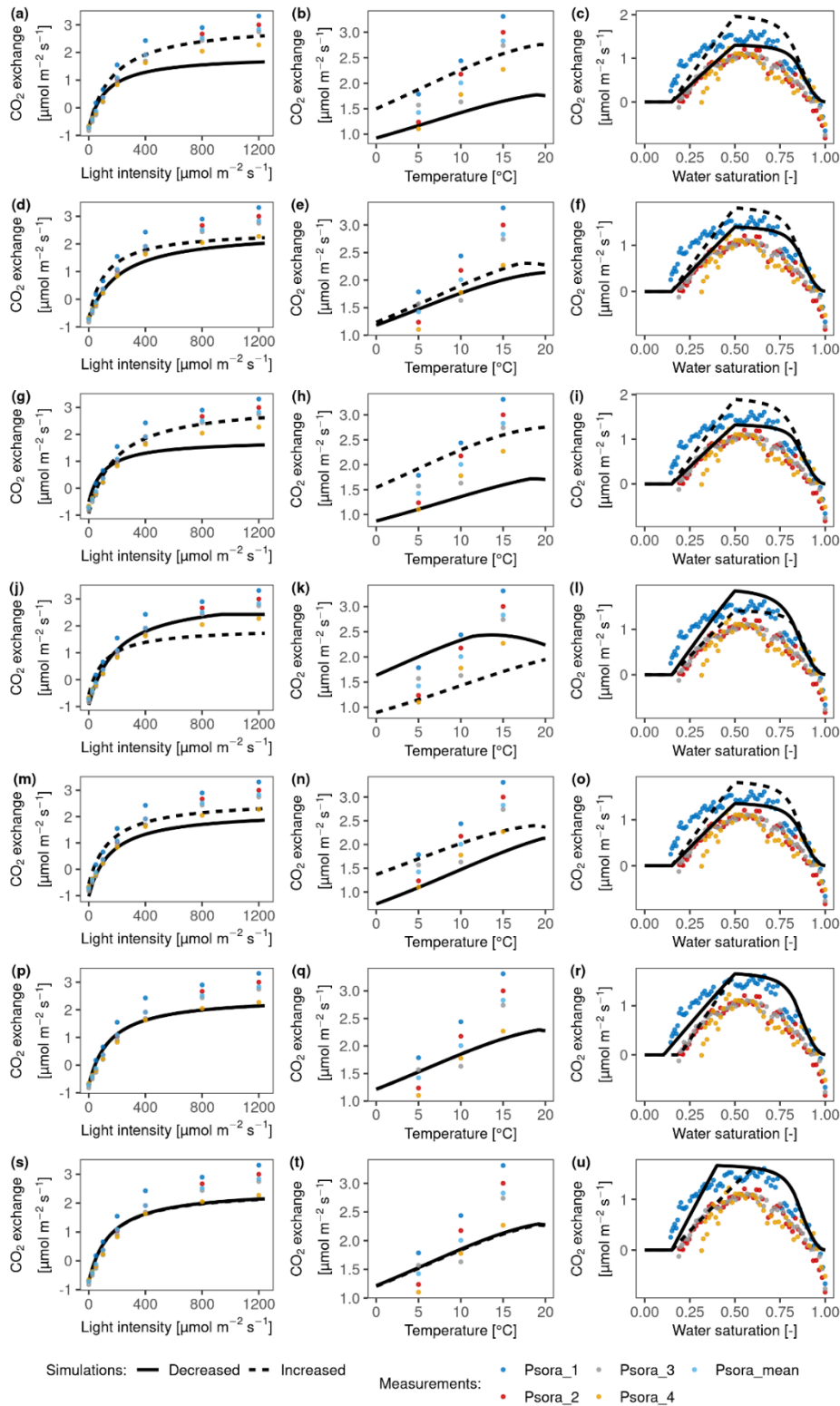
Figure S2.5: Simulated net photosynthesis rate in response to light (a, d, g, j, m, p, s), temperature (b, e, h, k, n, q, t) and water (c, f, i, l, o, r, u) at site D1 by the data-driven model with decreased or increased physiological parameters. These varying physiological parameters are respiration cost of RuBisCO enzyme (Rub_ratio) (a-c), light absorption fraction in cells (ExtL) (d-f),

metabolic respiration cost per surface area (Resp_main) (g-i), the optimum temperature for gross photosynthesis (Topt) (j-l), Q_{10} value of respiration (q10) (m-o), minimum saturation for activation (Sat_act0) (p-r) and minimum saturation for full activation (Sat_act1) (s-u). Resp_main, ExtL, q10, Sat_act0 increased or decreased by 30%, Rub_ratio and Sat_act1 by 20%, and Topt by 5 K. The colored points represent the measured CO_2 exchange rates of different replicates of lichen-dominated biocrusts.

Figure S2.6: Simulated net photosynthesis rate in response to light (a, d, g, j, m, p, s), temperature (b, e, h, k, n, q, t) and water (c, f, i, l, o, r, u) at site D2 by the data-driven model with decreased or increased physiological parameters. These varying physiological parameters are res-

piration cost of RuBisCO enzyme (Rub_ratio) (a-c), light absorption fraction in cells (ExtL) (d-f), metabolic respiration cost per surface area (Resp_main) (g-i), the optimum temperature for gross photosynthesis (Topt) (j-l), Q_{10} value of respiration (q10) (m-o), minimum saturation for activation (Sat_act0) (p-r) and minimum saturation for full activation (Sat_act1) (s-u). Resp_main, ExtL, q10, Sat_act0 increased or decreased by 30%, Rub_ratio and Sat_act1 by 20%, and Topt by 5 K. The colored points represent the measured CO_2 exchange rates of different replicates of lichen-domi-nated biocrusts.

Figure S2.7: Simulated net photosynthesis rate in response to light (a, d, g, j, m, p, s), temperature (b, e, h, k, n, q, t) and water (c, f, i, l, o, r, u) at site T1 by the data-driven model with decreased or increased physiological parameters. These varying physiological parameters are respiration cost of RuBisCO enzyme (Rub_ratio) (a-c), light absorption fraction in cells (ExtL) (d-f), metabolic respiration cost per surface area (Resp_main) (g-i), the optimum temperature for gross photosynthesis (Topt) (j-l), Q_{10} value of respiration (q10) (m-o), minimum saturation for activation (Sat_act0) (p-r) and minimum saturation for full activation (Sat_act1) (s-u). Resp_main, ExtL, q10, Sat_act0 increased or decreased by 30%, Rub_ratio and Sat_act1 by 20%, and Topt by 5 K. The colored points represent the measured CO_2 exchange rates of different replicates of lichen-dominated biocrusts.

Figure S2.8: Simulated net photosynthesis rate in response to light (a, d, g, j, m, p, s), temperature (b, e, h, k, n, q, t) and water (c, f, i, l, o, r, u) at site T2 by the data-driven model with decreased or increased physiological parameters. These varying physiological parameters are respiration cost of RuBisCO enzyme (Rub_ratio) (a-c), light absorption fraction in cells (ExtL) (d-f), metabolic respiration cost per surface area (Resp_main) (g-i), the optimum temperature for gross photosynthesis (Topt) (j-l), Q_{10} value of respiration (q10) (m-o), minimum saturation for activation

(Sat_act0) (p-r) and minimum saturation for full activation (Sat_act1) (s-u). Resp_main, ExtL, q10, Sat_act0 increased or decreased by 30%, Rub_ratio and Sat_act1 by 20%, and Topt by 5 K. The colored points represent the measured CO_2 exchange rates of different replicates of lichen-dominated biocrusts.

Figure S2.9: Simulated net photosynthesis rate in response to light (a, c, e, g, i, k, m) and temperature (b, d, f, h, j, l, n) at site T3 by the data-driven model with decreased or increased physiological parameters. These varying physiological parameters are respiration cost of RuBisCO enzyme (Rub_ratio) (a-b), light absorption fraction in cells (ExtL) (c-d), metabolic respiration cost

per surface area (Resp_main) (e-f), the optimum temperature for gross photosynthesis (Topt) (g-h), Q_{10} value of respiration (q10) (i-j), minimum saturation for activation (Sat_act0) (k-l) and minimum saturation for full activation (Sat_act1) (m-n). Resp_main, ExtL, q10, Sat_act0 increased or decreased by 30%, Rub_ratio and Sat_act1 by 20%, and Topt by 5 K. The colored points represent the measured CO_2 exchange rates of different replicates of lichen-dominated biocrusts.
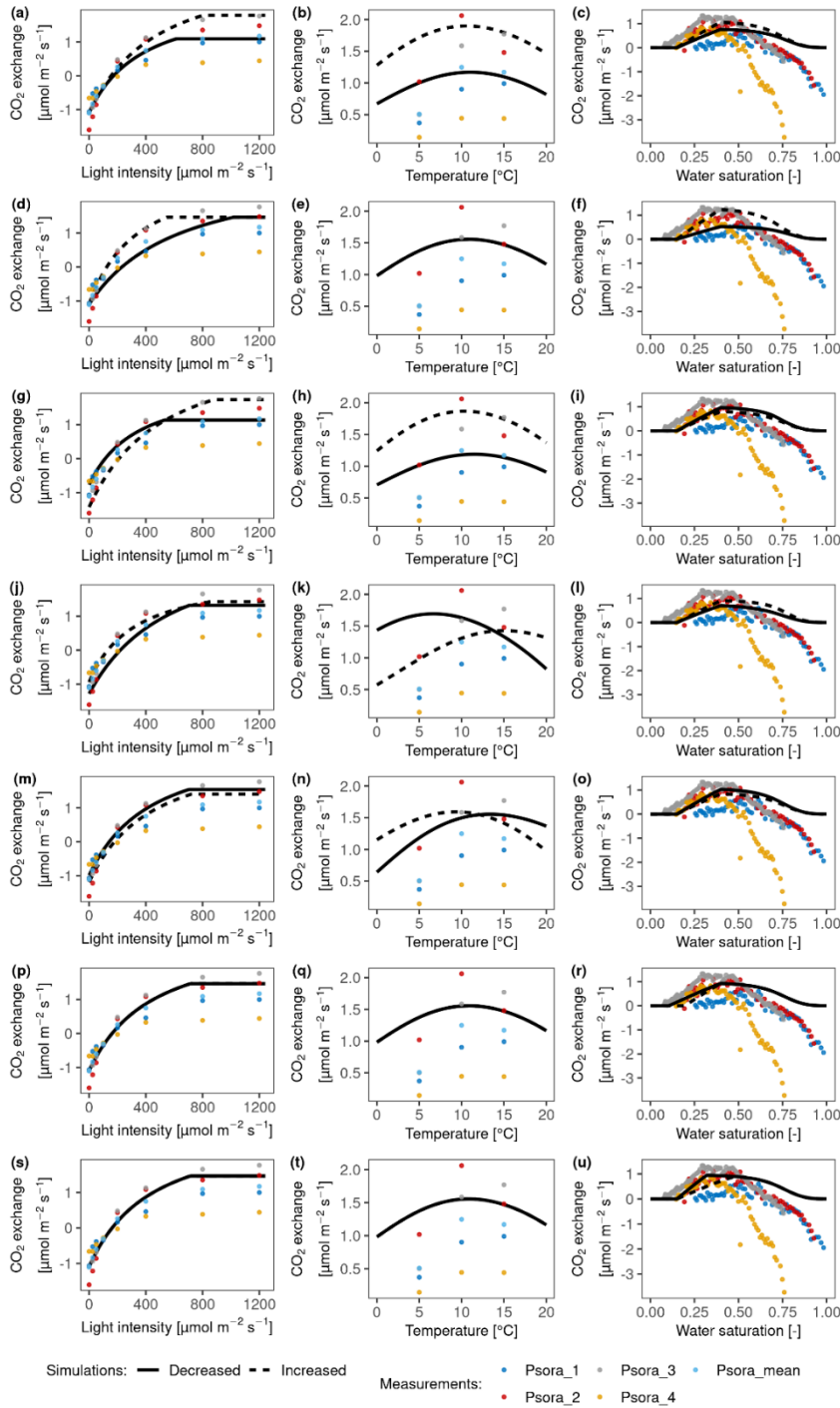
Figure S2.10: Simulated net photosynthesis rate in response to light (a, c, e, g, i, k, m) and temperature (b, d, f, h, j, l, n) at site A1 by the data-driven model with decreased or increased physio-

logical parameters. These varying physiological parameters are respiration cost of RuBisCO enzyme (Rub_ratio) (a-c), light absorption fraction in cells (ExtL) (d-f), metabolic respiration cost per surface area (Resp_main) (g-i), the optimum temperature for gross photosynthesis (Topt) (j-l), Q_{10} value of respiration (q10) (m-o), minimum saturation for activation (Sat_act0) (p-r) and minimum saturation for full activation (Sat_act1) (s-u). Resp_main, ExtL, q10, Sat_act0 increased or decreased by 30%, Rub_ratio and Sat_act1 by 20%, and Topt by 5 K. The colored points represent the measured CO_2 exchange rates of different replicates of lichen-dominated biocrusts.
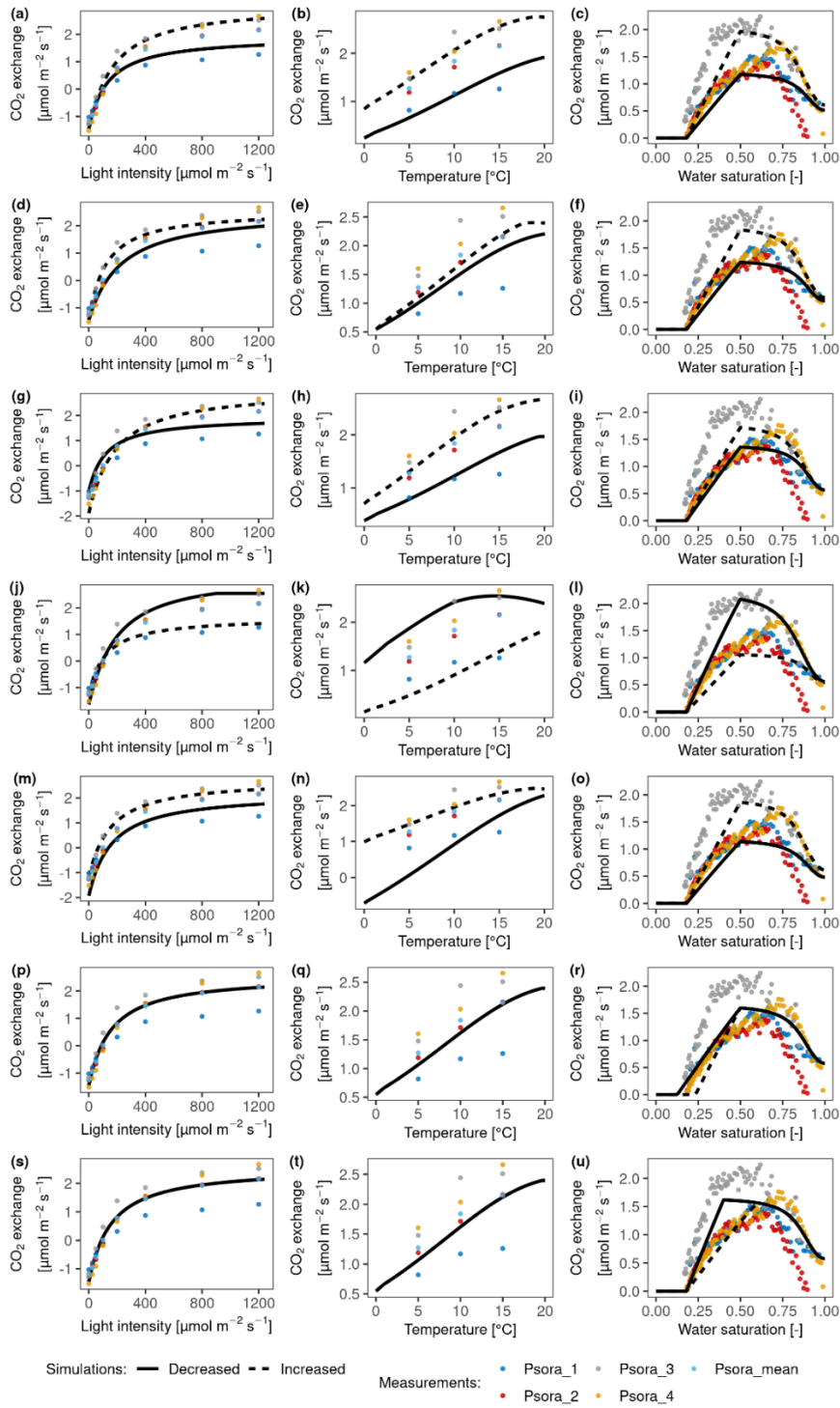

Figure S2.11: The C balance number estimated by the data-driven model without changing the parameters (Original), and with increasing and decreasing physiological parameters at all sites (Increased and Decreased, respectively). The changed parameters are respiration cost of RuBisCO enzyme (Rub_ratio), light absorption fraction in cells (ExtL), metabolic respiration cost per surface area (Resp_main), the optimum temperature for gross photosynthesis (Topt), Q_{10} value of respiration (q10), minimum saturation for activation (Sat_act0) and minimum saturation for full activation (Sat_act1). Resp_main, ExtL, q10, Sat_act0 increased or decreased by 30%, Rub_ratio and Sat_act1 by 20%, and Topt by 5 K.
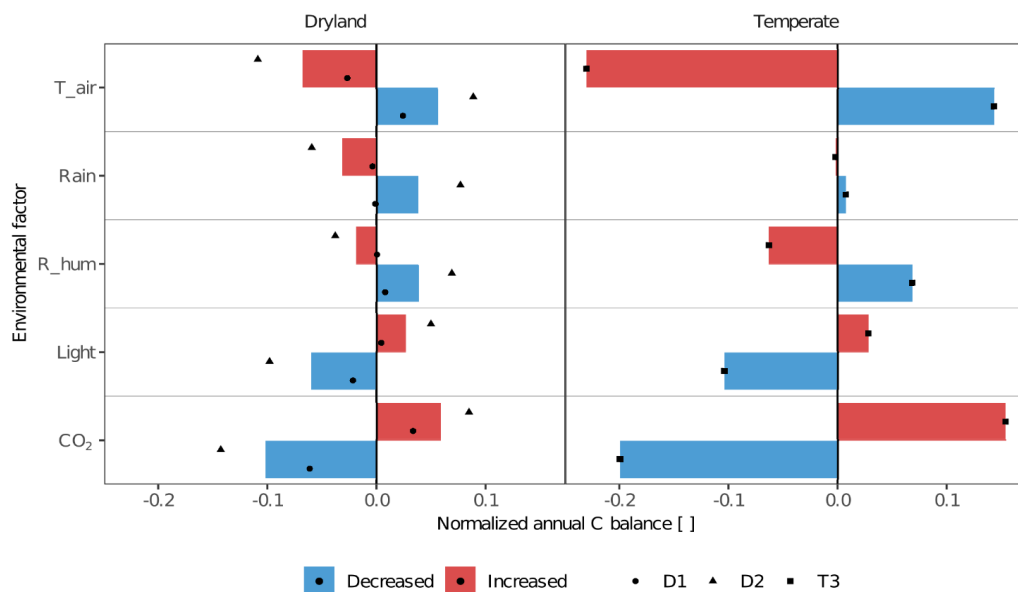
Figure S2.12: The effects of environmental factors - CO_2 concentration (CO_2), relative air humidity (R_hum), rainfall amount (Rain), air temperature (T_air) and light intensity (Light) on the annual C balance of lichen-dominated biocrusts at different sites with reasonable C balance estimates (excluding site T1, T2 and A1 with strongly negative C balance). The altered annual C balance resulting from increasing or decreasing environmental factors is normalized by the C balance under original environmental conditions. The colored columns indicate the average value of the normalized C balance at sites with similar climate conditions. Various styles of black points indicate different sites.
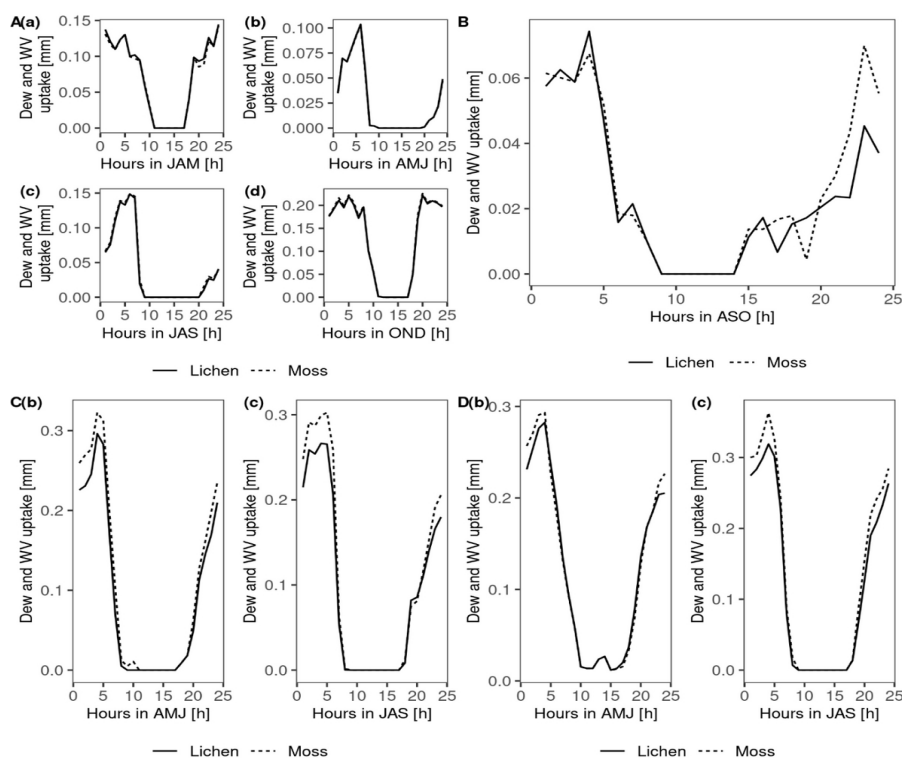
Figure S2.13: Modeled hourly sum of dew and water vapor uptake of lichen- and moss-domi-
nated biocrusts at site D1 (A), T1 (B), T2 (C) and A1 (D) during seasons when an obvious under-
estimation of activity at night and morning can be observed. (a): diurnal pattern during the period
January, February and March (JFM); (b): diurnal pattern during the period April, May and June
(AMJ); (c): diurnal pattern during the period July, August and September (JAS); (d): diurnal pat-
tern during the period October, November and December (OND); ASO represents August, Sep-
tember and October.

6.2   Details about the LiBry model

LiBry model was used to simulate the dynamics of non-vascular vegetation (including
lichens, bryophytes, and cyanobacteria) at various research sites (Porada et al.,
2013, 2014, 2017, 2018; Porada and Giordani, 2021). The LiBry model simulates the
responses of a large number of physiologically and morphologically different
strategies to environmental conditions and select strategies with optimal values for
functional traits, adapting to the predefined climatic conditions. Each strategy is
defined by a unique combination of parameter values and thus represents a group of
functionally identical individuals. The physiological and morphological parameters of
each strategy are photosynthetic capacity, thallus specific area, etc. The value of
each parameter is randomly generated from their respective possible ranges, which
are derived from the literature, with trait combinations subject to biophysical and
physiological constraints/trade-offs (see Porada et al., 2013). At the level of func-
tional properties (traits), several similar strategies together may represent a species,
thereby accounting for intra-specific trait variation.

The model is driven by a time series of climatic forcing data and other abiotic para-
meters describing the habitat, such as disturbance interval, the surface roughness
length, etc. Some of the abiotic parameters can be derived more easily by calibration.
Parameters like roughness length, soil thermal conductivity, or soil heat capacity, for
instance, are calibrated through the fitting of model equations concerning water and
energy fluxes to daily and diurnal patterns of measured surface temperature and
moisture. A large number of strategies with combinations of the different parameter
values are generated by the model before the start of the simulation. Then the car-
bon dynamics of each strategy is calculated based on physiological and biochemical
mechanisms during simulations. For example, an organism gains carbon through
photosynthesis and releases it by respiration. The gross photosynthesis rate is calcu-

lated based on the Farquhar photosynthesis scheme (Farquhar and von Caemmerer, 1982); respiration is temperature-dependent (Q_{10} relationship). Both photosynthesis and respiration depend on the water saturation of the strategy, which is regulated through the input rainfall, snowmelt, dewfall, and evaporation. The evaporation and dew are calculated via the energy balance approach, the negative energy balance leads to condensation at the surface and thus the dewfall. Unlike vascular plants that have stomata, biocrusts are poikilohydric, and cannot actively control water exchange. Uptake (or loss) of water from (or to) the air in the model depends on the net radiation and vapor pressure deficit. The vapor pressure deficit is the difference between saturation water vapor pressure at the surface corrected by water potential inside the biocrust thallus and the atmospheric water vapor pressure which is related to relative humidity.

The C balance then translates into biomass, resulting in growth in cover if this translated biomass is larger than the biomass lost due to tissue turnover, whereas a negative C balance, as well as disturbance, leads to mortality, and thus a shrinkage of the cover. In the end, the strategies that have a positive cover area in the long term survive in the model. In other words, the survival of strategies is determined by their C balance.

The LiBry model ran for 300 years to simulate the dynamics of generated 1000 strategies. The input of such a large number of strategies is to ensure that the combinations of all possible values of all functional traits in research sites are considered for selection by the LiBry model.

6.3 Supplementary analyses

6.3.1 Calibration

Fitting of surface temperature

The abiotic surface properties required by the data-driven model are obtained by fitting the daily and diurnal surface temperature to measurements. The results showed early peaks at site T1, T2, D1 and A1 and underestimation in several seasons. For instance, from January to March at site T2 (Fig. 2.1 (b)). This may result from the measured diurnal patterns of PAR or air temperature at 2 m being inconsistent with the measured surface temperature. We compared the diurnal patterns of the meas-

ured PAR, surface temperature (Measured_Ts) and air temperature at 2 m (Tair), and simulated surface temperature (Simulated_Ts) from January to March and found the different measured climate variables might have uncertainties against each other. For instance, Tair has an earlier increase than Measured_Ts, which is unusual, and also is always lower than Measured_Ts, even at night, which could partly explain the underestimated surface temperature there (Fig. S2.14 (a)). When we shifted the PAR data to 1 hour later, we found that the early peak of simulated surface temperature is corrected (Fig. S2.14 (b)).
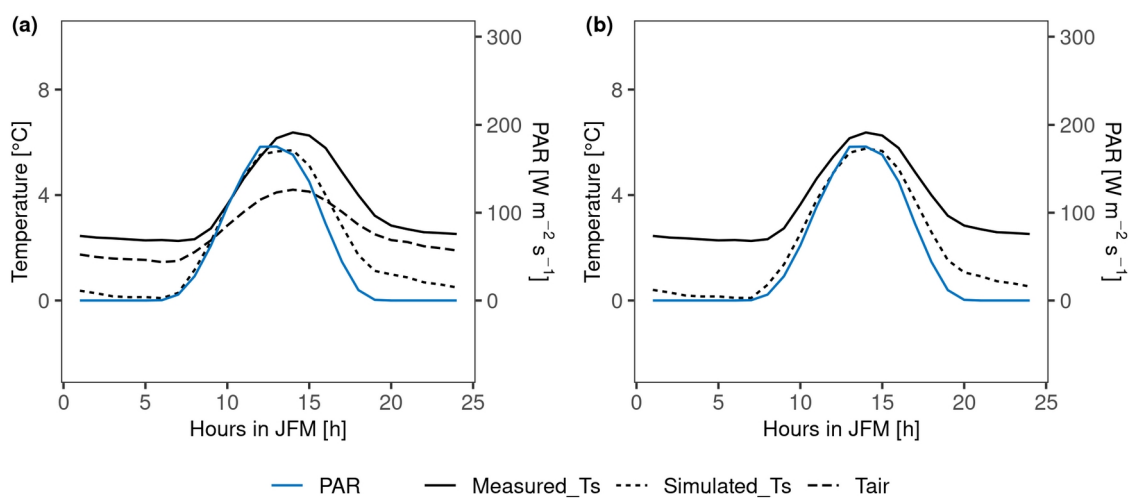
Figure S2.14: The diurnal patterns of PAR, measured surface temperature (Measured_Ts), measured air temperature at 2m (Tair), and simulated surface temperature (Simulated_Ts) from January to March at site T2. (a): The patterns of original measurements and simulation. (b): the patterns of measured variables and simulated surface temperature when PAR was shifted to 1 hour later.

Furthermore, the calibrated boundary parameters such as soil thermal conductivity in the model could affect the diurnal temperature difference, and thus partly lead to the mismatches in diurnal surface temperature patterns, although do not have a strong influence on the timing of the peak in surface temperature. A sensitivity analysis of soil thermal conductivity was conducted at T1 to check whether the bias in calibrated boundary parameters can have a large impact on the carbon balance of biocrusts. The results showed that changing soil thermal conductivity does not prevent a negative carbon balance value in the model (change from -42.8 to -37.1 and to -50.9 g C m-2 yr-1, respectively, for lichen-dominated biocrust when soil thermal conductivity increased or decreased 5 times).

Fitting of photosynthesis response curves

In the calibration of physiological properties, we can, however, only reduce the net photosynthetic rate close to 0 at high water saturation, but it is impossible to fit the strongly negative net C flux there.

The reason are the CO_2 diffusion pathways implemented in our data-driven model. We assume that CO_2 only leaves the thallus through the same route as it enters. Furthermore, we assume that the net flux between the interior of a lichen/bryophyte and the atmosphere has the same magnitude as the flux (respiration minus photosynthesis; see Fig. S2.15). This "steady-state" assumption is similar to vascular vegetation models and is justified by the comparably small internal space for CO_2 storage which prevents long-term (meaning minutes) maintenance of photosynthesis under insufficient influx of CO_2. These assumptions do not allow the simulation of a negative net C flux under the relatively high light of the response curve setup (see also Fig. S2.15 (a)). As the measured response curves show, the net C flux of one sample of lichen-dominated biocrust at high water saturation (Fig. 2.2 (c)) is similar to the dark respiration rate obtained from the light-response curve (Fig. 2.2 (a)), meaning that, for this sample, the flux of CO_2 out of the thallus to the atmosphere at high water saturation is likely similar in magnitude to respiration rate. In this case, the gross photosynthesis rate of the sample is likely approximately zero. But, in the model, the CO_2 concentration inside the thallus needs to be larger than the atmospheric CO_2 (400 ppm) in order to achieve a negative net flux. The relatively high CO_2 concentration together with the ambient light level of 400 µmol m^{-2} s^{-1} in the experimental setup of the water response curve, force the modelled gross photosynthesis rate to markedly exceed zero, and therefore it is impossible to achieve a large negative net C flux with the model.

The only way to simulate a negative net C flux under light is to assume that the largest part of CO_2 leaves the thallus via a different route (Fig. S2.15 (b)). In this case, the small flux of CO_2 from the atmosphere into the thallus at high water saturation and further into the chloroplasts, which leads to little gross photosynthesis, is overcompensated by a much larger respiration flux that directly enters the atmosphere through a different route. However, this is highly uncertain and also a bit questionable for most lichens and bryophytes. It may be possible in a lichen if the or-

ganism has a high amount of fungal biomass located above the photobionts that contain the chloroplasts, but without detailed information on the morphology, this would represent an arbitrary parametrization. Alternatively, we would have to assume that respiration of the sample in Fig. 2.2 (c) is substantially higher than in Fig. 2.2 (a), but this seems arbitrary, too.
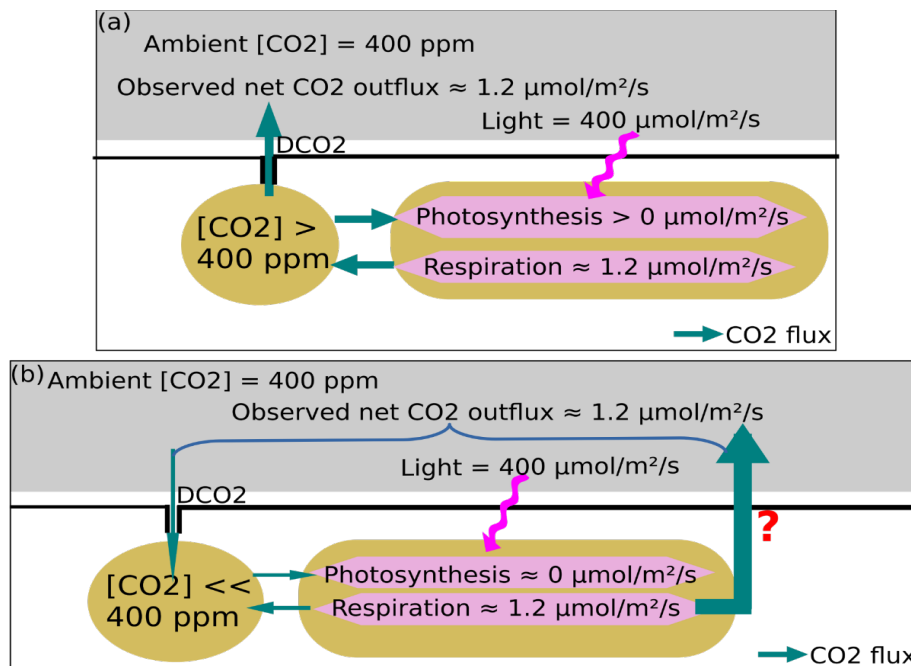
Figure S2.15: The schematic diagram of the CO_2 diffusion pathways. (a): the pathway in the data-driven model, which makes it impossible to fit a strongly negative net C flux. (b): The pathway that allows a simulation of strongly negative net C flux. Please note that the figure only shows CO_2 fluxes. Contrary to vascular plants, CO_2 and water exchange are not coupled in lichens and mosses, due to lack of stomata. The model thus calculates water fluxes independently based on the surface energy balance.

6.3.2 Effect of MWC on C balance

The estimated C balance may be inaccurate due to potential bias in estimated relative water saturation, which partly depends on prescribed MWC, a morphological model parameter that is obtained by measurements. We varied the MWC of lichen-dominated biocrust from site T1 by half (+/- 50%) to examine how important uncertainty in this parameter is for the estimation of the C balance. The outcome revealed that MWC has little effect on C balance (-40.0, -42.8, -44.5 g C m-2 yr-1 for reduced, original and increased MWC). Therefore, the annual carbon estimation is robust to the uncertainties with regard to the prescribed MWC.

Chapter 3 - Quantifying the effect of competition on the functional assembly of bryophyte and lichen communities: A process-based model analysis

Yunyao Ma, Maaike Y. Bader, Imke Petersen, Philipp Porada

Abstract

1. Environmental filtering and competition are two fundamental processes that shape plant community assembly in terms of functional composition, i.e., the distribution of trait values. Understanding the role of these two processes for the assembly of non-vascular vegetation, such as bryophytes and lichens, is important since these communities provide essential ecosystem services in many regions around the world, and these depend on functional composition. Responses of non-vascular communities to environmental selection pressures have been explored in a range of experimental and modelling studies. However, it is still largely unknown to what extent competition affects the distribution of functional traits of non-vascular communities. Moreover, it remains poorly explored which traits that are associated with competition are key for shaping community functional assembly.

2. Here, we integrated a field transplantation experiment with a process-based model to disentangle the effects of environmental filtering and competition on the assembly of non-vascular communities. Following the validation of environmental selection in the model using field observations, we performed a simulation experiment to understand the impacts of competition on trait distributions in non-vascular communities growing in two temperate locations that differ in microclimatic conditions (a shaded and an open location).

3. Our results suggest that the functional composition is likely a result of weak competition or may not depend on competitive exclusion at all while environmental filtering plays an essential role. Plant height seems to be a key trait for competition. However, no single-trait competition scheme could consistently explain the observed functional composition of the studied non-vascular communities.

4. Synthesis: The presented model provides a new trait-based approach for simulating the functional assembly of non-vascular communities. Environmental

filtering appears to be more essential than competition for predicting trait distributions of non-vascular communities under temperate climatic conditions and we recommend caution in associating competition to a single trait while analyzing community functional assembly.

1. Introduction

Communities of bryophytes (mosses, liverworts, hornworts) and lichens widely occur in various habitats around the globe and have a substantial impact on ecosystem functioning such as carbon, nitrogen, and hydrological cycling (Concostrina‐Zubiri et al., 2021; Porada et al., 2018). These vegetation effects are tightly linked to the functional assembly of communities, such as the distribution of functional traits (Conti & Díaz, 2013; Lavorel & Garnier, 2002). For example, the distribution of the maximum water-holding capacity in a lichen and bryophyte community may affect carbon sequestration by these communities, since it will affect community hydrology and thereby the duration of the metabolic activity (Lange et al., 2001). Because of such effects of functional trait distributions, there has been increasing interest in exploring the functional composition of lichen and bryophyte communities. However, the mechanisms of functional assembly leading to particular trait distributions in non-vascular communities are not well understood.

Environmental filtering and competition are two dominant processes in regulating local community structure and functional assembly (Chesson, 2000; Kraft et al., 2015; Soliveres & Eldridge, 2020), and thus may affect distributions of functional traits within communities. Several studies have examined how functional traits of non-vascular vegetation and functional diversity respond to the environment, although much work still needs to be done to fully understand these relationships (e.g., Coyle, 2017; Färber et al., 2014; Gheza et al., 2021; Roos et al., 2019). In contrast, the response of functional assembly to competition is, to our knowledge, addressed only by very few studies (e.g., Maestre et al., 2008; Mälson & Rydin, 2009; Rydin, 1997; Soliveres & Eldridge, 2020).

A better understanding of the role of competition in the functional assembly of non-vascular communities is needed. Observational monitoring of the impacts of competition on any community is challenging as it requires setting up long-term field

experiments that are continuously observed to obtain the final outcome of species interactions. Apart from being laborious, observations alone may be insufficient to separate the role of environmental filtering from biotic interactions without further experiments or modelling (Kraft, Adler, et al., 2015). Therefore, process-based ecological models that integrate both competition and abiotic filtering based on related ecological assumptions and theories have been developed to simulate biodiversity and community dynamics for vascular plant communities (e.g., Chalmandrier et al., 2022). For non-vascular vegetation, Gong et al. (2020) developed a process-based model to simulate the population dynamics of peat moss (Sphagnum) communities. However, this model is not focused on the simulation of functional assembly but on habitat differentiation based on the (fixed) traits of the Sphagnum species involved.

Dynamic global vegetation models (DGVM), as mechanistic numerical models, are commonly driven by climate variables and soil properties to explicitly simulate vegetation dynamics and biogeochemical processes (Maréchaux et al., 2021; Prentice et al., 2007). DGVMs have been advanced for more realistic representation and prediction of functional diversity (Pavlick et al., 2013; Sakschewski et al., 2015; Scheiter et al., 2013; Verheijen et al., 2015). Therefore, DGVMs may serve as an efficient approach to simulate functional community assembly and quantify the role of each potential driving mechanism. However, in this type of model, non-vascular vegetation is usually neglected. Here, we apply a process-based DGVM that is explicitly designed for non-vascular vegetation, called LiBry, to predict the non-vascular community composition with regard to functional traits (Porada et al., 2013). The model mimics natural selection by simulating a large range of different physiological and morphological types (strategies) that are characterized by unique sets of functional traits. The strategies are selected during the simulation based on their responses to multiple environmental drivers and competition processes. This model can therefore not only help to estimate the contribution of these strategies to element fluxes (Porada et al., 2013, 2014) but additionally shed light on the mechanisms that drive the functional diversity and composition of non-vascular communities.

Lichens and bryophytes may compete with each other for light or space for lateral expansion (Rydin, 1997). Both light-competition- and expansion-related processes, such as growth and propagule production, are associated with carbon costs, and a trade-off likely exists between the traits optimizing these processes in a species. Generally, the organisms that are more productive and can allocate more carbon for spreading and horizontal growth are stronger competitors when they compete for space, while those that invest in vertical growth can better compete for light. Competition is thus likely to be associated with multiple traits, which is also proposed by trait-based ecology (Kraft, Godoy, et al., 2015). It is largely unknown, however, which traits are key for predicting competition.

The main objective of this paper is to address the following questions: (i) What role does competition play in the emergence of the functional composition of lichen and bryophyte communities? (ii) Which traits are key for shaping the community functional assembly through competition processes? To answer these questions, we first transplanted samples of lichen and moss species collected at natural open and shaded sites to two open and shaded experimental plots (fully factorial), thereby separating the transplanted samples to prevent competition between them. In this way, the pure impacts of different microclimatic conditions on the physiological responses of the samples could be studied. The outcome of this experiment was used to validate the LiBry model with regard to processes of environmental selection (without competition). Subsequently, we applied the model to assess the effect of competition on community functional assembly. To this end, we varied the intensity of competition processes in LiBry and estimated the effects on the distributions of several functional traits in the simulated lichen and moss communities, namely height, specific thallus area, and maximum water content. We then identified the degree of competition that best matched observations by comparing the simulated trait distributions with those observed at the natural sites. In this way, we could determine the relative roles of competition and environmental filtering on the functional assembly of lichen and moss communities under temperate climatic conditions.

2. Materials and Methods
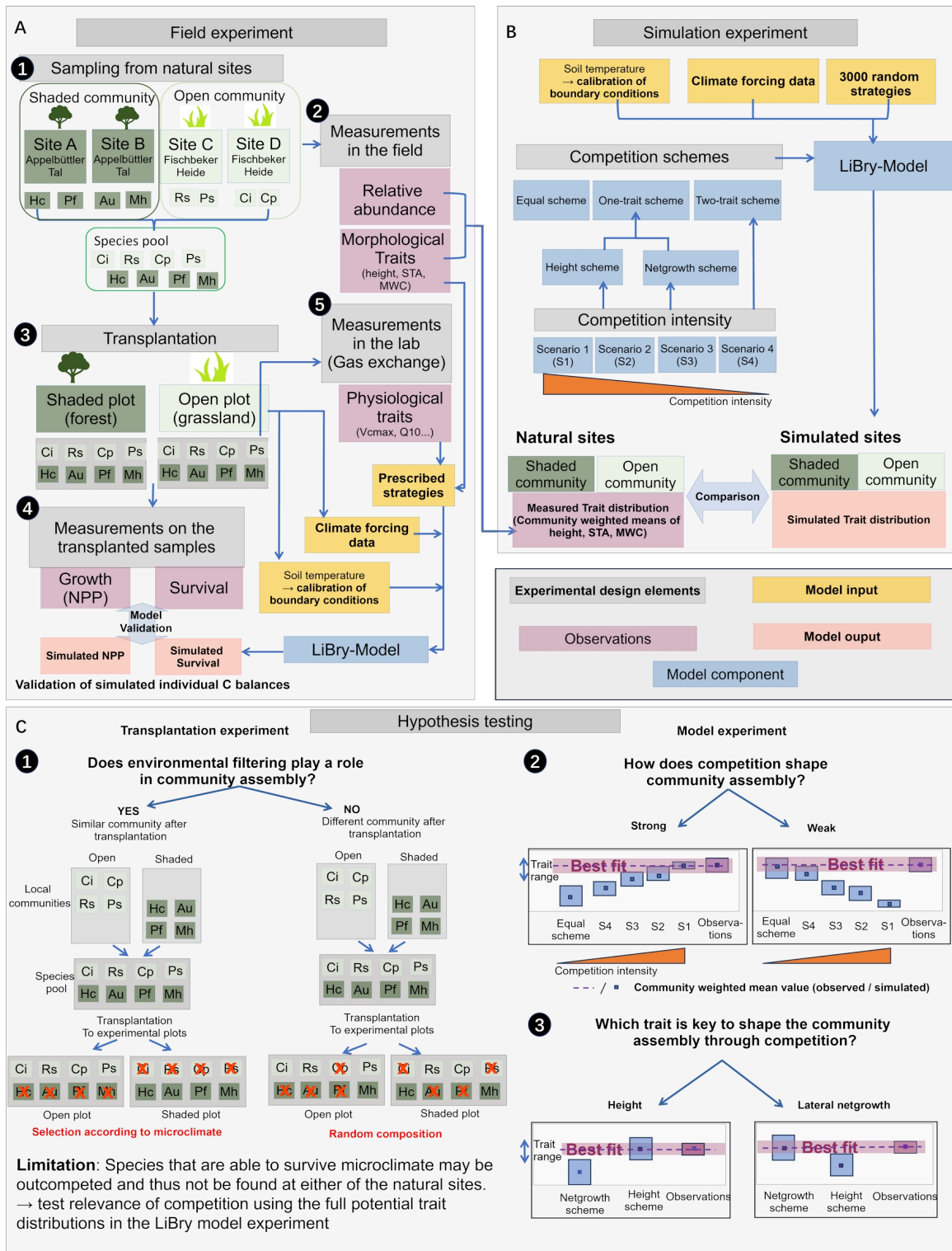
Figure 3.1: Illustration of workflow and hypotheses. (A) Observations from natural sites and a transplantation experiment, combined with laboratory measurements on samples, provide functional-trait data of lichen and moss species *Cladonia portentosa* (Cp), *Atrichum undulatum* (Au),

Campylopus introflexus (Ci), *Hypnum cupressiforme* (Hc), *Mnium hornum* (Mh), *Pleurozium schreberi* (Ps), *Polytrichum formosum* (Pf), and *Rhytidiadelphus squarrosus* (Rs) for model validation and model hypothesis testing. (B) Model experiments provide information on the impact of competition on the functional assembly of lichen and bryophyte communities, based on comparison of simulated and observed functional traits (height, specific thallus area (STA), and maximum water content (MWC)). (C) Potential outcomes of transplantation and model experiments. (1) Transplanting samples of eight species to two experimental plots where competition is excluded, provides insights into the role of environmental filtering for the relative performance of species and thus the assembly of lichen and bryophyte communities. (2) Variation of competition intensities in model simulations and subsequent comparison to measured trait distributions indicates the role of competition for functional assembly. (3) Comparing different trait-based model competition schemes to measurements may point at key competition-related traits for functional assembly.

2.1   Model description

The dynamic global vegetation model LiBry is a process-based mechanistic model designed for non-vascular vegetation, which represents their unique properties such as lack of roots and stomatal control, or variation in activity depending on water status (poikilohydry).

LiBry is driven by a continuous time series of climate-forcing variables, including short- and long-wave radiation, air temperature, wind speed, rainfall, snowfall, and relative air humidity, and parameters describing boundary conditions such as roughness length and soil thermal conductivity.

In contrast to most DGVMs, which simulate a low number of plant functional types (PFTs) via fixed average trait values that are based on a wide spectrum of species, LiBry explicitly simulates large functionally diverse communities based on trait distributions and accounts for processes of community assembly. In LiBry, each simulated location (cell), which may range in size from a local site to a quadratic box in a global grid, is initialized with a large number of "strategies", i.e., functionally distinct types characterized by a unique combination of 11 trait values each, representing all potential "species" of the location. These 11 traits include morphological and physiological traits such as growth height, the optimum temperature for gross photosynthesis, and photosynthetic capacity (Vcmax). The trait values are randomly sampled from their possible observed global range (see Porada et al., 2013) and then selected for (resp. filtered out) by the model based on their

71

carbon balance under the simulated conditions. In previous versions of the model, competition played no role: all species that managed to obtain a positive carbon balance were maintained in the community, albeit with differing abundances. In this study, we introduced competition.

The new model version simulates competitive exclusion of strategies, but not explicitly at a small scale, i.e., between neighbours. Instead, it indirectly simulates competition via the allocation of free area to the strategies in a community, which they need for the establishment and maintenance of their dynamic cover under turnover and disturbance. Competition reduces the available area for each strategy based on the other strategies. In the competition experiments (see Sect. 2.4.2), the allocation of area could be symmetric (i.e., simply proportional to the carbon balance), or modified so that additional competitive traits influenced the allocation further, resulting in asymmetric competition and stronger competitive exclusion. Various trait-based competition schemes were employed to quantify the competition (Fig. 3.1B).

2.1.1 One-trait competition scheme

In the model, we linked the competitive ability (Comp) to height or to the lateral net growth of strategies (the corresponding competition formulations are called the Height scheme and Netgrowth scheme, respectively). We selected these two traits as they are related to different potential competition strategies: Organisms are likely to compete either for light or for space for their lateral expansion.

The competition formulation of the trait-based schemes in the model is related to concepts from competitive hierarchy theory (Chesson, 2020; Silvertown & Dale, 1991), which also applies to non-vascular communities (Mälson & Rydin, 2009). The theory proposes that resource competition among plant species within a community results in a hierarchical distribution: dominant species with superior trait values occupy a higher position in the hierarchy and have strong competitive impacts on species with inferior trait values. For instance, taller species have a higher competitive ability to capture light and are likely to outcompete shorter species. The strategies with the same trait values would coexist since competition is symmetrical and does not lead to the exclusion of either species.

Therefore, we assume that the competitive ability in the model follows a power function of the normalized value of one trait (equation 1; height or lateral net growth), which enables a wide range of relationship shapes between the normalized trait values and competitive ability (Fig. 3.2).

$$Comp(i) = \left(\frac{T(i)}{\sum_{i=1}^{n} T(i)} \right)^{\alpha} \tag{1}$$

where Comp(i) represents the competitive ability of strategy i; n is the total number of living strategies; T is the trait that we assume can determine the vegetation community assembly (height or lateral net growth); the exponent "α" in the equation determines the shape of the relation between normalized trait value and competitive ability.

For a value of α = 0, each strategy has an identical competitive ability of 1, the available area will be equally distributed among all still living strategies. Hence there is no competitive exclusion between strategies since the new cover is not reduced by competitors. The model without competitive exclusion is referred to as "Equal scheme" (Table 2).

2.1.2 Two-trait competition scheme

The competition formulation can be then extended to two trait dimensions to assess the response of community trait composition to the balance of two competition pro-cesses (for vertical and for lateral growth) using a multivariate power distribution (equation S1 in the Supplement). Here, two traits (height and net growth) jointly but independently contribute to the competitive ability.

Additional details on the competition schemes and other model processes can be found in the Sect. S1 of the Supplement and Porada et al. (2013, 2019).

2.2 Field experiment

To provide the necessary data for model validation and hypothesis testing, a field experiment was conducted, and moss and lichen traits were measured (Fig. 3.1A). We sampled eight common species of lichens and mosses in the surroundings of the city of Hamburg, Germany, from four natural sites distributed across two locations that differ in microclimate (open grassland and shaded forest floor) but have similar

soil properties (Table 1). By including a diverse range of species, we aimed to capture the variation in growth strategies and traits that occur under the same macroclimate, covering two contrasting microclimates. The species included were one lichen (*Cladonia portentosa* (Cp)) and seven mosses (*Atrichum undulatum* (Au), *Campylopus introflexus* (Ci), *Hypnum cupressiforme* (Hc), *Mnium hornum* (Mh), *Pleurozium schreberi* (Ps), *Polytrichum formosum* (Pf), and *Rhytidiadelphus squarrosus* (Rs)). Species from different natural sites with similar open or shaded microclimates are regarded as members of the same either open or shaded local community (Table 1). They may not always grow together at each site but are assumed to compete at some point either directly for space or light or indirectly during dispersal and establishment (see Supplement S2 for details).

2.2.1 Measurements in the field

To create reference community-weighted means (CWM) of trait values against which to compare the different competition schemes (see 2.4), we measured two morphological traits on 3 samples per species in these natural sites: the height of green tissue (Height) and specific thallus area (STA, projected surface area per dry weight of samples).

To calculate the CWM from the measured trait values, we calculated the relative abundance of each species at the natural sites (Table 1) by estimating and averaging the fractional cover area of existing species in 48 squares (15cm x 15cm) across three plots (3m x 3m) for each natural site. We then calculated CWMs for all four sites using equation S7 in the Supplement and averaged the CWMs of the two sites within the same community (open or shaded).

2.2.2 Transplantation experiment

To create the necessary data for evaluating if the LiBry model is able to reproduce the individual effect of environmental filtering, five samples of each of the eight selected species were transplanted into each of two experimental plots (open and shaded; more details in Sect. S3 of the Supplement) in the Botanical Garden of the University of Hamburg with similar microclimates as the natural sites. Samples were grown in baskets covering 19.6 cm2, placed on artificial substrates based on quartz sand, and spatially separated to avoid competition among them. We monitored the

survival of samples for two years from September 2020 to August 2022. Furthermore, we collected field data on the change in biomass every half year over the two-year period. The growth data were then converted to net primary production (NPP) based on the area of the baskets in which they were cultivated. These field data were used for validating environmental selection in the LiBry model (see Sect. 2.3).

Table 3.1: Sites of origin of lichen and moss samples used for transplantation experiments and trait measurements. +/- sign indicates the survival/death of the sample one year after transplantation to open and shaded plots.

Location	Natural site	Habitat condition	Sampled species	Abbreviation	Community	Survival in the open plot	Survival in the shaded plot
Appelbüttler Tal	A	shaded	*Hypnum cupressiforme*	Hc		-	+
			Polytrichum formosum	Pf		-	+
			Atrichum undulatum	Au		-	+
Appelbüttler Tal	B	shaded	*Mnium hornum*	Mh	shaded	-	+
Fischbeker Heide	C	open	*Rhytidiadelphus squarrosus*	Rs	open	+	+
			Pleurozium	Ps		+	-

			m schreberi			
			Cladonia portentosa	Cp	+	-
Fischbeker Heide	D	open	*Campylopus introflexus*	Ci	+	-

Gas-exchange measurements were subsequently conducted to determine the physiological traits of the transplanted samples at the experimental plots, which were then used to parameterize the species in the LiBry model for validation of the simulated environmental selection processes (see Sect. 2.3). For these measurements, one subsample from three to four surviving samples for each species (32 in total; see Table 1) was collected after one year of transplantation. Gas exchange was measured under controlled laboratory conditions using a GFS 3000 system (Walz GmbH, Effeltrich, Germany). Net photosynthesis (NP) was measured at various levels of light intensity, CO_2 concentration, temperature, and water saturation to determine light, CO_2, temperature, and water-content response curves (see S5.1 in the Supplement for more details).

2.2.3 Climate forcing data and boundary conditions

For our study, all climate-forcing variables necessary for the LiBry model (see Sect. 2.1) were monitored by weather stations installed on the ground in the grassland and under the canopy next to the experimental plots, with sensors at a standard height of 2 m and an hourly temporal resolution (see further details in Sect. S3 of the Supplement). However, the weather station at the shaded plot was not directly under the tree canopy due to the necessary solar electricity supply. This may have caused an overestimation of shortwave radiation compared to the experimental plot. We thus carried out a sensitivity analysis to assess the impact of potentially overestimated shortwave radiation on the simulated results (details in Sect. S12 of the Supplement).

Moreover, snowfall data were not available for the two experimental plots and were therefore estimated as the average of data from the ERA5 reanalysis dataset (https://www.ecmwf.int/en/forecasts/datasets/reanalysis-datasets/era5) spanning 41 years (from 1979 to 2019) for the region of Hamburg. Additionally, we observed a much lower amount of rainfall at the open experimental plot than under the canopy, which is strange considering the expected rainfall interception by the canopy. We therefore attribute this to a measurement error caused by missing data records and thus corrected this bias (details in Sect. S3 of the Supplement).

The parameters describing boundary conditions (including soil thermal conductivity, soil heat capacity, non-vegetated surface albedo, and roughness length) were not available for the two experimental plots. Therefore, these parameters were calibrated by fitting the measured daily and diurnal patterns of the mean value of monitored soil temperature at different depths (details in Sect. S4 of the Supplement).

2.3   Model validation

In the model validation, we aimed to assess the ability of the LiBry model to reproduce the carbon balance (NPP) and survival of individual samples under two different microclimate conditions without being affected by competition. To this end, the 32 transplanted species subsamples were represented in the model by calibrating simulated NP-response curves against measured curves obtained from gas-exchange measurements and prescribing further morphological parameters (details in Sect. S5 and Table S1 in the Supplement, see also Fig. 3.1A). In addition to these sample-specific parameters, several physiological traits, such as thallus albedo and maximum molar carboxylation rate of Rubisco (VcmaxM), were set to fixed values based on literature (see Table S2; Petersen et al., unpublished data).

We then ran the 32 prescribed samples in LiBry driven by hourly local climate forcing data provided by the weather stations from mid-August 2021 to mid-August 2022 at open (or shaded) experimental plots. We validated the model by comparing the simulated annual and seasonal NPP (summer months from 2022-03-02 to 2022-09-05; winter months from 2021-08-20 to 2022-02-22) as well as the survival of the modelled samples with the measured net growth (i.e., NPP) and survival of transplanted real species at the open and shaded experimental plots.

2.4   Simulation experiment

After validating the environmental selection processes of the model, we explored the impacts of competition on the community assembly of lichen and moss communities by conducting several model simulations using different competition schemes under various scenarios with different competitive intensities (Fig. 3.1B).

2.4.1 Model implementation and setup

The model simulations were each initialized with 3000 strategies that were generated in advance by randomly sampling the distributions of 11 functional traits from ranges based on globally occurring values (see Sect. 2.1 and further details in Sect. S8 of the Supplement). The number of 3000 is usually sufficient to sample the 11-dimensional trait space and ensure consistency of the simulation outcomes (see Sect. S10 in the supplement for details). We did not constrain the ranges of trait values a priori based on the measured values (in contrast to the validation), since we wanted to avoid an arbitrary reduction of potential functional diversity in the model. In reality, species that may survive under the microclimate of one of the natural sites may be outcompeted and thus not be represented in the field samples. If we excluded their trait combinations (=strategies) from the simulation we would artificially improve the fit to observations of modelled trait distributions that correspond to weak or no competition, by making them narrower than they potentially are, and introduce a bias in our interpretation of results.

LiBry was driven by the same input data as the validation run but ran for 600 years to obtain a stable community. We compared the modelled CWMs of all surviving strategies (quantified using equation S7) against measured CWMs of two morphological traits (Height and STA; 24 samples of 8 species) collected in natural sites and one hydrological trait (maximum water content (MWC); 28 samples of 8 species) in experimental plots. MWC is an essential trait affecting the photosynthesis rate of non-vascular vegetation at high water saturation, where it is limited by CO_2 diffusion (Lange et al., 1993). We assume consistency between the distributions of MWC in the experimental plots and natural sites since it is a structural trait that is unlikely to change markedly within months.

2.4.2 Competition scenarios

We performed model simulations under four scenarios (S1 to S4) to test the effect of varying competition intensity between strategies on the trait distribution. To this end, we varied the value of the factor α of the Height and Netgrowth scheme (equation 1; Table 2; Fig. 3.2; Sect. S1). If little area for expansion is available for the strategies, due to a high total cover fraction (csum), for instance, the simulated competition is more selective under S1 than S4. In scenario S4, differences in competitive ability between the strategies are not that large, for most of the possible trait values. In scenario S1, however, most strategies have very low competitive ability, and the few strategies with the highest relative trait value can exclude the others (Fig. 3.2). As a result, competition becomes highly asymmetrical, i.e., from a certain trait value onwards, being taller (or growing faster) gives an over-proportional advantage. Such asymmetry is commonly seen in light competition, for example, since this resource is directional, and taller individuals shade out smaller ones and have a large advantage.

Table 3.2: The shape parameter α of the Equal scheme and the power function of the one-trait competition scheme varies with the total cover fraction occupied by all surviving strategies (csum) in different scenarios. A lower value of α implies a lower competition intensity among strategies.

	Factor α	Competition intensity
Scenario 1 (S1)	5 + csum * 10	High
Scenario 2 (S2)	1 + csum * 5	Intermediate
Scenario 3 (S3)	1	Moderate
Scenario 4 (S4)	0.05 + csum * 0.3	Low
Equal scheme	0	None
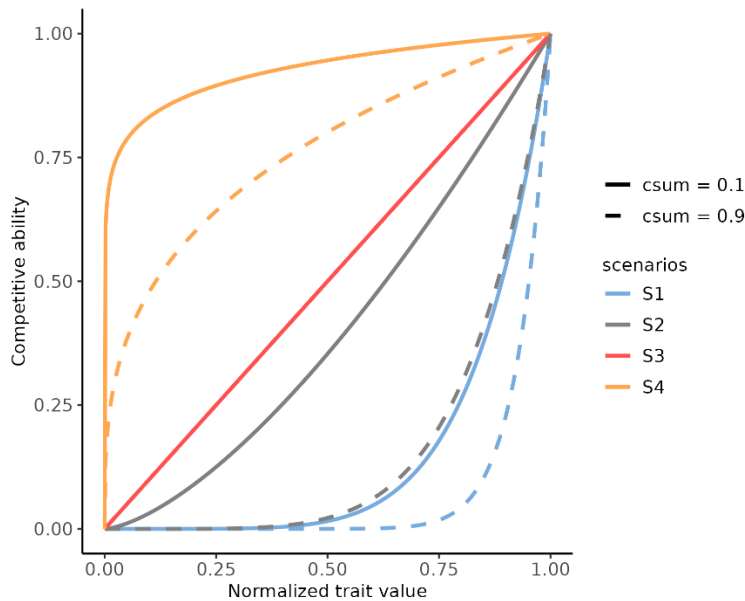
Figure 3.2: Implementation of the concept of the one-trait competition scheme. The relationship between competitive ability and normalized trait value when the available area (1- total cover fraction occupied by all surviving strategies (csum)) is sufficient (csum = 0.1) and limited (csum = 0.9). Different scenarios represent different competitive intensities from high (S1) to low (S4). In the scenario with high competition intensity (S1, S2 at high cover values), most strategies have a similar low competitive ability and only a few strategies with high trait values relevant for selection have a high competitive ability. At low competitive intensities (S4, especially at low cover values) all species have similar competitive abilities with no single one dominating, and hence strong competitive exclusion is not expected.

We subsequently applied these four scenarios to the two-trait competition scheme (see details in Sect. S1 of the Supplement).

Moreover, to test the robustness of the results against different competition functions, we ran the model with the Gaussian function that is commonly applied in theoretical ecology models of species interactions (e.g., Chalmandrier et al., 2022), instead of the power function described above. A detailed description of the Gaussian competition scheme is included in the Sect. S13 of the Supplement.

3. Results

3.1 Model validation
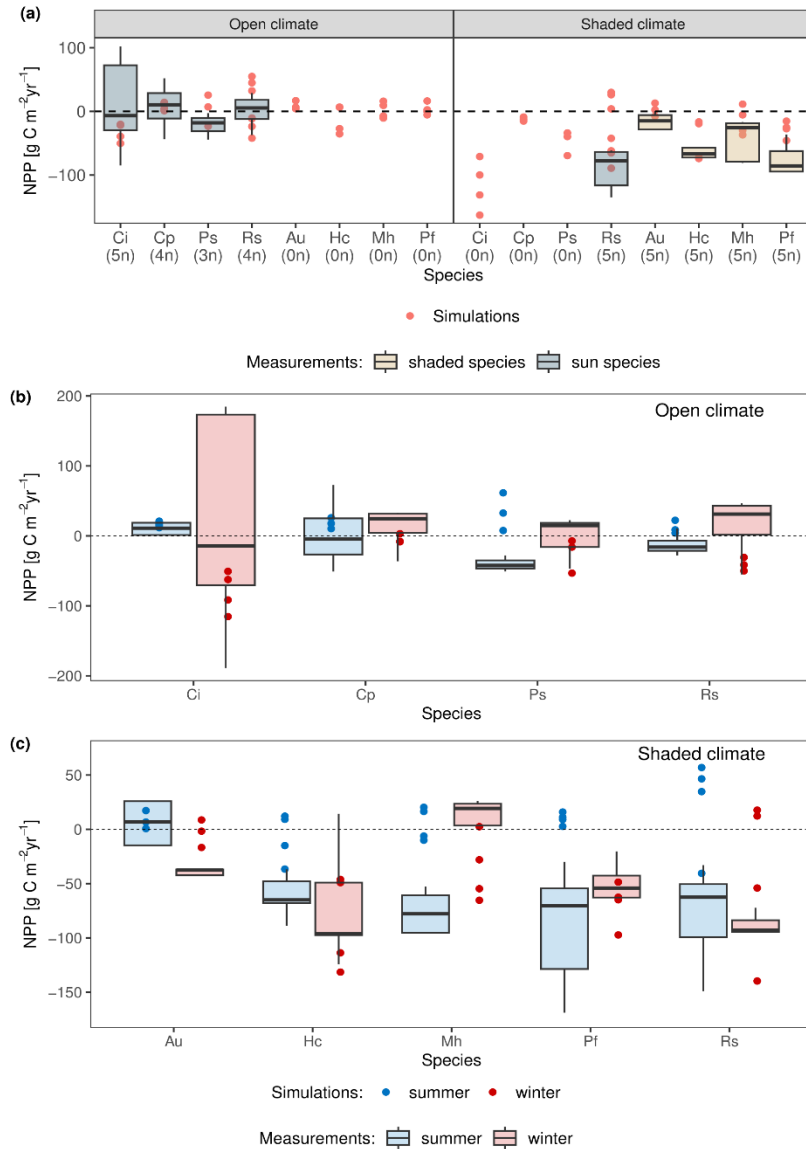
Figure 3.3: Comparison of measured (boxplots) and simulated (dots) annual (a) and seasonal (b and c) net primary production (NPP) of transplanted samples of moss and lichen species collected from open and shaded communities in northern Germany. (a) shows the comparison of the measured (only surviving) to simulated NPP. The numbers in parentheses below the species names represent the number of surviving samples after transplantation for each species. (b) measured and simulated NPP of surviving samples at the open experimental plot in the summer months (2022/03/02 – 2022/09/05) and winter months (2021/08/20 - 2022/02/22). (c) measured and simulated NPP of surviving samples at the shaded experimental plot in the summer and winter months.

Our model could successfully predict the selection of samples by climatic conditions at the shaded experimental plot: only the modelled strategies that were calibrated for samples from the original shaded natural sites could survive (i.e., had a positive NPP) in the model simulation driven by climate from the shaded plot. In the simulation driven by climate data from the open plot, however, not only strategies calibrated for the samples from the original open natural sites survived but also some that fit the shade-adapted samples (Fig. 3.3a). The model predicted death (i.e., a negative annual NPP) for multiple samples that in reality survived for two years, both at the shaded and the open plot (Table 1, Fig. 3.3a). On the other hand, the model also predicted survival of some shade-adapted samples at the open plot that died in reality. To evaluate the simulation accuracy of the model in more depth before testing competition effects, we investigated the seasonal patterns of NPP in addition to the survival (annual NPP), as explained below.

The simulated NPP was notably overestimated for most species in the summer months at the shaded plot (Fig. 3.3c), while NPP was slightly underestimated in winter months at both plots (Fig. 3.3b and 3.3c). The discrepancy in summer at the shaded experimental plot may be attributed to the overestimation of monitored shortwave radiation, as the weather station was not situated entirely under the dense canopy of the samples. We then reduced the shortwave radiation by 90% in the summer months (from the 1st of May to the 5th of September) at the shaded plot to test its impact. The results illustrated a much better match of simulated NPP in summer to measurement at the shaded plot (Fig. S3.7). However, we kept using the measured potentially overestimated shortwave radiation at the shaded plot for further simulations, since this seemed to us a better solution than arbitrarily reducing radiation. We conducted a sensitivity analysis to evaluate the impact of overestimated shortwave radiation on functional composition and found only a small influence on the simulated trait distributions (Fig. S3.11 in the Supplement).

The underestimation of NPP in winter could result from the missing seasonal acclimation of respiration rate in the model (Ma et al., 2023). We thus reduced the physiological parameter reference maintenance respiration rate ($Resp_{main}$) so that it moderated the respiration rate by 70% between September and February (because the simulated samples were collected in September, having acclimated to summer

conditions) to examine its effect. We found that a reduction of $Resp_{main}$ could result in an improved fit of NPP to the measurements during winter, particularly for the open plot (illustrated in Fig. S3.8), which experienced greater variability in terms of radiation and water availability between the winter and summer seasons. However, we did not keep the seasonal acclimated parameter $Resp_{main}$ for the next model experiments, as the relation between the parameter value and seasonal variation in climate is poorly constrained so far due to little research on the topic. A sensitivity analysis revealed that the impact of the seasonally acclimated parameter on the trait distribution is relatively minor (Fig. S3.12 in the Supplement).

3.2 Predicted trait distributions by the one-trait competition scheme.

83
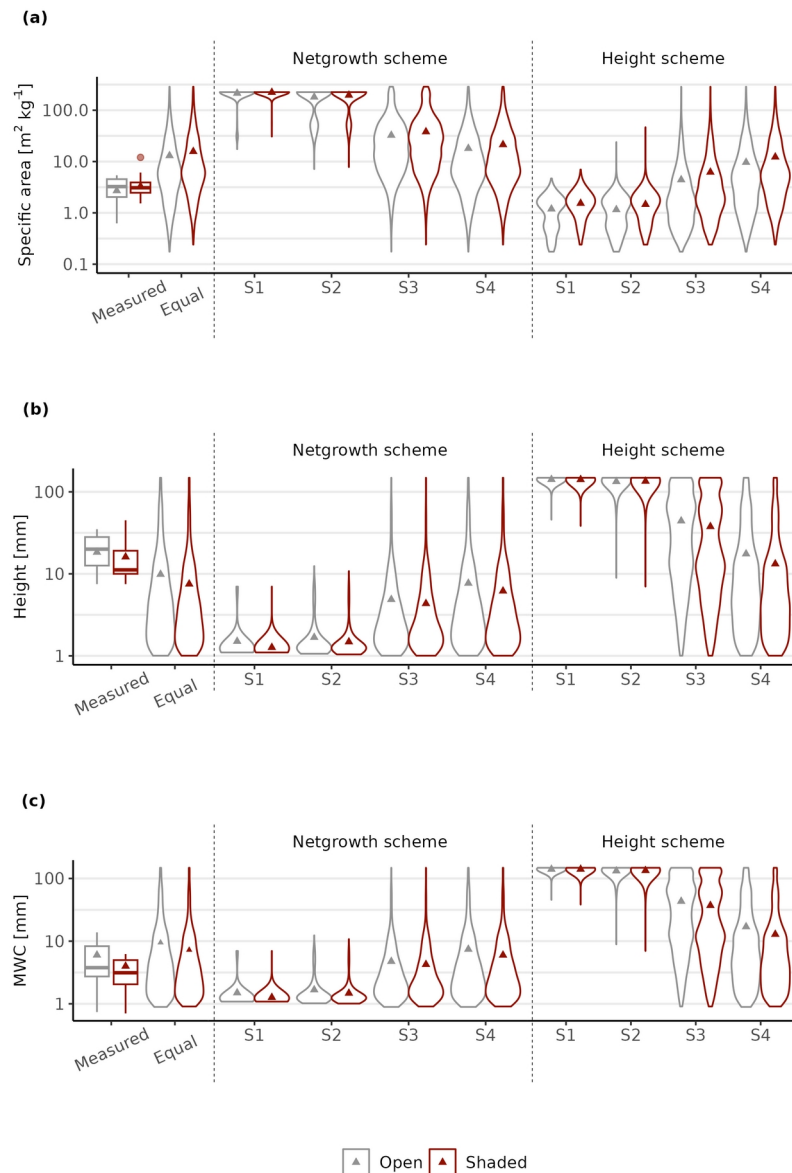
Figure 3.4: Observed and modelled distributions of morphological and hydration traits of the open and shaded communities. a: specific thallus area (STA), b: Height, c: maximum water content. The simulated values are estimated by the LiBry model with a one-trait (Height or Netgrowth) competition scheme with different competitive intensities (S1-S4) or without competition exclusion ("Equal"). The width of violin plots is proportional to the simulated cover fraction of the surviving strategies selected by the model. These strategies are characterized by randomly generated physiological and morphological parameters. Points in the box and violin plots demonstrate the community-weighted mean values of measured shaded and open communities for mosses and lichens, and the simulated community-weighted mean values, respectively.

Modelled competition strongly affected the trait distributions of the communities. The effects were consistent between shaded and open communities despite their different microclimates. The modelled CWM (community-weighted mean value) of the trait Height, specific thallus area (STA), and maximum water content (MWC) were predicted to differ between shaded and open communities by the model without competitive exclusion ("Equal"), with slightly higher values at the shaded community for STA, while lower for Height and MWC. These patterns are consistent with the tendencies of the measured values, although the differences of the measured traits were not statistically significant (p-values of Wilcoxon test > 0.1) and for the modelled distributions they were rather small.

The model overestimated STA in scenarios without competitive exclusion or with strong competition based on net growth, while it underestimated STA in scenarios based on strong height-based competition. The best fit to the data was in the scenario with a linear increase in competitive ability with growth height (Height scheme-S3; Fig. 3.4a). The model underestimated plant Height in the scenario without competitive exclusion and with competition based on net growth, but in the scenarios with relatively strong height-based competition, the model overestimated the Height. The scenario exhibiting the most accurate fit to the measured data entailed competition based on height, with the least degree of intensity (Height scheme-S4, Fig. 3.4b). While the simulations with weak height-based competition performed best for distributions of STA and Height, the model results suggested that weak growth-based competition was most effective for reproducing the distribution of MWC (Netgrowth scheme-S3 and S4, Fig. 3.4c). MWC was overestimated in model simulations without

competitive exclusion and with height-based competition, whereas it was underestimated in simulations with strong net growth-based competition.

To test the robustness of results against uncertainties in climate forcing data, we used macroclimate data for Hamburg to simulate competition effects on the community functional composition and found that the results remained consistent (more details in Supplement Sect. S14 and Fig. S3.17).

3.3 Predicted trait distributions by the two-trait competition scheme.
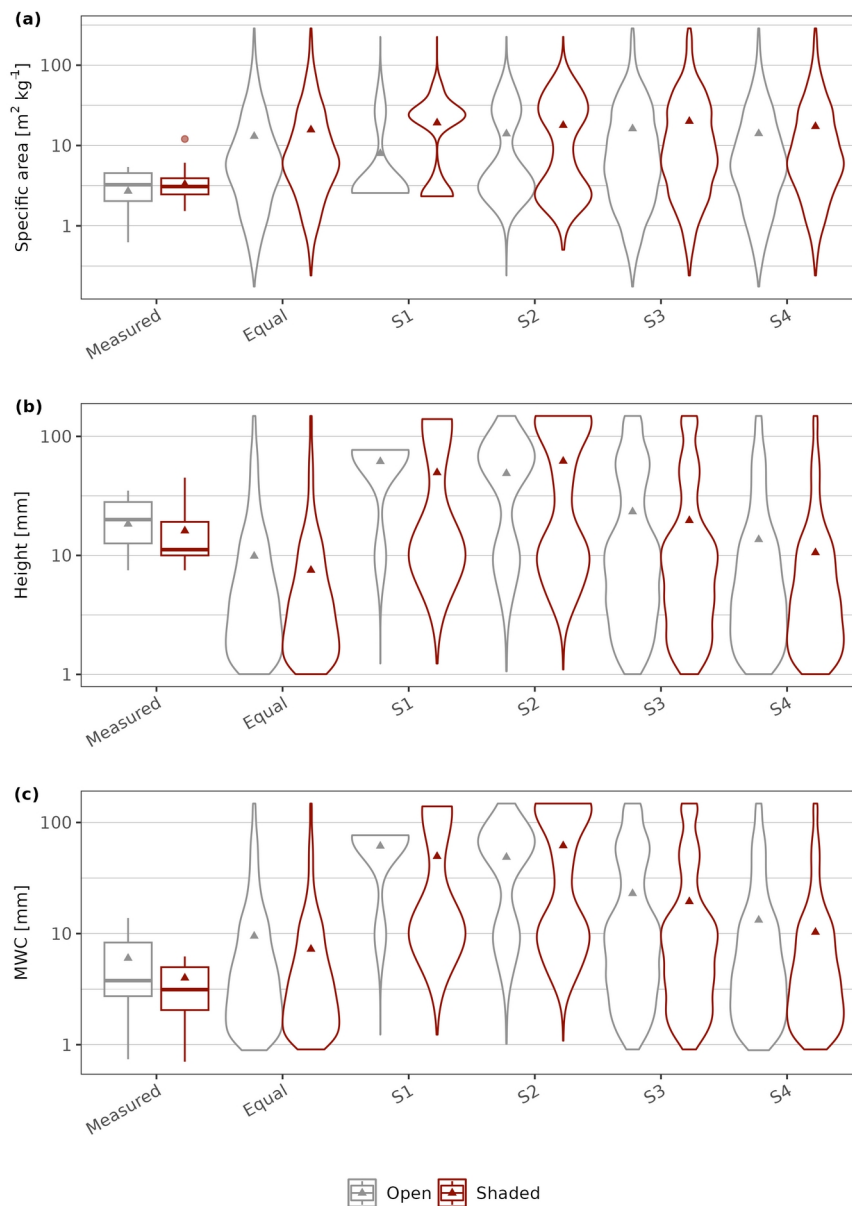
Figure 3.5: Observed and modelled distributions of morphological and hydration traits of the open and shaded communities. a: specific thallus area (STA), b: Height, c: maximum water content. The simulated values are estimated by the LiBry model with a two-trait competition scheme

with different competitive intensities (S1-S4) or without competitive exclusion ("Equal"). The width of violin plots is proportional to the simulated cover fraction of surviving strategies selected by the model. These strategies are characterized by randomly generated physiological and morphological parameters. Points in the box and violin plots demonstrate the community-weighted mean values of measured shaded and open communities for mosses and lichens, and the simulated community weighted mean values, respectively.

The simulated trait distributions with competition based on both height and net growth showed much less variation between competition intensities (Fig. 3.5) than the one-trait-based competition. While the Height distribution could be well reproduced by the model with a linear increase in competitive ability with both traits (S3, Fig. 3.5b), STA and MWC were overestimated by the model with all two-trait competition schemes (Fig. 3.5a, 3.5c), with the overestimation getting stronger with stronger competition.

The results of trait distributions estimated by the model using the Gaussian function, both with one and two-trait competition schemes, delivered identical conclusions, namely that the model with the weak competition resulted in a better match of the simulated functional trait distributions to the measured data (see Fig. S3.14 and S3.16 in the Supplement).

4. Discussion

Understanding community functional assembly (represented by trait distributions) is critical to predict ecosystem functions (Díaz & Cabido, 2001). However, the mechanisms of functional assembly within non-vascular communities are not well understood, especially the role of competition. Our results suggested that environmental filtering has a strong influence on the survival of real species and also affects their trait distributions, while competition may play only a minor role in the assembly of the studied lichen and moss communities and the distribution of traits in the community.

4.1 Effect of environment and competition on community assembly

The important role of environmental filtering is illustrated by the differential survival of species in the two experimental plots, with species from natural shaded sites surviving only in the shaded experimental plot and species from open sites surviving only in the open plot, with just one exception also surviving in the shaded plot. The

survival of the sampled moss species after transplantation to plots with a different substrate, but climatic conditions similar to those of their natural sites, suggests a minor impact of the substrate on moss community composition, consistent with the findings of Spencer (2001). Nevertheless, the physical and chemical properties of the substrate can clearly affect non-vascular community composition, which has been shown, for instance, for soil pH value (Spencer, 2001; Zraik et al., 2018).

In contrast to these results, the model predicted the survival of several shade-adapted samples under the open conditions (Fig. 3.3a). This may result from missing processes in the model regarding potential negative effects of frequent dry-wet cycles at the open plot on shade-adapted species (Hu et al., 2016). On the other hand, the model simulated the death of several shade/sun-adapted samples at their corresponding plots, which may be attributed to potentially suboptimal climatic conditions in the year of the climate time series used to drive the model (August 2021 to August 2022) while conditions were probably more optimal when the transplantation took place (September 2020 to August 2021).

Even though the transplantation experiment supports the important role of environmental filtering, an important role of competition in the assembly of lichen and moss communities cannot be ruled out. Next to dispersal limitation, competition may explain the absence of species at natural sites where they would be physiologically able to survive based on the microclimate but are outcompeted and thus not found in nature. The LiBry model, as a complementary tool, can be used to test the hypothetical "species" that may be able to survive in a particular microclimate and explore the reasons that it is not found, including additional physiological constraints, time constraints (disturbance), dispersal limitation and competition.

Our model results demonstrate that tendential differences in trait distributions between the two communities with different microclimatic conditions (shaded and open community) could be captured by similar tendencies in the model without competitive exclusion (Fig. 3.4), which indicates that the trait difference tendency between shaded and open community results to a large part from environmental filtering. It would be interesting to test this finding for other traits that may respond more strongly to the light environment, like the chlorophyll content (Kershaw & Webber, 1986).

Moreover, our results found that the observed traits in the studied temperate-zone communities were best reproduced by the model with no competitive exclusion or weak competition, i.e., with minor differences in the competitive strengths of the species. In the very few studies of the impact of competition on non-vascular community structure in temperate regions, competition seems to play a minor role (During & Tooren, 1990), consistent with our results. The number of surviving strategies simulated in our study (as detailed in Table S4 of the Supplement) is generally higher than the number of species or samples from the sites or plots. This is due to the concept of a "strategy", which represents a sample from an 11-dimensional trait space and does not directly correspond to an "average" species, but rather includes variation between as well as within species. Since we used 3000 strategies to sufficiently sample the potential trait space, the CWM computed from the surviving strategies is representative. For the real samples, however, 24 samples (including within- and between-species variation in 8 species) should be sufficient to estimate the CWM, since the real populations are already the outcome of a process of natural selection. Thus, we do not need to consider all hypothetical trait combinations in this case. The trait distributions derived from the model simulations should be broader than the distributions found in real species in a particular location (Fig. 3.4-S2, S3, S4, Equal) since only a subset of possible trait combinations will actually have evolved and only a subset of these will be available at a particular location. In theory, it would be possible to compare the simulated and observed trait distributions in more detail, but hundreds to thousands of samples would have to be collected from natural populations at large spatial scales to capture the tails of their distributions, which is why we focus on the CWM comparison.

In fact, it has been suggested that in interactions among bryophytes, facilitation may play a more important role than competition. A shift from competitive to facilitative interactions is expected with increasing abiotic stress (Maestre et al., 2009; Sun et al., 2021), with the type of stress playing an important role. For example, for bryophytes, low-light stress would result in competition, while desiccation stress may lead to facilitation since dense communities can hold their water longer than single shoots through larger capillary space of surface (Dilks & Proctor, 1979; Rice, 2012). If there is a balance of competitive and facilitative interactions, this may result in a

weak net effect in either direction. This may provide a potential explanation for the modelling result that no or weak competitive exclusion best explains observed trait distributions. While facilitative interactions are not explicitly included in the model, some positive community-level effects are represented by parameterized ecophysiological relations of the strategies, such as the decreasing effect of height on evaporation (Di Nuzzo et al., 2022), which only becomes effective when growing in a cushion. Several studies have found that facilitation arises frequently between associated lichens and bryophytes (Colesie et al., 2012), and when interacting species acquire resources in complementary ways (Bowker et al., 2010). Accordingly, future studies are necessary to distinguish between the role of competition and facilitation in lichen and moss community assembly, both experimentally and using models like LiBry.

4.2   Key traits for community assembly via competition processes

Our study considered two traits as factors determining competition, namely growth height and lateral growth. We found that height may be slightly more suitable than net growth at predicting distributions of morphological traits via competition, although no single trait was consistently better than the other in shaping the distributions of all traits. Thus, our results suggest being cautious to use solely a single trait to describe competition processes and infer community functional assembly.

Rather, competition is likely to be affected by the combination of multiple traits. Several studies have shown that multiple traits interact to generate a plant community composition different from that based on a single trait (Doebeli & Ispolatov, 2010; Falster et al., 2017). Thus, extending the analysis to have multiple traits alter the modelled competitive outcome is an area worthy of future study. As a step towards a multi-trait perspective, we applied a two-traits competition scheme to assess how the balance of the two competitive processes, namely vertical and lateral growth, affected the trait distribution in lichen and moss communities. Our results showed that in the scenarios with strong competition, the two-trait scheme, which assigned equal weight to trait height and net growth in determining competitive ability, reduced the extreme estimations of trait distributions of the one-trait schemes. This could be due to the trade-off between the two traits associated with carbon allocation to either vertical or lateral growth processes. Further traits and trait combinations that

present no direct trade-offs may also be involved in determining competitive strength (e.g., growth height and nitrogen use efficiency).

4.3 Limitations and Future Perspectives

We provide the first results on the role of competition for trait distributions and functional composition of non-vascular vegetation. More studies on similar communities in temperate regions are needed to confirm our findings, while their generality needs to be tested across other habitat types and climate zones. Currently, we cannot assess the role of competition in the functional assembly of non-vascular communities across environmental gradients due to the limited availability of measurements of trait distributions in other climatic regions. Applying the LiBry model in other ecosystems across different environmental gradients is thus a possibility for further research on the effects of competition on community functional assembly.

Additionally, we assessed the distributions of only three traits and the measured trait values represent a snapshot in time. Other traits may respond more strongly to competition, and larger temporal heterogeneity in measurements may change the coexistence of species and the community trait distribution (Usinowicz et al., 2017). This may partly explain the fact that not all shade- and sun-adapted samples are predicted to survive under the corresponding shaded and open experimental plots in the model validation. Therefore, more long-term empirical studies on other trait distributions and competition among non-vascular species in a wide variety of communities in various climatic zones are needed to evaluate the generality of our results.

We defined the competitive ability by height and lateral net growth. Nevertheless, there may be other relevant traits associated with competition that affect functional assembly, such as the chlorophyll content. Species with higher chlorophyll content may be more efficient in absorbing and utilizing light to maximize the photosynthetic rates (Kershaw & Webber, 1986), enabling them to outcompete neighbors for light resources. Furthermore, the assumed functions describing the relationship between trait and competitive ability affect the results on the role of competition. The tested Power and Gaussian functions produced highly similar results, indicating that our finding of weak competition in shaping functional assembly is robust. Nevertheless, the function may not necessarily be a Power or Gaussian function. Falster et al.

(2021) found mismatches between the shape of the competition relationship that emerged from the theoretical function and the shape that emerged from a mechanistic model that linked traits to competition based on a species' ability to consume resources. To avoid uncertainty in modelling the trait distributions depending on theoretical functions and abstract concepts of competition, future developments could focus on simulating the competition among strategies in an explicit mechanistic way. For instance, the taller strategies reduce the light for smaller strategies and thus affect the carbon gain of smaller strategies, while smaller strategies with more lateral growth occupy more space and thus may prevent the establishment of other species. Although we determined the competitiveness of each strategy based on a comparison with all other strategy traits in our competition scheme, we do not take into account how one competitor modifies the interaction between other competitors in the community, e.g., growing wide may be competitively advantageous only in the absence of tall species overshadowing all smaller species. Thus, the high-order interactions perspective on the competitive outcome warrants further investigation, as consideration of multi-species interactions may lead to different competitive outcomes (Kleinhesselink et al., 2022).

5. Conclusions

This is one of the few studies to investigate the role of competition in the functional assembly of non-vascular communities. By combining a transplantation experiment of non-vascular communities in two types of microclimates with the mechanistic model LiBry, we showed the important role of environmental filtering in shaping community assembly. Competition based on height or lateral growth strongly affected trait distributions in the model simulations, but the observed trait distributions were best explained by model configurations corresponding to weak or no competitive exclusion, which indicates a minor role of competition in community functional assembly. Our study emphasizes the need to consider a high-dimensional trait space that affects non-vascular community assembly via competition processes since we found that using only one or two traits to represent competition could not predict the functional composition with high accuracy.

In community ecology, functional traits have been used mainly to describe plant strategies and ecosystem functions, and to assess community assembly based on

empirical approaches. Our study applied the process-based LiBry model to explicitly simulate assembly processes from a biochemical perspective and models directly local functional trait distributions. As a process-based approach driven only by climate data and other environmental boundary conditions, it is designed to be more transferable than statistical models. As a result, models such as LiBry might be appropriate for generating estimates outside of the study site and projections for the future (Higgins et al., 2020). By further developing the competition processes in the model, process-based growth models may open a new general way to represent and quantify the relative role of different community assembly processes in shaping non-vascular communities and they may enhance our understanding of the community functional structure and dynamics under climate change.

Acknowledgements

6. Supporting information

S1 Detailed description of LiBry model and competition scheme

S2 Coexistence of collected species within a community

S3 Detailed description of weather stations and observed climate data

S4 Boundary condition calibration results and analysis

S5 Detailed description of model parametrization

> **S5.1 Calibration of sample-specific physiological properties**

> **S5.2 Fixed physiological parameters**

S6 Validation results and analysis

S7 Community weighted mean value

S8 Traits allowed to vary randomly in the model simulations

S9 Number of surviving strategies in model simulations

S10 Sensitivity analysis of different input strategies

S11 Sensitivity analysis of disturbance parameter

S12 Sensitivity analysis of adjusted shortwave radiation and physiological parameter

S1 Detailed description of LiBry model and competition scheme

A simulated non-vascular community (open or shaded) is located on a cell, in which a large range of strategies were initialized with a set of randomly generated trait values. These strategies are not explicitly put as shapes or volumes onto a given area. Instead, each strategy has a certain (dynamic) share on the total cover per unit area. The dynamic water, energy, and carbon fluxes as well as the fractional cover of each strategy are simulated per this unit area based on its responses to the input climatic conditions of the cell, which are regulated by trade-offs in biophysical, physiological, and ecological processes.

Specifically, the photosynthesis rate in the model is calculated based on the Farquhar scheme (Farquhar & Von Caemmerer, 1982) and respiration is modelled based on temperature following a Q_{10} relationship. Net primary productivity (NPP) is calculated as the difference between photosynthesis and respiration and, together with losses from tissue turnover, drives biomass dynamics and thus lateral growth.

Positive changes in biomass result in increased fractional cover of a strategy. However, as the total cover fraction occupied by all living strategies (csum) increases, the available area (1-csum) becomes insufficient for their potential expansion, and the available space for expansion is constrained by competition with other strategies, which is determined by various trait-based competition schemes that linked the competitive ability to various functional traits (height and lateral net growth). Growth height is a fixed trait of a strategy positively related to the amount of captured light for photosynthesis, whereas lateral net growth is an emerging trait that depends both on other traits and on climate. Both traits are positively related to competitive ability. These two traits form a trade-off in the model due to the mass balance constraints, wherein strategies face a trade-off between allocating carbon to vertical growth to gain access to light or to lateral growth to compete for space.

Negative biomass changes and disturbance cause a decrease in the fractional cover of a strategy. Disturbance (e.g., wildfire, windthrow) is an essential process shaping community structure (Mouillot et al., 2013). In LiBry, we account for this effect by

defining a disturbance rate each year based on the literature (Porada et al., 2013) that applies equally to all strategies, meaning that their shares on the total cover are reduced proportionally to their cover fractions. In this way, the new available area for expansion and establishment is generated, which also affects competition intensity in the model. Competition increases generally with decreasing free area, i.e., at a low disturbance rate. Furthermore, a sensitivity analysis was conducted to examine the role of the prescribed disturbance rate in shaping the community functional composition (see Sect. S11 and Fig. S3.10).

The strategies that maintain a positive fractional cover area in the long term during the simulation are identified as survivors and constitute the predicted community. Thereby, the model is able to simulate functional diversity patterns and trait distributions of local communities and also has the potential to provide global-scale estimates, by simulating the patterns across a large number of grid cells, driven by time series of maps of global weather patterns. For a more detailed description of the process representation, please refer to studies by Porada et al. (2013, 2019).

Competition scenarios

Various scenarios with different levels of competition intensity can be studied by setting the α value in the competition formations, i.e., setting a starting value or function of change with the trait values (Table 2). A value of α of 0 indicates the Equal scheme where there is no competitive exclusion between strategies. In simulations with a competition process (i.e., where α>0), α will increase with the total cover fraction occupied by all living strategies (csum), which indicates that as the available area (1-csum) becomes less, the competition becomes more intense, but to varying degrees, depending on the scheme and scenario chosen for α (Table 2; Fig. 3.2).

Two-trait competition scheme

The competition formulation of two-trait competition scheme uses a multivariate power distribution (Eq. S1).

$$Comp(i) = \left(\frac{T_1(i)}{\sum_{i=1}^{n} T_1(i)} \right)^{\alpha 1} * \left(\frac{T_2(i)}{\sum_{i=1}^{n} T_2(i)} \right)^{\alpha 2} \qquad \text{Eq. S1}$$

where T1(i) and T2(i) are the traits, height and net growth, of strategy i. Factor α1 and α2 in the equation determine the shape of the power distribution of each trait (see the one-trait scheme).

For feasibility, α1 and α2 are assumed to be equal to each other. We ran the model in four scenarios under different competitive intensities, the same as in the one-trait scheme (Table 2). Having lower values of both α1 and α2 implies a lower competition intensity among strategies while fewer strategies are likely to be competitively excluded, and vice versa. The relationship between competitive ability and normalized trait value varies with csum and different scenarios are shown in Fig. S3.1.
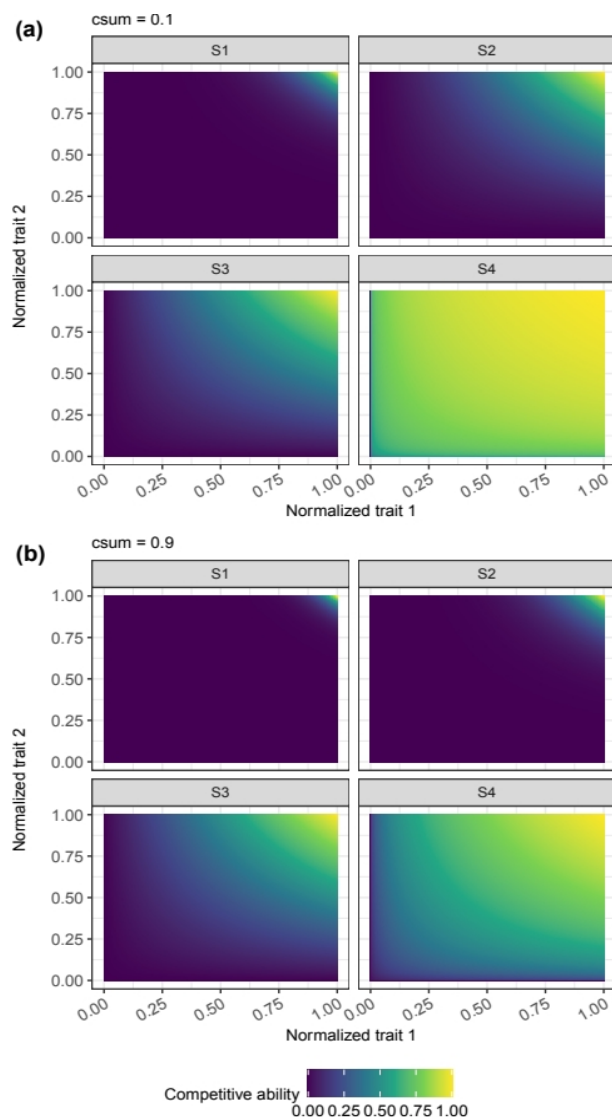
Figure S3.1: Implementation of the concept of the two-trait competition scheme, which demonstrates the competitive ability changing with two traits (normalized). (S1) - (S4) demonstrate four scenarios where the competitive intensities change from high to low by varying

the values of factor α1 and α2 of the two-trait competition scheme at the condition that the total cover fraction area occupied by all surviving strategies (csum) is low (a, 0.1) and high (b, 0.9).

S2 Coexistence of collected species within a community

The species that we collected at different natural sites in either a shaded or an open location are assumed to be part of the same shaded (or open) community, even though we did not observe the co-occurrence of all species at one shaded or open site. We make this assumption due to spatial proximity and similar environmental conditions (climate, substrate, etc.). The absence of observed co-occurrence at a particular site may be attributed to various factors, such as the small size of the sampling sites, and collection only at one point in time, for instance. The species *Pleurozium schreberi* (Ps) and *Rhytidiadelphus squarrosus* (Rs) have been documented to occur in heathlands in north-east Scotland (Welch, 1984), which indicates that their favoured habitats are similar to the habitat where we observed *Campylopus introflexus* (Ci) and *Cladonia portentosa* (Cp). Furthermore, we noted the co-occurrence of *Polytrichum formosum* (Pf) with *Mnium hornum* (Mh) or *Atrichum undulatum* (Au) during our observations in the field close to the shaded sampling site (Fig. S3.2).

Figure S3.2: Coexistence of *Polytrichum formosum* (Pf) with *Atrichum undulatum* (Au) (left) and *Mnium hornum* (Mh) (right).

S3 Detailed description of weather stations and observed climate data

We transplanted samples into two experimental plots. The open experimental plot is in a grassland while the shaded plot is situated beneath a beech tree canopy *(Fagus sylvatica).* The weather stations installed next to these two experimental plots monitored the net short- and long-wavelength radiation using the SN500SS Apogee four-component net radiometer; the wind speed was measured by a WindSonic4 gill ultra-sonic anemometer at 2 m; The relative humidity and air temperature at 2 m were recorded by HygroVUE10 Temperature and Relative Humidity Sensor while rainfall was

measured automatically by an unheated Campbell Scientific tipping bucket raingauge. Furthermore, soil temperatures at different depths (0.0, 6.5, 13.0, 20.0, 40.0, 65.0 cm) were measured by a Campbell Scientific CS230 temperature profiler. These climate data were monitored at an hourly resolution.

The weather station at the open and shaded experimental plots showed that air temperature at the open plot is a little higher particularly in summer months (averaging 18.2 °C from June to August) than at the shaded plot (averaging 17.5°C from June to August). The daily patterns of air temperature in the two plots are shown in Fig. S3.3(a). Moreover, the daily mean short wavelength radiation at the open plot was markedly higher than at the shaded plot, which was situated beneath the canopy. There were only a few days in winter when the beech tree was without leaves, that showed relatively high radiation at the shaded plot. Notably, the daily radiation at the shaded plot decreased dramatically from May onward, owing to the dense canopy formed by the growth of tree leaves (the daily course of the short wavelength radiation at two plots is shown in S3(b)). Relative humidity was slightly higher at the shaded plot (daily minimum mean value is 66% and 61% at shaded and open plots, respectively), whereas the annual rainfall reaching the ground at the shaded plot, measured manually every two weeks with rain gauges that were placed close to the samples, was lower (597 mm) than that at the open plot (721 mm).
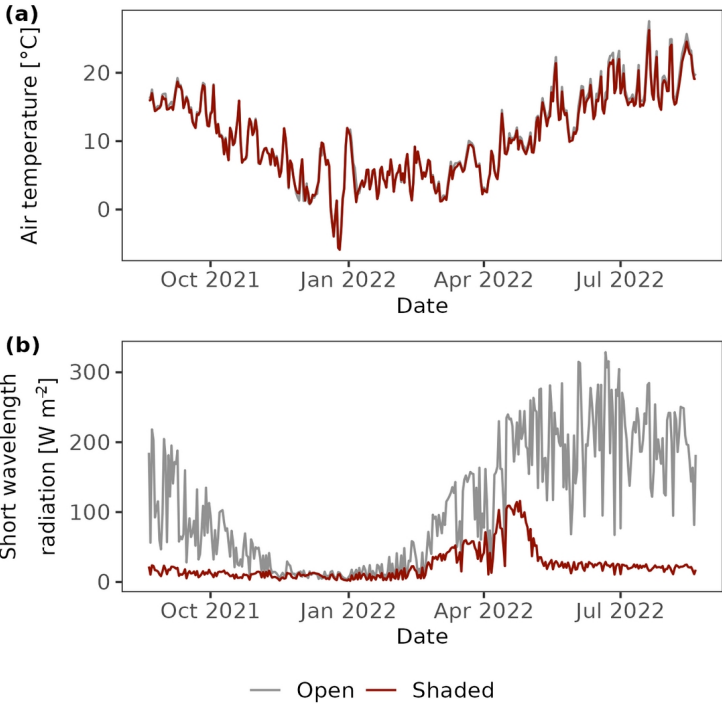
Figure S3.3: the daily patterns of air temperature (a) and short wavelength radiation (b) monitored at shaded (red) and open (grey) experimental plots.

Notably, the automatically monitored annual rainfall amount at the open experimental plot was less than the value measured manually with rain gauges during the same rainfall monitoring period. Additionally, the monitored hourly rainfall at the open experimental plot is often much less than that at the shaded plot, which is also inconsistent with the manually measured difference between the two plots (see Fig. S3.4). We thus attributed the much smaller rainfall data at the open plot to a measurement error caused by missing data records there and reduced the resulting bias by replacing the hourly rainfall data at the open plot with the rainfall at the shaded plot whenever the shaded rainfall was higher.
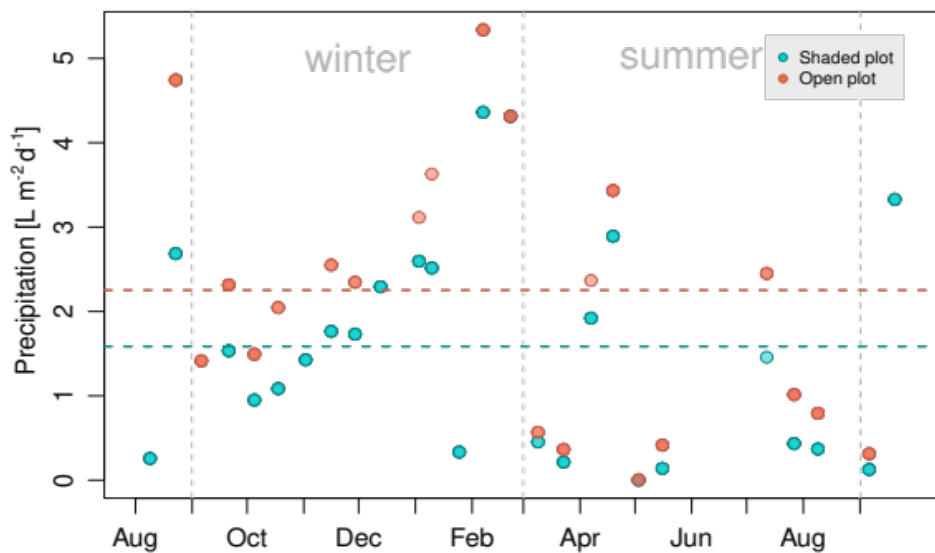
Figure S3.4: the precipitation amounts at shaded and open experimental plots measured manually every two weeks from Aug. 2021 to Aug. 2022. The dashed lines indicate the average values of precipitation amount in two plots.

S4 Boundary condition calibration results and analysis

The parameters describing boundary conditions were calibrated by fitting the average of the measured soil temperature at different depths (open plot: two sensors at 8 cm; shaded plot: at 6.5 cm, 13 cm, 20 cm; Fig. S3.5). The calibration was assessed by a metric RMSE, quantifying the difference between measured and simulated soil temperature and we adopted the combination of parameter values that minimized RMSE.
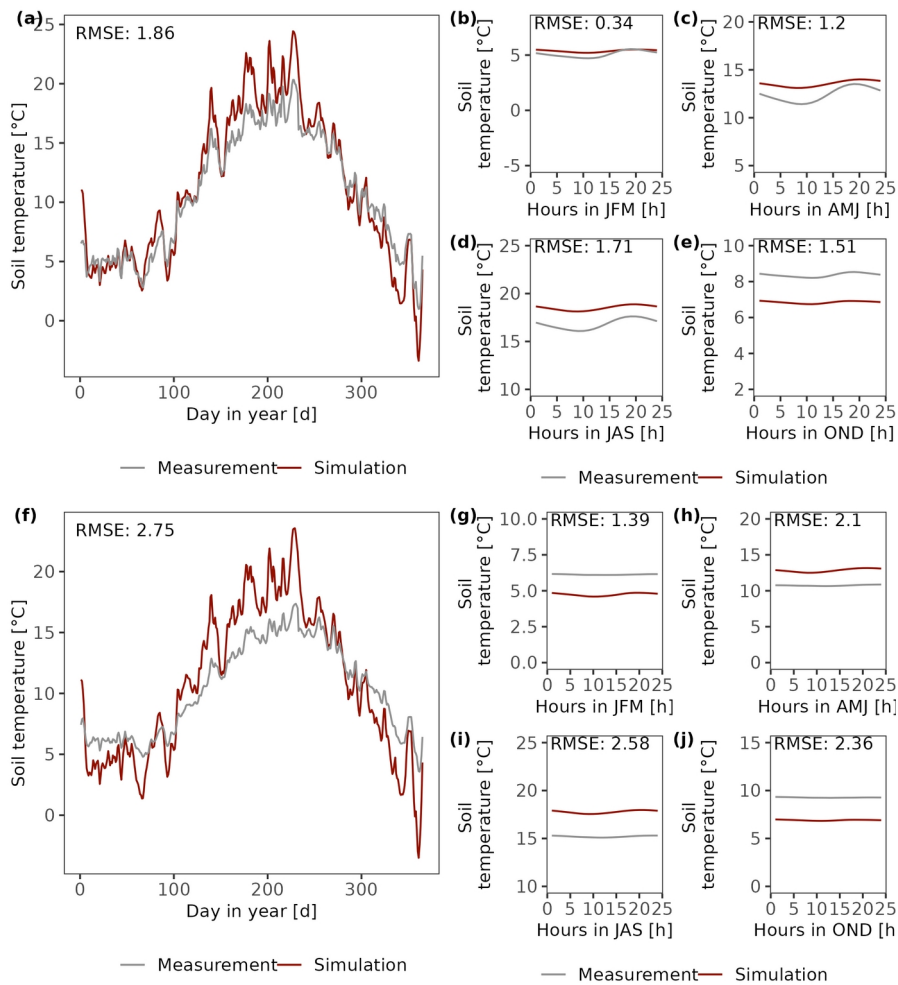
Figure S3.5: Calibration results of abiotic parameters describing boundary conditions by fitting the daily (a, f) and diurnal (b-e; g-j) patterns of the soil temperature at the open (a-e) and shaded plots (f-j). (b) to (e) and (g) to (j) represent the patterns of average hourly soil temperature from January to March (JFM), April to June (AMJ), July to September (JAS), and October to December (OND) at the open and shaded plot, respectively.

The calibration results showed an overall satisfactory fit between measured and simulated soil temperature at the studied shaded and open plots. However, a minor underestimation of soil temperature was observed during the winter, whereas an overestimation was observed during the summer in both plots (Fig. S3.5). This may

have resulted from the missing coupling of soil moisture and soil energy exchange in the model.

With coupled effects, soil can lose energy due to soil evaporation in warm summer. Consequently, the soil temperature could be lower in summer than the simulated values. In cool winter, the liquid water may move into the soil and transfer heat into the soil system by substituting soil air with water that has a higher enthalpy per unit volume (Heitman & Horton, 2011). To test the robustness of the results with regard to the uncertainties in calibrated soil properties, we performed a sensitivity analysis related to soil thermal conductivity (ksoil) using the model with no competitive exclusion (Equal scheme) and with height or net growth-based competition under scenario S2 (see Table 2) to test whether the simulated trait distribution differs largely (varied ksoil from the calibrated value of 0.25 to 0.025 and 3). The newly simulated trait distribution with varied ksoil differs little from the original (Fig. S3.6). Thus, the missing coupling effect may not make a difference in the simulated trait distribution.
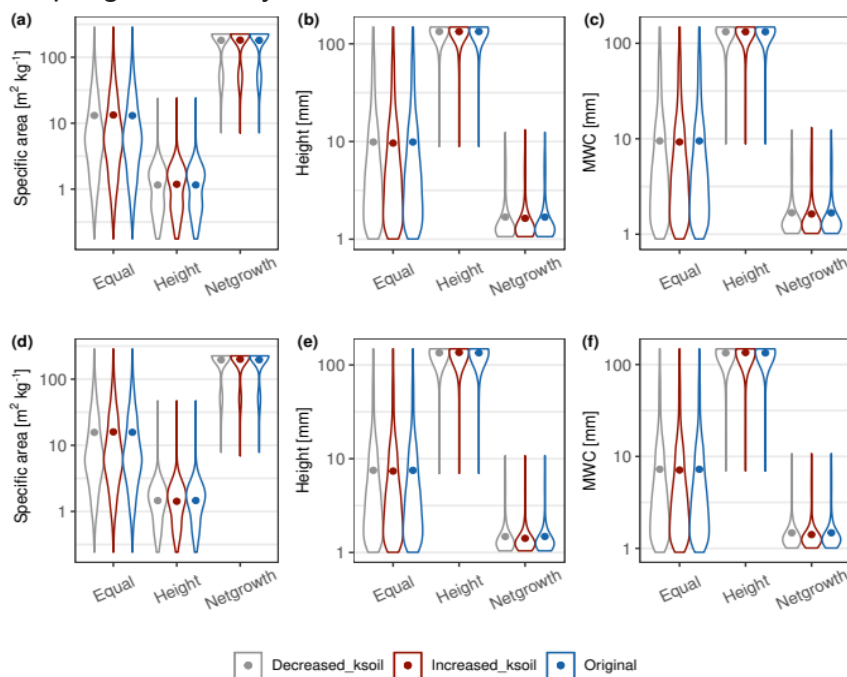
Figure S3.6: The simulated distribution of trait specific thallus area (a, d), Height (b, e), and maximum water content (MWC; c, f) in open (a, b, c) and shaded (d, e, f) communities, by model without competitive exclusion (Equal), with competition depending on height (Height) or net growth (Netgrowth). In the model simulations, the parameter soil thermal conductivity (ksoil) decreased from calibrated value (0.25; Original) to 0.025 (Decreased_koil) and increased to 3 (Increased_ksoil).

S5 Detailed description of model parametrization

S5.1 Calibration of sample-specific physiological properties

Gas exchange measurements were performed to determine the physiological traits of 32 transplanted samples. Light response curves, for instance, were determined at 400 ppm CO_2 concentration and 17 °C, at optimum relative water saturation, which was based on the water-response curves. The temperature response curves were measured for species *Cladonia portentosa (Cp)*, *Hypnum cupressiforme (Hc),* and *Mnium hornum (Mh)* at CO_2 concentration of 400 ppm, light of 1000 µmol m^{-2} s^{-1}, and water saturation of approximately 100%.

The calibration of physiological properties is based on the relevant net photosynthesis calculation module isolated from the LiBry model. The relation between metabolic activity and the water saturation (sat) depends on parameters sat_{act0} and sat_{act1} (Eq. S2), which represent the minimum saturation required to activate the organisms for respiration and photosynthesis, and the water saturation required for full activation. Both traits were derived by fitting the water-response photosynthesis curves.

$$Activity = max\left(0, min\left(1.0, \frac{sat - sat_{act0}}{max\left(p_{critD}, sat_{act1} - sat_{act0}\right)}\right)\right)$$

Eq. S2

where p_{critD} is a critical value of 1^{-12}, needed due to the computer precision limit, to prevent division by 0.

The parameters DCO2min and DCO2max represent the minimum and maximum CO_2 diffusivity (DCO2; mol m^{-2} s^{-1}), and kCO2g1 and kCO2g2 are two parameters regulating the shape of the dependence of DCO2 on water saturation (Eq. S3). All these parameters were calibrated by fitting the CO_2 diffusivity along water saturation using a logistic function. The CO_2 diffusivity values were calculated based on CO_2 response curves as the slope of a linear regression on CO_2-limited net assimilation, requiring correction for the dependence of activity on water saturation.

$$DCO2 = DCO2max + \frac{DCO2min - DCO2max}{1 + kCO2g1 * e^{-kCO2g2 * sat}}$$

Eq. S3

The Q_{10} value (q10), describing the increase of respiration per 10°C increase in temperature, was calibrated based on the measured temperature response of respiration, as shown in Eq. S4. Due to time constraints, these temperature measurements were conducted only for four species (Mh, Hc, Cp, and an additional species *Peltig-*

era rufescens), for species not included in the measurements, Q_{10} was set to the mean of the four parameterized Q_{10} values.

$$q10 = \left(\frac{Resp1}{Resp2} \right)^{\frac{10}{|T1-T2|}}$$ Eq. S4

Resp1 and Resp2 are the respiration rate at the temperature of T1 and T2, respectively.

The reference maintenance respiration rate ($Resp_{main}$) was then calculated as the respiration rate at 17°C, scaled by the temperature response, based on Eq. S5.

$$Resp_{main} = \frac{Resp}{\left(q10^{\left(\frac{xT_s - 17}{10} \right)} \right)}$$ Eq. S5

where Resp is the respiration rate measured at the temperature of xT_s.

The parameter o_extinct represents the absorption efficiency for photosynthesis of light that has not been reflected (1- albedo). Since albedo is a fixed parameter (see Table S2), o_extinct can be obtained by fitting the slope of the CO_2 assimilation depending on light intensity for light-limited photosynthesis.

The parameter prr is the factor to convert respiration to Rubisco content, which was calibrated by fitting the light-response curves since it can influence the light-saturated photosynthesis rate by affecting the photosynthetic capacity (Vcmax) along with the maximum molar carboxylation rate of Rubisco (VcmaxM) and $Resp_{main}$ (Eq. S6), both of which are already calculated or fixed.

$$Vcmax = VcmaxM * prr * Resp_{main}$$ Eq. S6

The range and averages of the calibrated physiological parameter values of each species in the experimental plots are demonstrated in Table S1.

Table S3.1: The range and average values of the calibrated parameters of eight species, derived from gas-exchange measurements across 32 samples. Parameter o_extinct indicates the absorption rate of input light intensity; MWC is the maximum water content; sat_{act0} and sat_{act1} indicate minimum saturation required to activate the organisms and the water saturation for full activity; $Resp_{main}$ is reference maintenance respiration rate, while q10 is the respiratory Q_{10} value. DCO2min and DCO2max represent the minimum and maximum CO_2 diffusivity; kCO2g1 and kCO2g2 represent the shape of the dependence of CO_2 diffusivity on water saturation; prr indicates the factor to convert respiration to Rubisco content.

Species (#replicates)	Range	$o\_extinct$ [ ]	MWC [wet mass dry mass^{-1}]	sat_{act0} [ ]	sat_{act1} [ ]	$Resp_{main}$ [µmol m^{-2} s^{-1}]	q10 [ ]	DCO2min [mol m^{-2} s^{-1}]	DCO2max [mol m^{-2} s^{-1}]	kCO2g1 [ ]	kCO2g2 [ ]	prr [ ]
Pf (4)	min	1	4.6	0.05	0.2	1.51	1.53	0.0065	0.025	1000	15	6.7
	mean	1.65	5.8	0.12	0.31	1.62	1.53	0.0075	0.025	3000	16.1	12.9
	max	2	6.8	0.19	0.42	1.67	1.53	0.01	0.025	5000	18.5	20
Hc (4)	min	1.1	12.2	0.02	0.32	1.05	1.7	0.007	0.0145	5000	15	2.2
	mean	2.05	15.8	0.08	0.43	1.41	1.7	0.0076	0.0145	5000	15	4.6
	max	3.5	18.6	0.1	0.6	2.2	1.7	0.008	0.0145	5000	15	6.5
Mh (4)	min	2.5	8.3	0.05	0.6	0.51	1.44	0.005	0.005	5000	15	10
	mean	2.85	13.4	0.26	0.87	0.98	1.44	0.0055	0.0055	5000	15	12.3
	max	3.1	18.5	0.45	0.98	1.39	1.44	0.006	0.006	5000	15	15
Au (3)	min	3.2	5.8	0.08	0.55	0.3	1.44	0.0041	0.005	5000	13	10
	mean	4.33	11.2	0.09	0.79	0.40	1.44	0.0045	0.0055	5000	14.3	13
	max	5	14.1	0.1	0.93	0.54	1.44	0.005	0.006	5000	15	16
Rs (7)	min	1.3	10.7	0.01	0.36	0.69	1.53	0.006	0.013	1000	10	2.5
	mean	2.71	14.5	0.06	0.53	1.21	1.53	0.007	0.014	2714	11.3	12.4
	max	4	19.8	0.15	0.69	1.89	1.53	0.011	0.019	6000	15	24
Ps (3)	min	1.8	8.2	0.02	0.33	1.17	1.53	0.007	0.019	8000	12	7
	mean	2.73	11.1	0.03	0.4	1.38	1.53	0.008	0.019	8000	13.3	11

	max	4	13.9	0.04	0.45	1.68	1.53	0.009	0.019	8000	14	16
Cp (3)	min	4.1	4.8	0.03	0.32	0.47	1.7	0.01	0.016	8000	13	5.5
	mean	5.2	5.9	0.03	0.46	0.58	1.7	0.011	0.016	8000	13	8.3
	max	6	7.2	0.04	0.65	0.69	1.7	0.013	0.016	8000	13	12
Ci (4)	min	3.4	7.8	0.01	0.36	1.04	1.53	0.0035	0.0095	3000	11	6.8
	mean	3.78	9.6	0.05	0.43	1.53	1.53	0.005	0.0106	5750	11.8	9.7
	max	4.2	12.3	0.08	0.49	2.02	1.53	0.006	0.011	9000	12	12

S5.2 Fixed physiological parameters

In addition to the calibrated sample-specific physiological parameters, several parameters were fixed to values based on literature (Petersen et al., unpublished data; Table S2). These fixed parameters were also used to describe the physiological properties of the species.

Table S3.2: Fixed parameters values for physiological properties of species *Cladonia portentosa* (Cp), *Atrichum undulatum* (Au), *Campylopus introflexus* (Ci), *Hypnum cupressiforme* (Hc), *Mnium hornum* (Mh), *Pleurozium schreberi* (Ps), *Polytrichum formosum* (Pf), and *Rhytidiadelphus squarrosus* (Rs) chosen for parameterizing the model for validation. These values were determined based on the literature.

Parameter	value	References
albedo	Pf = 0.10	moss: Petzold & Rencz,
	Hc, Mh, Au, Rs (survives in shaded plot) = 0.15	1975 Cp: Heim & Lundholm, 2014
	Rs (survives in open plot),	
	Ps = 0.20	
	Cp=Ci= 0.25	

Maximum molar oxygenation rate of Rubisco (VomaxM) [s⁻¹]	1.2	Calculated from Savir et al., 2010
Maximum molar carboxylation rate of Rubisco (VcmaxM) [s⁻¹]	4.5	Savir et al., 2010
Enzyme activation energy of Kc (Eact_Kc) [J mol⁻¹]	85000	Porada et al., 2013
Enzyme activation energy of Ko (Eact_Ko) [J mol⁻¹]	30000	Porada et al., 2013
Enzyme activation energy of Vcmax (Eact_Vm) [J mol⁻¹]	75000	Porada et al., 2013
Enzyme activation energy of Jmax (Eact_Jm) [J mol⁻¹]	55000	Porada et al., 2013

S6 Validation results and analysis:
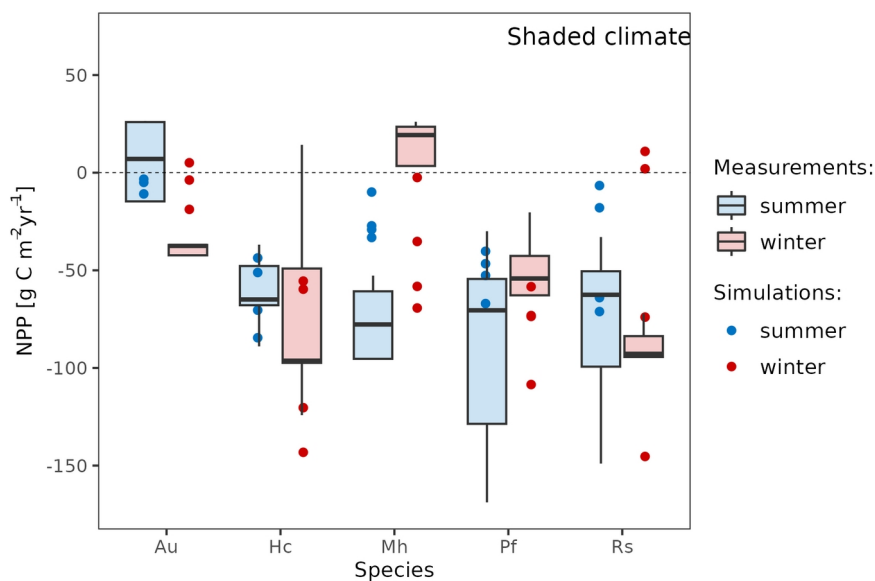
Figure S3.7: The comparison of the measured net primary productivity (NPP) of surviving trans-planted species samples at the shaded experimental plot within the winter and summer months to

the simulated NPP of all samples of the species and driven by the shaded climate with reduced short wavelength radiation by 90% when there is a relatively dense canopy covering (during 1st of May and the 5th of September).
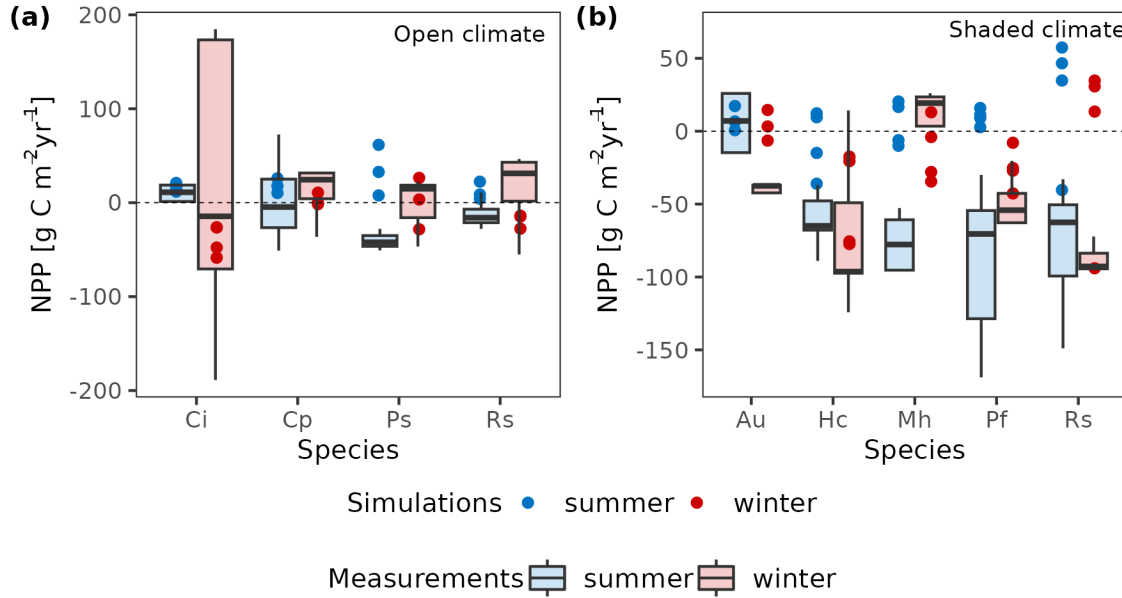
Figure S3.8: The comparison of measured net primary productivity (NPP) in summer and winter months to simulated NPP when including the acclimation of parameter reference maintenance respiration rate ($Resp_{main}$) during winter for species samples that survive at the open experimental plot (a) and at the shaded plot (b) after transplantation. The parameter $Resp_{main}$ reduced by 70% during September and February but remained unchanged for the other months.

S7 Community weighted mean value

The equation used to calculate the community weighted mean (CWM) of both simulated and measured communities is delineated as follows:

$$CWM = \frac{\sum\limits_{i=1}^{n}\left(trait(i) * cover(i)\right)}{\sum\limits_{i=1}^{n} cover(i)} \qquad \text{Eq. S7}$$

where n is the number of surviving strategies (or samples), trait(i) is the trait value of the strategy (sample) i while cover(i) is the cover fraction (relative abundance) of the strategy (sample) i.

S8 Traits allowed to vary randomly in the model simulations

The 11 traits that combine to characterize the model strategies were chosen randomly within their potential global ranges (as described in Sect. 2.1), which also

leads to variation in the values of several other traits that are determined by these 11 traits (the randomly generated traits are listed in Table S3). A few physiological parameters, however, such as sat_{act0}, prr, and the shape parameters for the CO_2 diffusivity curve, were kept at constant values across all strategies in the model simulation since they correspond to no physiological trade-offs that need to be constrained. To this end, the values of these parameters were averaged from all species samples collected from the open (or shaded) experimental plots. These averaged values were subsequently applied in the model simulations.

Table S3.3: Traits that are randomly chosen from their possible range in the simulations

Random Trait	Unit
Albedo	-
Thallus height	m
Total thallus porosity when wet	-
Minimum saturation needed for full activity	-
Minimum thallus CO_2 diffusivity	mol m^{-2} s^{-1}
Specific thallus area	m^2 kg^{-1}
Water storage capacity	kg H_2O kg biomass^{-1}
Maximum molar carboxylation rate of Rubiscos^{-1} (VcmaxM)	
Maximum molar oxygenation rate of Rubiscos^{-1} (VomaxM)	
Reference maintenance respiration	mol m^{-2} s^{-1}
Turnover	year^{-1}
Optimum temperature for photosynthesis	K

Q$_{10}$ value of respiration   -

Enzyme activation energy of Kc (Eact_Kc)   J mol^{-1}

Enzyme activation energy of Ko (Eact_Ko)   J mol^{-1}

Enzyme activation energy of Vcmax (Eact_Vm) J mol^{-1}

Enzyme activation energy of Jmax (Eact_Jm)   J mol^{-1}

S9 Number of surviving strategies in model simulations

Table S3.4: Number of simulated survivors for 3000 initial strategies, using the Equal, Height/Net-growth-based competition scheme, under various scenarios of different competition intensities within open and shaded local communities.

Associated trait	Scenario	Community	Surviving strategies
Equal scheme	-	Open	1239
		Shaded	961
Height scheme	S1	Open	47
		Shaded	26
	S2	Open	167
		Shaded	115
	S3	Open	1221
		Shaded	954
	S4	Open	1235
		Shaded	961
Netgrowth scheme	S1	Open	19

	Shaded	16
S2	Open	117
	Shaded	98
S3	Open	1236
	Shaded	959
S4	Open	1240
	Shaded	961

S10 Sensitivity analysis of different input strategies

To assess the influence of the sample size of the initial strategies on the simulated trait distributions, and the convergence of the strategy space, we performed a sensitivity analysis involving four simulation replicates with different sets (three new sets and one original set) of 3000 randomly generated strategies, and also subsets of these four including 30 and 300 strategies each, respectively. Comparisons of simulated community-weighted mean trait values (CWMs) using the Equal scheme across the four simulation replicates revealed a higher degree of convergence in the strategy space when utilizing 3000 strategies, in contrast to lower numbers (Fig. S3.9). Furthermore, no significant differences were observed among the simulated distributions of traits across the four simulations when generating 3000 strategies (p-value of Kruskal test > 0.1).
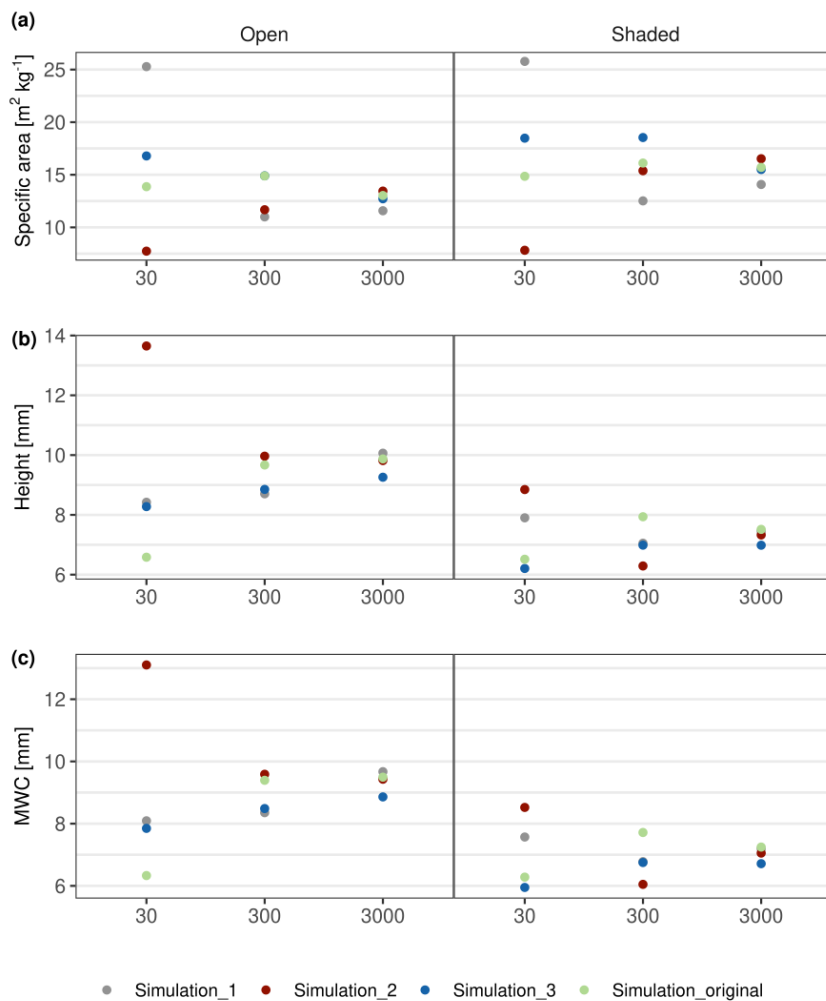
Figure S3.9: The simulated community-weighted mean values of specific thallus area (a), Height (b), and maximum water content (MWC; c) in open and shaded communities, initialized with 30, 300, and 3000 strategies, respectively. Four replicate simulations are run that differ in the random number sets for the initial strategies (simulation_original, simulation_1-3).

S11 Sensitivity analysis of disturbance parameter

We simulated trait distributions of the open and shaded communities based on the Equal scheme, Height- and Netgrowth-based competition schemes under scenario 2 (see Table 2), while varying the parameter disturbance rate by +/-20% in the model. The results (Fig. S3.10) indicate that the disturbance rate may alter the range of simulated trait distributions but has little impact on the CWMs. With decreasing disturbance, competition increases and strategies with low relative abundance are more likely to die out, thus narrowing the distribution, but with little effect on the CWM that is dominated by the highly abundant strategies. Note that we did not increase disturbance to unrealistically high values, which would again narrow the distributions, not

due to competition, but due to the inability of some strategies to replace their cover losses.
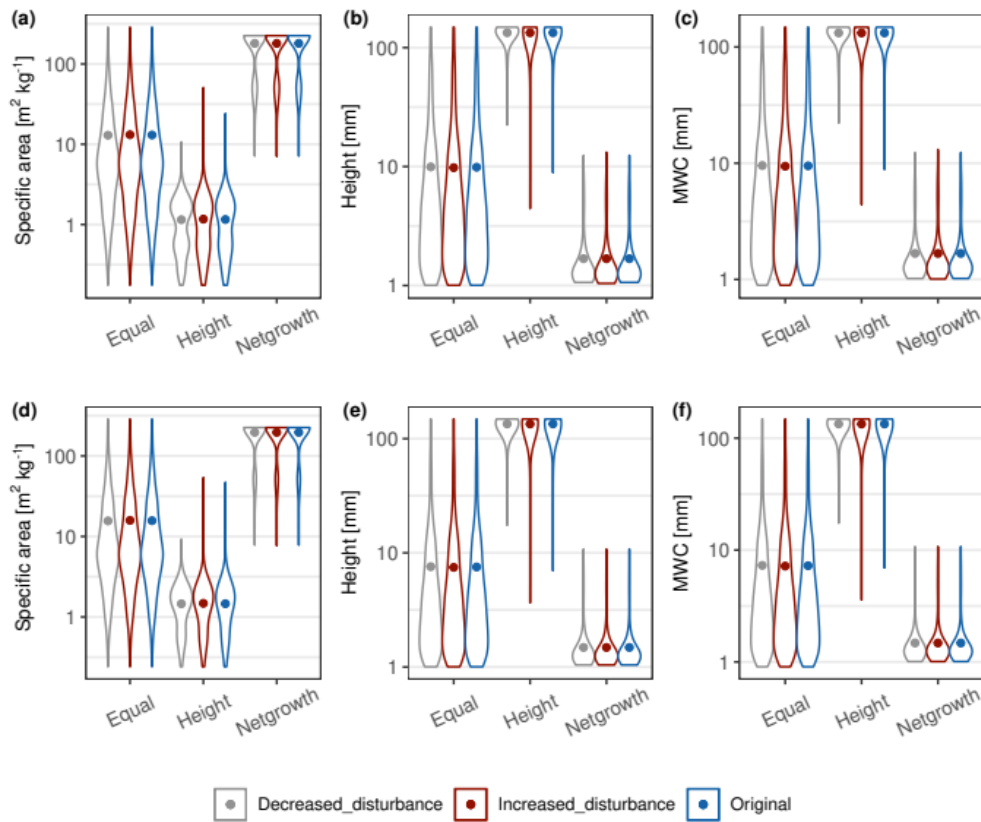
Figure S3.10: Simulated distributions of the specific thallus area (a, d), Height (b, e), and maximum water content (MWC; c, f) in open (a, b, c) and shaded (d, e, f) communities, based on model schemes without competitive exclusion (Equal), with competition depending on height (Height) or net growth (Netgrowth). In the model simulations, the parameter disturbance rate was increased by 20% (Increased_disturbance) from the original value (Original) or decreased by 20% (Decreased_disturbance).

S12 Sensitivity analysis of adjusted shortwave radiation and physiological parameter
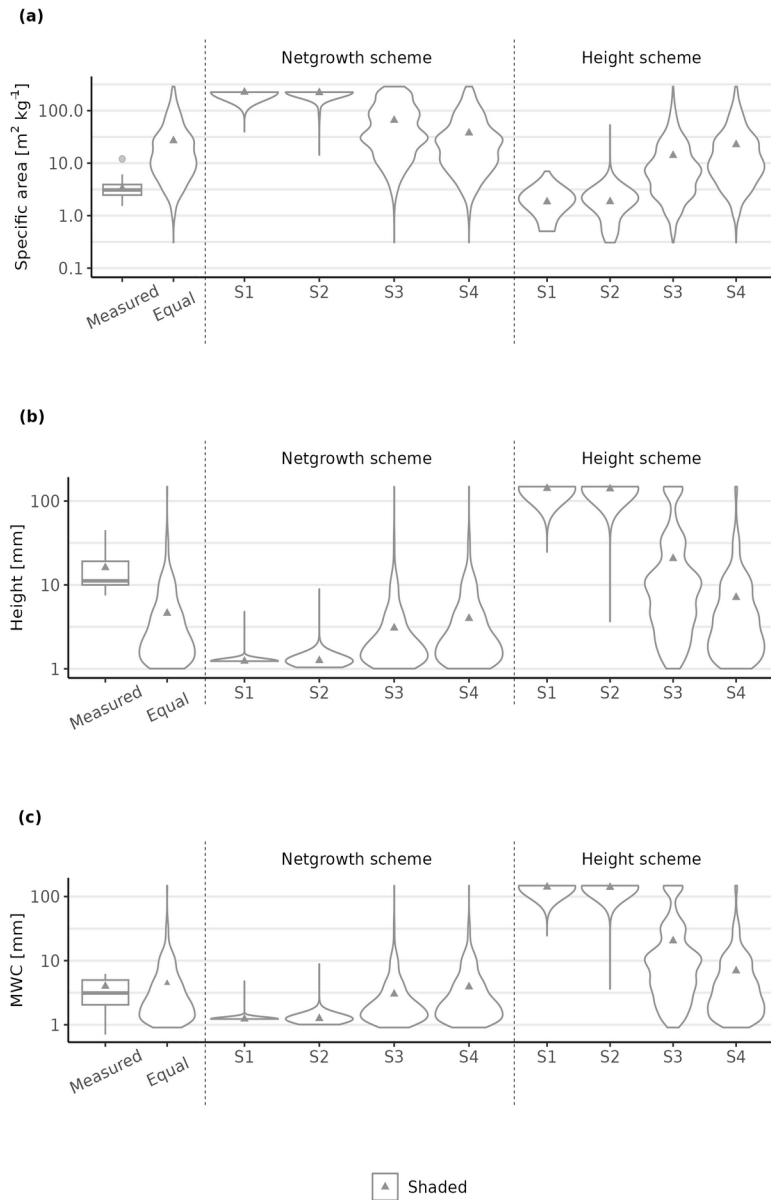
Figure S3.11: Observed and modelled distributions of morphological and hydration traits of a shaded community. a) specific thallus area, b) Height, c) maximum water content. The simulated values are estimated by the LiBry model driven by weather data collected at the shaded experimental plot with shortwave radiation reduced by 90% in the summer months (from the 1st of May to the 5th of September 2022), and with a one-trait (Height or Netgrowth) competition scheme with different competition intensities (S1-S4) or without competitive exclusion ("Equal"). The width of violin plots is proportional to the simulated cover fraction of the surviving strategies selected by the model. Points in the box and violin plots demonstrate the community-weighted mean value of the measured shaded community for mosses and lichens, and the simulated community-weighted mean values, respectively.
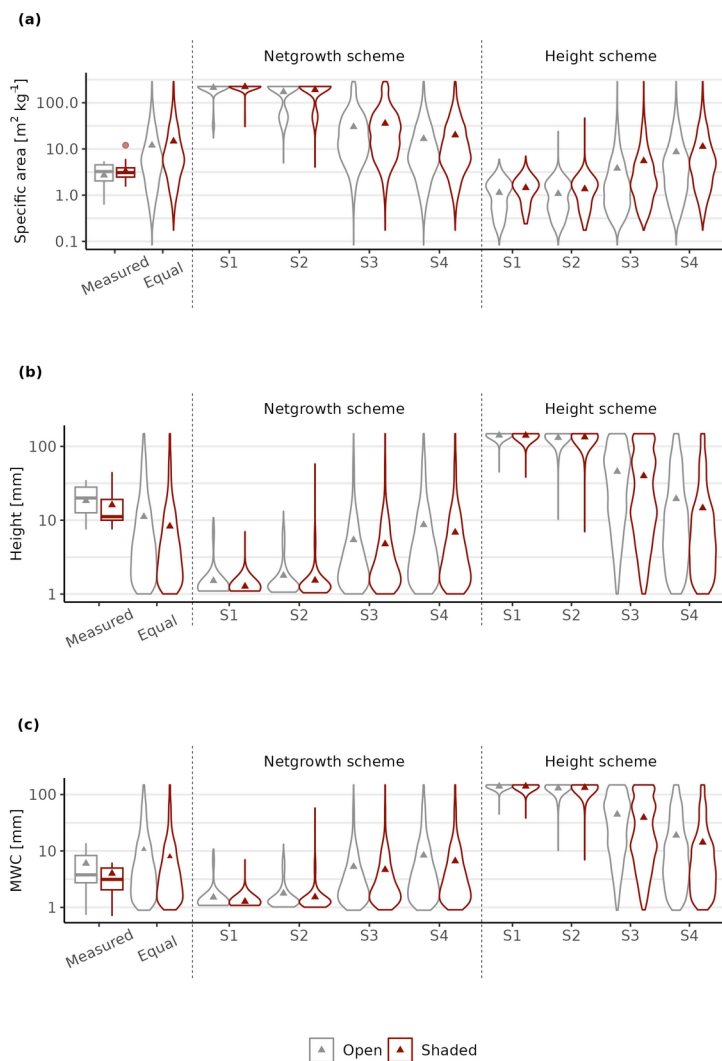
Figure S3.12: Observed and modelled distributions of morphological and hydration traits of the open (grey) and shaded (red) communities. a) specific thallus area, b) Height, c) maximum water content. The simulated values are estimated by the LiBry model with the physiological parameter reference maintenance respiration rate (Resp$_{main}$) adjusted to 70% for all strategies between September and February, and using a one-trait (Height or Netgrowth) competition scheme with different competitive intensities (S1-S4), or without competitive exclusion ("Equal"). The width of violin plots is proportional to the simulated cover fraction of the surviving strategies selected by the model. Points in the box and violin plots demonstrate the community-weighted mean values of measured shaded and open communities for mosses and lichens, and the simulated community-weighted mean values, respectively.

S13 Sensitivity analysis of competition formation

In addition to the power distribution, the relationship between competitive ability and functional trait could be in other forms such as the Gaussian function, which is com-

monly applied in community ecology models. To examine the robustness of the results against the equation we assumed for estimating the competitive ability based on trait values, we performed additional model simulation analyses where the trait-based competition in the model was calculated using univariate and multivariate Gaussian function.

One-trait competition scheme

The functional traits were first normalized by dividing the sum of trait values of all surviving strategies, and then the normalized trait values were log-transformed prior to the calculation of competitive ability to approach a normal distribution.

$$x(i) = -\log 10\left(max\left(1.0\,E^{-12}, \frac{T(i)}{\sum_{i=1}^{n} T(i)} \right) \right) \qquad \text{Eq. S8}$$

where n is the total number of surviving strategies, T indicates the trait height or net growth as a determinant trait for competition; T(i) is the trait value of strategy i; and x(i) is the transformed height or net growth of strategy i.

Then the competitive ability of each strategy is calculated following Eq. S9

$$Comp(i) = e^{\frac{-1}{2}\left(\frac{x(i)}{\sigma}\right)^2} \qquad \text{Eq. S9}$$

where σ controls the width of the Gaussian function curve. Comp(i) represents the competitive ability of strategy i.

We also relate σ to csum in each scenario and vary the range value of σ in three scenarios to explore the effect of different competition intensities on trait distribution (Table S5). A higher value of σ^2 implies that a larger number of strategies have similar competitive abilities independent of their trait values, with no single strategy dominating and excluding the others. Hence the higher value of σ^2 exhibits a lower competition intensity among strategies. We also applied the model with Height- and Net-growth-based competition schemes. The relationship between competitive ability and normalized height or net growth value varies with csum and different scenarios are shown in Fig. S3.13.

Table S3.5: The values of shape factor σ^2 of the Gaussian function of the one-trait based competition scheme changed with the total cover fraction occupied by all surviving strategies (csum) in different scenarios. The lower value of factor σ^2 implies a higher competition intensity among strategies and vice versa.

	Factor σ²
Scenario 1 (S1)	0.2 – csum * 0.1
Scenario 2 (S2)	1
Scenario 3 (S3)	6 – csum * 4
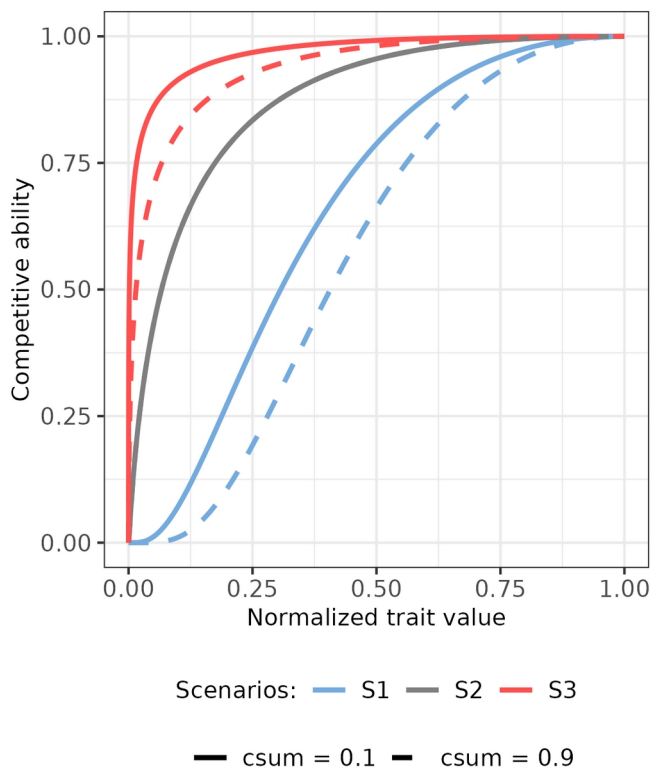
Figure S3.13: Implementation of the concept of the one-trait based competition scheme using the Gaussian function. The relationship between competitive ability and normalized determinant trait value when the available area (1- total cover fraction occupied by all surviving strategies (csum)) is sufficient (csum = 0.1) and limited (csum = 0.9). Different scenarios represent different competitive intensities from high (S1) to low (S3). In the scenario with high competition intensity (S1 at high cover values), differences in competitive ability between the strategies are relatively large, hence most strategies could be competitively excluded by a few strategies with extremely high trait value that have much higher competitive ability. At low competitive intensities (S3, especially at low cover values) all species have similar competitive abilities, and hence competitive exclusion is not expected.

The results of comparisons between simulated trait distributions under different scenarios and measurements in shaded and open communities are shown in Fig. S3.14.

(a)

(b)

(c)
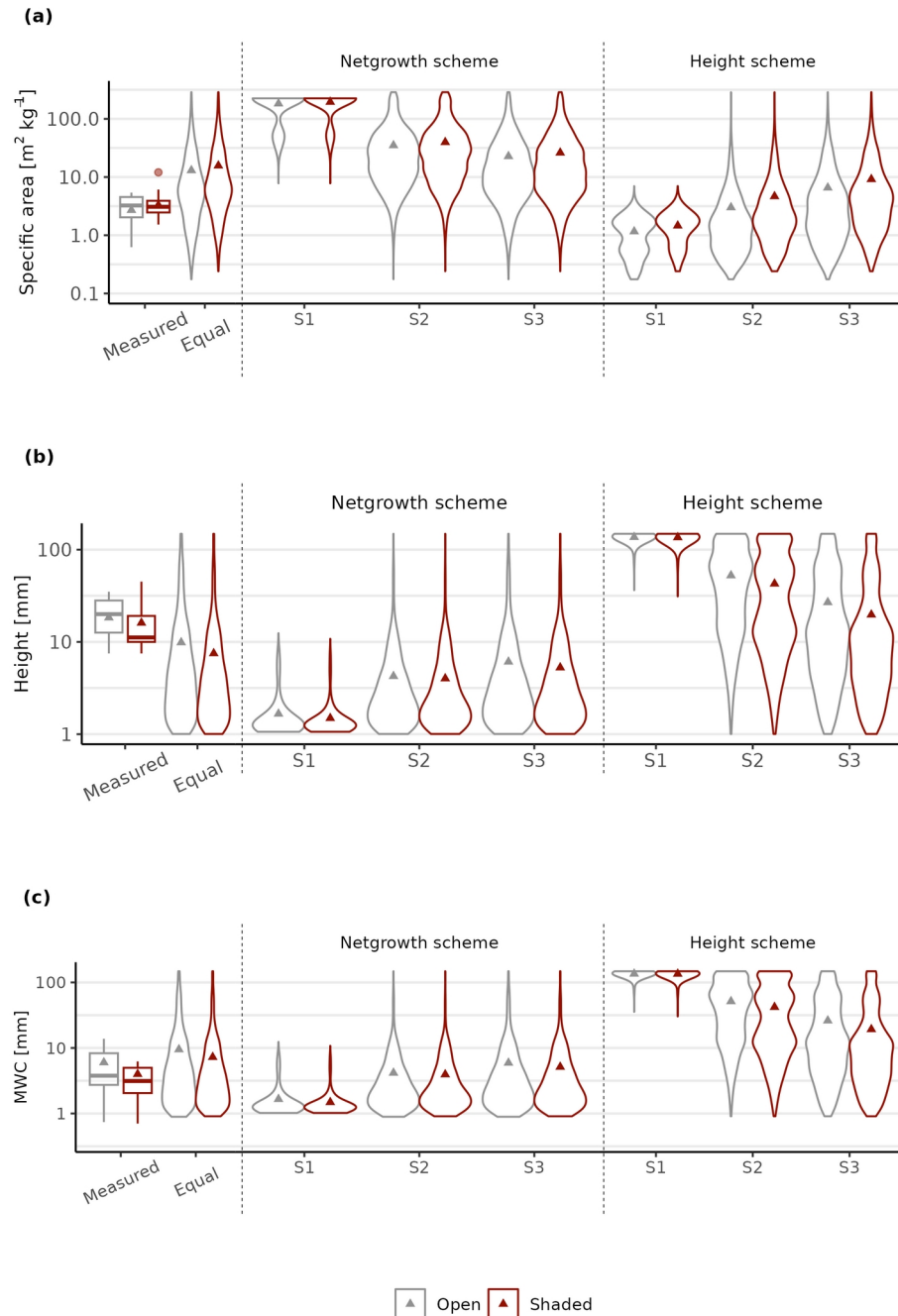
Figure S3.14: Observed and modelled distributions of morphological and hydration traits of the open and shaded communities. a: specific thallus area, b: Height, c: maximum water content. The simulated values are estimated by the LiBry model with a one-trait based Height or Netgrowth competition scheme with different competitive intensities (S1-S4) or without competition exclusion ("Equal"), using the Gaussian function. The width of violin plots is proportional to the simulated cover fraction of the surviving strategies selected by the model. These strategies are character-

ized by randomly generated physiological and morphological parameters. Points in the box and violin plots demonstrate the community-weighted mean values of measured shaded and open communities for mosses and lichens, and the simulated community-weighted mean values.

Two-trait competition scheme

We also estimated the impacts of two-trait competition using multivariate Gaussian function, which is commonly used in theoretical models of species interactions based on multiple trait dimensions (e.g., Chalmandrier et al., 2022). Here two traits (height and net growth) jointly but independently contribute to the competitive ability. Identical to the one-trait based competition scheme, both traits were first normalized for each strategy (i), and then the normalized trait values were log-transformed prior to the calculation of competitive ability to approach a normal distribution (Eq. S8; x1 and x2). The competitive ability was then calculated based on the log-normalized trait value:

$$Comp(i) = e^{-\left(\frac{1}{2}\right) * \left[\left(\frac{x1(i)}{\sigma X1}\right)^2 + \left(\frac{x2(i)}{\sigma X2}\right)^2\right]} \qquad \text{Eq. S10}$$

where parameters $\sigma X1$ and $\sigma X2$ in the equation determine the width of the normal distribution of each trait. Comp(i) represents the competitive ability of strategy i.

$\sigma X1$ and $\sigma X2$ are assumed to be equal for feasibility and related to csum as well to show a higher competition intensity when the available area (1-csum) is limited. We ran the model in four scenarios under different competitive intensities to assess the trait distributions by varying the range values of $\sigma X1^2$ and $\sigma X2^2$ (Table S6). Having both larger values of $\sigma X1^2$ and $\sigma X2^2$ implies that more strategies have a similar competitive ability with no single strategy dominating and excluding the others. Hence, both higher values of $\sigma X1^2$ and $\sigma X2^2$ exhibit a lower competition intensity among strategies. The relationship between competitive ability and normalized trait value varies with csum and different scenarios are shown in Fig. S3.15.

Table S3.6: The values of shape factor $\sigma X1$ and $\sigma X2$ of the multivariate Gaussian function of the two-trait based competition scheme changed with the total cover fraction occupied by all surviving strategies (csum) in different scenarios.

	Factor $\sigma X1^2$	Factor $\sigma X2^2$
Scenario 1 (S1)	0.2-csum*0.1	0.2-csum*0.1

Scenario 2 (S2)	0.6-csum*0.2	0.6-csum*0.2
Scenario 3 (S3)	1	1
Scenario 4 (S4)	6-csum*4	6-csum*4
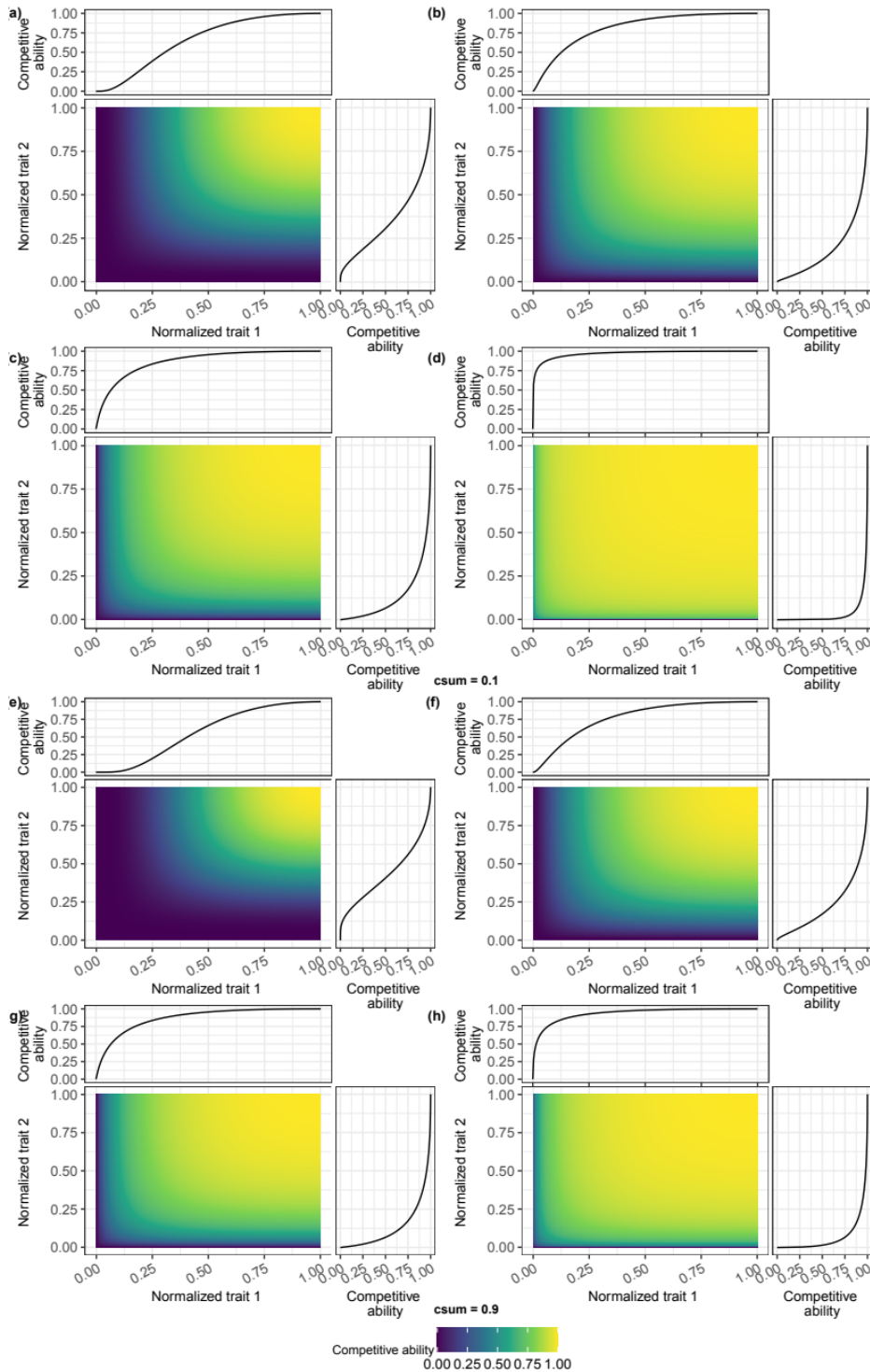
Figure S3.15: Implementation of the concept of the two-trait competition scheme, which demonstrates the competitive ability changing with two traits in normalized value. (a)-(d) demonstrate four scenarios where the competitive intensities change from high to low by varying the values of parameter $\sigma X1$ and $\sigma X2$ of the two-trait competition scheme at the condition that the total cover fraction area occupied by all surviving strategies (csum) is low (0.1). (e)-(f) demonstrate four scenarios of different competitive intensities when csum is high (0.9).

The results of comparisons between simulated trait distributions under different scenarios and measurements in shaded and open communities are shown in Fig. S3.16:
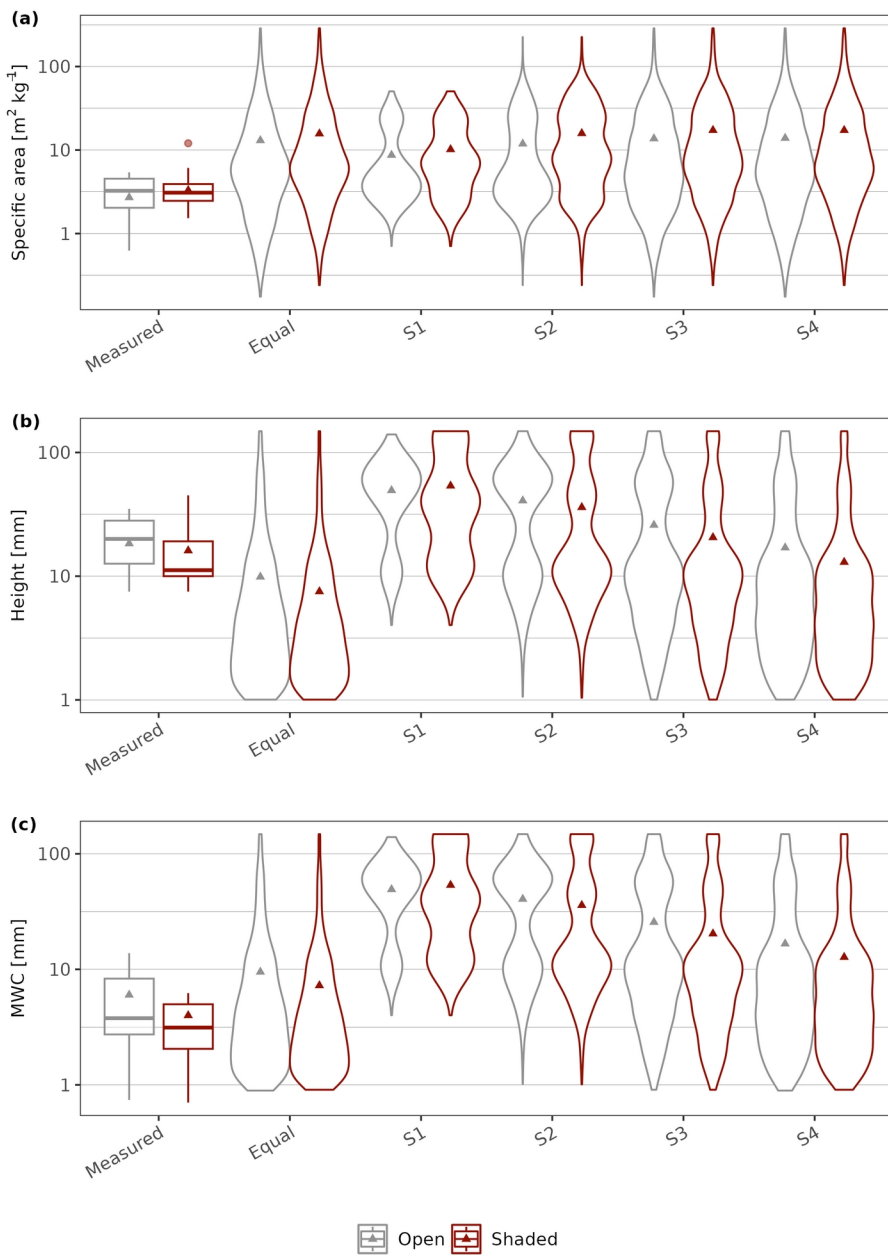
Figure S3.16: Observed and modelled distributions of morphological and hydration traits of the open and shaded communities. a: specific thallus area (STA), b: Height, c: maximum water content (MWC). The simulated values are estimated by the LiBry model with a two-trait based competition scheme using multivariate Gaussian function with different competition intensities (S1-S4) or without competition exclusion ("Equal"); The width of violin plots is proportional to the simulated cover fraction of surviving strategies selected by the model. These strategies are characterized by randomly generated physiological and morphological parameters. Points in the box and violin plots demonstrate the community-weighted mean values of measured shaded and open communities for mosses and lichens, and the simulated community-weighted mean values.

S14 Sensitivity analysis of climate forcing data

To examine the robustness of the results of competition effects against potential deviations in microclimate forcing data measured in experimental plots from those in the natural sites, we repeated the analysis with the data retrieved for Hamburg from ERA5 reanalysis data from Hamburg as an alternative set of microclimate variable. The results of comparisons between simulated trait distributions under different scenarios and measurements in shaded and open communities are shown in Fig. S3.17. We found the results are consistent: the best fit to the CWM data of specific thallus area (STA) was in the scenario with a linear increase in competitive ability with height growth (Height scheme S3, Fig. S3.17(a)). The scenario exhibiting the most accurate fit to the measured Height entailed competition based on height, with the least degree of intensity (Height scheme-S4, Fig. S3.17(b)). The weak growth-based competition was most effective for reproducing the distribution of MWC (Netgrowth scheme-S3 and S4, Fig. S3.17 (c))
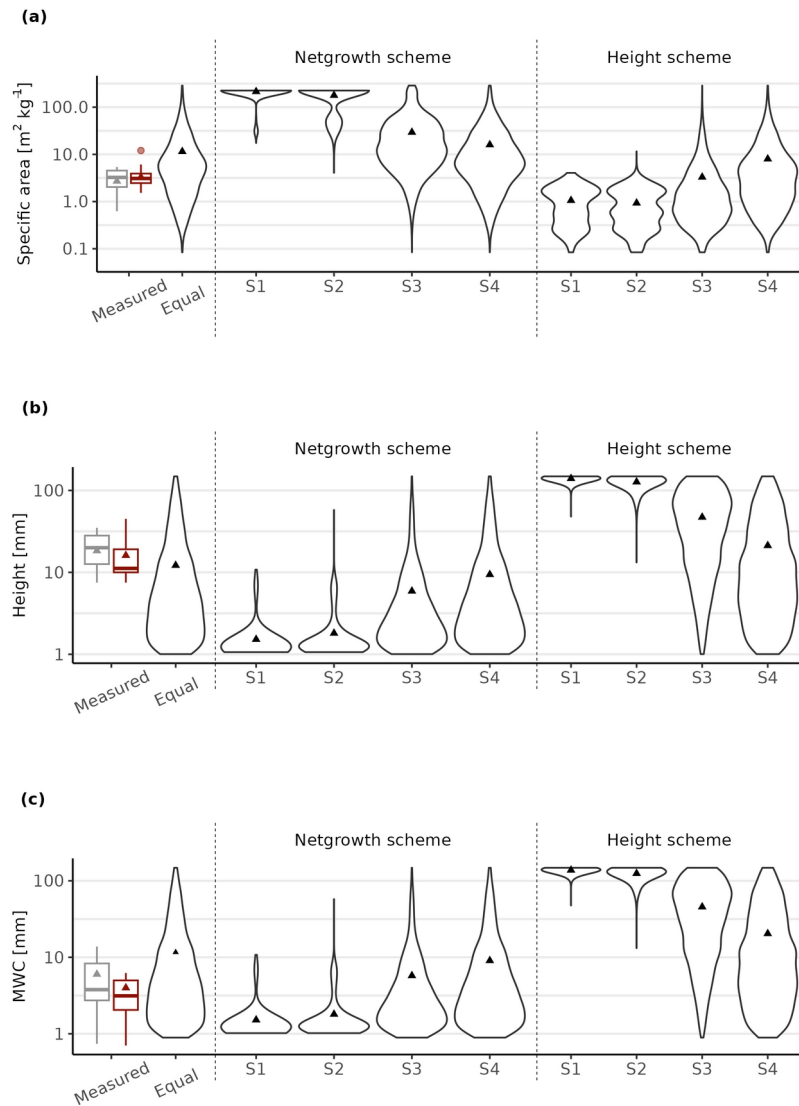
Figure S3.17: Observed and modelled distributions of morphological and hydration traits of non-vascular communities grown in Hamburg, northern Germany. a: specific thallus area, b: Height, c: maximum water content. The simulated values were estimated by the model with the one-trait based Height or Netgrowth competition scheme with different competitive intensities (S1-S4) or no competitive exclusion ("Equal"), driven by ERA5 reanalysis data of Hamburg. The width of violin plots is proportional to the simulated cover fraction of the surviving strategies selected by the model. These strategies are characterized by randomly generated physiological and morphological parameters. Points in the box and violin plots demonstrate the community-weighted mean values of measured shaded and open communities for mosses and lichens, and simulated community-weighted mean values.

Chapter 4 - General Discussion

This dissertation mainly elaborates on studies on the community assembly processes in terms of abiotic and biotic filtering, which are essential to understand the diversity pattern of non-vascular vegetation and the various ecosystem functions they provide. In this synthesis, I will summarize the outcomes of all studies, placing them within a larger scientific context. Additionally, I will further discuss the implications and provide directions for future research. In the first part of the synthesis, I will summarize and analyze the impacts of both the abiotic and biotic factors on community assembly of NVV (Fig. 4.1). The following section will also involve a discussion of how other ecological processes contribute to NVV community assembly. Subsequently, I will present the implications of the studies for interpreting the global diversity pattern of NVV and further discuss the impact of climate change on NVV communities.
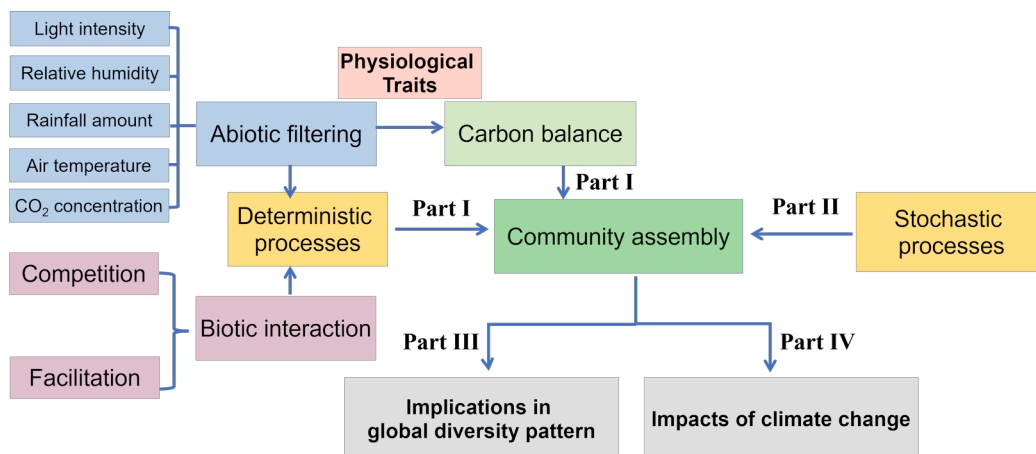
Figure 4.1: Conceptual diagram of the general discussion outline. Part I summarizes and discusses how the deterministic processes (abiotic filtering and biotic interaction) shape the NVV community structure. Part II discusses the stochastic factors that may shape the community assembly. Part III presents implications of the studies for analyzing the mechanisms resulting in the global diversity pattern of NVV. Part IV discusses the impact of climate change on NVV communities.

4.1 Abiotic and biotic factors in NVV community assembly

Abiotic (environmental) and biotic filtering are extensively studied and considered to be the most important assembly processes that structure natural plant communities and functional composition (Kraft, Adler, et al., 2015; Kunstler et al., 2012). Yet, the

impacts of abiotic and biotic factors on non-vascular communities, which provide essential ecosystem functions worldwide despite their small size, has received limited attention.

4.1.1 Abiotic filtering

The abiotic environment shapes the structure of plant communities by filtering for species that are able to establish and persist in the environment, depending on their ecological strategies, and thus the functional traits (Cornwell et al., 2006; Keddy, 1992). Species with different trait values exhibit varying tolerances in response to abiotic stressors, ultimately influencing their ability to survive and coexist within a particular environment (Beltrán-Sanz et al., 2023). For instance, NVV species with high optimum water saturation for photosynthesis may be excluded in dry environments, while the species with lower values may be tolerant to the drought. This could contribute to the observed similarities in phenotypic traits that convey these tolerances among coexisting community members, as indicated by many studies (e.g., Cornwell et al., 2006; Weiher et al., 1998).

In my research, the crucial contribution of environment filtering to community assembly was demonstrated by the relatively match of the observed tendential variations in trait distributions between shaded and sun-exposed communities to the simulations conducted without competitive exclusion (detailed in Chapter 3). In addition to examining the overall environment, I explored the relative influence of several key individual environmental filters (air temperature, relative humidity, annual rainfall amount, short-wave radiation, CO_2 concentration) on shaping the community structure. This was done by quantifying the annual carbon balance, a crucial indicator reflecting the growth and survival of organisms, for lichen- and moss-dominated biocrust collected from six sites across diverse climate zones (Chapter 2). The study showed the essential impacts of all examined climatic factors on the annual carbon balance of biocrusts at all sites, with air temperature and CO_2 concentration emerging as the most important. This suggests that climate change, potentially resulting in elevated air temperatures and CO_2 concentration (IPCC 2021), could potentially affect the long-term carbon balances of biocrusts distributed across various climate zones and ultimately their community assembly.

However, the relative importance of these climatic factors differs across climate

zones. For instance, the air temperature has largest impact on carbon balance at the alpine site, while CO_2 concentration is the most essential factor in drylands. Relative humidity, capable of regulating non-rainfall water sources like water vapor and dew, generally plays a more important role than rainfall amount at all sites except one dryland (Chapter 2, Fig. 2.6). The varying role of rainfall amount in this dryland may be attributed to differences in rainfall frequency, which is also recognized as an important factor for carbon balance (Reed et al., 2012). In sites with limited and evenly distributed rainfall, alterations in the magnitude of single rainfall events may largely affect the metabolic activity of the organisms and thus influence their long-term carbon balance.

Moreover, the carbon balances of biocrust species in response to environments are moderated by the physiological traits of biocrust species. For instance, the respiratory Q_{10} value determines the response of respiration rate and thus the net photosynthetic CO_2 assimilation rate to temperature. The water saturation required for the initial activation of organisms may contribute to the duration of inactive period throughout the year particularly in sites with limited water availability, thereby influencing the annual carbon balance. Despite the key roles of these physiological traits, their relative importance for carbon balance is different (Chapter 2, Fig. 2.7). My study revealed a more substantial impact of respiration-related traits on the carbon balance estimation of biocrusts.

Therefore, uncertainties in monitored climatic factors (particularly air temperature and the CO_2 concentration) can lead to uncertainties in simulated carbon balances and thus the community assembly. In addition, the large uncertainty in the respiration-related physiological traits calibrated from the photosynthesis response curves may also result in uncertainty in the simulation results. This might account for the simulated substantial loss of carbon from biocrusts in humid alpine and temperate sites in my study, which contradicts the real field where all species survive.

Apart from uncertainties in the values of physiological traits, the absence of seasonal acclimation of these traits in the model may also be a main error source. I observed a substantial improvement in carbon balance of biocrusts in a humid temperate site when physiological traits were acclimated to the winter climate (Chapter 2, Fig. 2.8). The acclimation of respiration rate to environmental change, such as warming (Drake

et al., 2016) and elevated CO_2 (Smith & Dukes, 2013), has been observed by regulating the reference maintenance respiration rate for vascular plants (Crous et al., 2022; Smith & Dukes, 2013). A similar downregulation of respiration rate in warmer summers was also observed in lichens (Lange & Green, 2005). Temporal acclimation of respiration rates, associated physiological traits and implications for carbon balance estimation have been widely recognized; however, this acclimation remains poorly quantified and addressed in many DGVMs and land surface models (Crous et al., 2022). Some models have attempted to incorporate temporal acclimation using empirical functions and parameters (e.g., the rate of thermal acclimation, Butler et al., 2021; Haverd et al., 2018), which, in turn, introduces additional uncertainties (Smith & Dukes, 2013). Consequently, further efforts are necessary to comprehensively quantify the temporal acclimation of traits in response to environmental changes to improve the accuracy of simulations on carbon balance and community assembly.

Furthermore, the carbon balance estimation by the model (Chapter 2) might be uncertain due to the lack of consideration for nutrient limitation on the growth of biocrusts. For instance, nitrogen is crucial for net primary production as it is a key component of proteins necessary for the production of chlorophyll and many enzymes (e.g., Rubisco), which are critical for photosynthesis (Shehawy & Kleiner, 2001; Vitousek & Howarth, 1991). Hence, the nitrogen shortage, notably prevalent in tropical regions (LeBauer & Treseder, 2008), can inhibit the carbon balance of individual NVV organisms as well as ecosystem productivity.

4.1.2 Biotic filtering

Among biotic filtering processes, competition has been shown by numerous studies to have a critical impact on shaping the community structure and multi-dimensional trait space (Bittebiere et al., 2019; Keddy 1989; Kunstler et al., 2012). However, the role of competition is less studied for non-vascular vegetation. We found that the functional composition of lichen and moss communities in temperate regions are likely to be shaped by weak rather than strong competition (Chapter 3), aligning partly with the study by During & Tooren (1987), which suggests that competition may be less essential for bryophyte communities in a Dutch forest. However, I expect that competition may play a different role in other climate zones, as studies have

found substantial impacts of competition on non-vascular community composition in semi-arid regions (Maestre et al., 2008; Soliveres & Eldridge, 2020); and competition tends to be strongly asymmetric but does not lead to competitive exclusions in boreal regions (Mälson & Rydin, 2009).

In addition to competition that was explored in my study (Chapter 3), facilitative interaction is also commonly recognized as an essential plant community assembly process (Brooker et al., 2008). Two different non-vascular organisms can exhibit a symbiotic and mutualistic relationship. For example, lichens growing on mosses might exhibit enhanced photosynthetic production due to the elevated CO_2 concentration beneath moss-associated lichen thalli and slower desiccation, leading to prolonged periods of optimal net photosynthesis (Colesie et al., 2012). Furthermore, mosses can be colonized by cyanobacteria to form a moss-cyanobacteria association. In this association, cyanobacteria receive protection, carbon, and a suitable habitat from the mosses, while in return, they contribute to enhancing the growth of the mosses by fixing and supplying nitrogen, thereby enhancing nutrient availability (Rousk, 2022). In these cases, the cyanobacteria-associated mosses and moss-associated lichens are thus more likely to survive in the community than the free-living mosses and lichens. However, the mutualistic moss-cyanobacteria symbiosis may shift to a parasitic relationship, as abiotic conditions change (e.g., limiting nitrogen becomes more abundant; Neuhauser & Fargione, 2004; Rousk, 2022). Furthermore, the facilitative interaction between NVV species can shift to competition, depending on the environmental conditions (Maestre et al., 2010). Several studies found empirical evidence to support the conceptual model known as the stress gradient hypothesis (SGH). The SGH presumes that facilitation usually dominates biotic interactions in stressful conditions, while competition increases as the environment becomes more favorable (e.g., Li et al., 2013; Sun et al., 2021). Nevertheless, the validity of the SGH has been found to depend on the type of abiotic stress, spatial scale, and the studied community (Maestre et al., 2009, 2010). For instance, the transition from competition to facilitation along a water stress gradient was not confirmed between bryophyte colonies by Spitale (2009), but was observed between biological soil crusts-forming lichens at fine spatial scales (Maestre et al., 2009).

Biotic interactions can be linked with functional traits through, for example, the competitive ability of species (Kraft, Godoy, et al., 2015; Kunstler et al., 2012). For instance, growth height and lateral growth rate are two critical traits that influence the ability of species to capture light and space for growth and thus fitness (Chapter 3). However, although the competitive advantage is well correlated with single trait (Kraft, Godoy, et al., 2015), my study suggests that using a single trait to represent the competitive ability of species should be done with caution as no single-trait competition scheme could consistently explain the observed functional composition of the studied non-vascular communities (Chapter 3; Fig. 3.4). Furthermore, facilitative interactions may also be related to functional traits, such as the nitrogen use efficiency of moss-cyanobacteria association, which might be quantified by the energy cost for nitrogen fixation or the ratio of nitrogen supply to fixation. This trait determines the extent of gain on both sides of the facilitation, and thus plays a crucial role in determining their primary production and the assembly of the community. Therefore, trait-based approaches (e.g., LiBry model) are appropriate for quantifying the contribution of biotic interactions within NVV communities to community assembly.

4.2 Stochastic processes in NVV community assembly

In addition to environmental and biotic filters as deterministic processes, coexistence theories propose that stochastic processes (e.g., demographic drift, dispersal) act simultaneously with deterministic processes to shape the community structure (Hubbell, 2001; Vellend, 2010). For instance, dispersal limitation can constrain the establishment and expansion of NVV, even though they are well adapted to environmental conditions and produce high net growth (carbon balance). Therefore, dispersal limitation increases the randomness in community assembly and the resulting community structure (Munoz & Huneman, 2016). Furthermore, the priority effect is also a stochastic process that may affect the assembly of communities during species colonization, such as during recovery following a disturbance (Fukami, 2015; Fukami et al., 2010). After disturbance, the random arrival sequence can result in diverse successional trajectories for the community, since species arriving earlier may change environmental conditions and resources that impact the establishment of species arriving later.

The relative importance of deterministic and stochastic processes in community assembly varies with the studied habitats. Dispersal processes, for instance, play a crucial role in the assembly of savanna tree communities (van der Plas et al., 2015) but contribute less to shaping the tropical tree community structure in defaunated forests, where seed dispersal depends on large-bodied vertebrates (Hazelwood et al., 2020). Furthermore, the relative importance of species filtering and dispersal limitation in microbial communities in maize fields differs across latitudes (Jiao et al., 2020). In the case of NVV, stochastic processes dominate boreal bryophytes community assembly after fire disturbance (Fenton & Bergeron, 2013). However, the importance of stochastic processes relative to deterministic processes may fluctuate across spatial scales. Environmental filtering, for instance, tends to dominate in bryophyte communities at fine scales, whereas stochastic processes are more prominent at broad spatial scale (Monteiro et al., 2023). Therefore, the inclusion of stochastic processes in LiBry model is warranted for future studies to enhance the simulation of NVV community structure.

The relative importance of deterministic and stochastic processes can be analyzed by assessing the trait distribution patterns within the community (Gross et al., 2021; Monteiro et al., 2023), which is commonly quantified by using a variety of metrics such as trait variance, kurtosis, functional dispersion etc. (Aiba et al., 2013; Cornwell & Ackerly, 2009). Convergence of traits is expected when the trait combinations are selected and constrained by environmental filtering and competitive exclusion, based on competitive hierarchy (Chapter 3). Conversely, a random trait distribution from the potential range is expected when stochastic processes play a dominant role. However, this framework encounters challenges when the traits are not closely associated with environmental filtering and biotic interaction, such as respiratory Q_{10} value (Fig. 4.2). The trait distributions do not demonstrate clear convergence or divergence, posing difficulties in drawing conclusions based on the comparison of the simulated trait distribution to a random distribution.
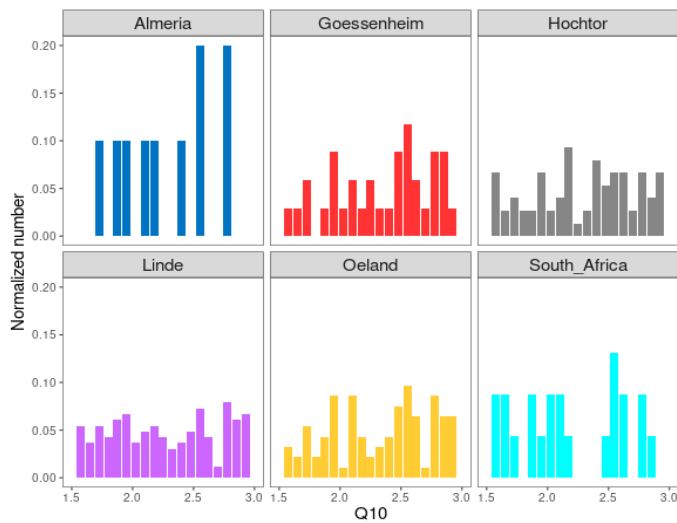
Figure 4.2: Frequency distribution of respiratory Q_{10} values for six study sites with different climatic conditions. The trait distributions were generated based on the selection of climatic factors and competition in LiBry model on surviving strategies with specific Q_{10} values. The survival is selected from 1000 randomly generated values with uniform probabilities between 1.5 and 3.0.

4.3 Implications for interpreting global diversity pattern

The global diversity pattern has always been a heated subject over the years in the field of ecological geography. The latitudinal diversity gradient (LDG) along which species richness increases from the poles towards the tropics is one of the most noticeable patterns, which has been widely recognized across diverse taxa including most vascular plants (Hillebrand, 2004). Nevertheless, this general global pattern seems not to be applicable to NVV such as mosses (Geffert et al., 2013). The general mechanisms driving these observed differences, however, are largely unknown.

A range of hypotheses have examined the drivers of this global diversity pattern (e.g., Currie et al., 2004; Mittelbach et al., 2007). A fundamental hypothesis is the tolerant hypothesis, which suggests that species assemblages are composed of a variety of functional strategies, each characterized by a combination of different physiological and morphological traits that enable their adaptation to environmental constraints (Bruelheide et al., 2018; Currie et al., 2004). In favourable climates, species assemblages can support a greater variety of trait combinations. In contrast, in more stressful climates, the potential trait space is constrained. Thereby, the difference in

LDG between NVV and vascular plants may be due to their different responses to community assembly drivers that shape the functional diversity and composition. Nevertheless, the specific community assembly drivers that shape the functional structure across spatial scales and contribute to the difference in LDG are poorly understood.

The insights acquired from studying key drivers of NVV community assemblages at local sites could provide hints to elucidate the different global diversity patterns. More specifically, the different patterns might be attributed to different microclimatic drivers of NVV (i.e., light and water), as well as to their different biochemical and ecophysiological trade-offs, which may lead to contrasting adaptations to the environment. For example, NVV possesses a functional trade-off between CO_2 diffusivity and metabolic activity that links to water saturation, inhibiting their growth in humid tropics. Thereby, adequate water input promotes the full activity of organisms, but it restricts the diffusion of CO_2 for photosynthesis, consequently limiting the growth of NVV organisms. However, vascular plants that lack this trade-off can maintain both high activity and CO_2 diffusivity by regulating stomata in humid regions. Therefore, having a better understanding of the community assembly of NVV and the functional diversity pattern can provide new insights into the mechanisms leading to this different global species richness pattern of NVV compared to vascular plants, and predict the change of richness pattern under climate change.
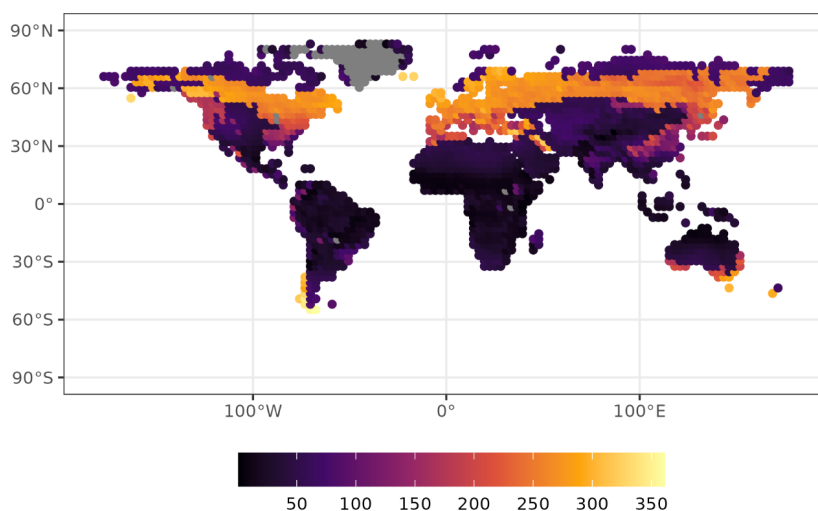
Figure 4.3: The global mean functional richness of non-vascular vegetation in grassland, forest floor, forest stem and canopy, simulated by the LiBry model.

I thus propose four hypotheses (H1-H4) to account for the observed variations in latitudinal diversity patterns:

H1: the different diversity pattern might result from the shading effect of the dense forest canopy in tropical lowlands, on NVV that usually grow in the tree canopy or understory. The lower light input would inhibit the photosynthetic productivity and fitness of NVV in the tropical lowland, consequently leading to a decrease in the diversity. However, the shading effect is less pronounced in boreal and temperate forests compared to tropical lowlands, as the forests in these regions are typically less dense.

H2: the different diversity pattern might stem from the unfavorable conditions of frequent wet-dry cycles during night and daytime for NVV in tropical lowland. NVV might become metabolically active, engaging in respiration and losing carbon, during the wet night, while it tends to become inactive during the warm and dry daytime because of high evapotranspiration.

H3: the different diversity pattern may be attributed to the typical trade-off between CO_2 diffusivity and metabolic activity of NVV, which is regulated by the water status. The high water input and low CO_2 diffusivity of NVV in tropical lowland may contribute to a low photosynthesis rate while vascular plants are well-adapted due to stomata regulation.

H4: the different diversity pattern may be due to lower temperatures of boreal and tundra regions compared to the tropical lowlands. These lower temperatures can be beneficial for the net productivity for NVV, coupled with the unique ability of NVV to remain inactive under freezing conditions, enhancing their survival in boreal and tundra regions. In contrast, vascular plants may be under water stress due to the lack of water input into the frozen soil surface during such conditions.

These hypotheses can be tested by conducting several sensitivity analyses of LiBry model that simulates the global functional diversity of NVV (the simulated distribution pattern of the number of surviving functional strategies by LiBry model is showed in Fig. 4.3). Completely testing and illustrating these four hypotheses in the model requires a substantial amount of effort, exceeding the scope of the current thesis.

Consequently, due to time constraints, this extensive implementation has not been included in the present study.

This study aims to explain the different global diversity pattern of NVV from the perspective of ecophysiological mechanisms and its regulation on community assembly at local scale. I have not considered the effects of stochastic ecological processes (e.g., limited dispersal and establishment rates of propagules especially in fragmented landscapes) on the assembly of NVV communities and the diversity pattern. Furthermore, the diversity pattern of vegetation may also be affected by geological and evolutionary processes at regional and continent scale (Antonelli et al., 2015; Moura et al., 2016). For instance, geographic isolation makes populations less connected and promotes extinction (Ouborg, 1993) and speciation over time (Kisel & Barraclough, 2010). High speciation and low extinction rates in an area with relatively stable climates such as humid tropical forests allow for a high number of species (Mittelbach et al., 2007). Climatic historical processes also have legacies in current plant distributions and biodiversity (Eiserhardt et al., 2015; Svenning et al., 2015).

4.4 Research perspectives in climate change impact

Climate change involves global warming that is particularly rapid in tundra regions (Bjorkman et al., 2018), elevated atmospheric CO_2 concentration, nitrogen deposition, and altered precipitation patterns etc. (IPCC 2021). Moreover, the climatic variability has notably intensified in recent times, leading to frequent occurrences of extreme events such as droughts and flooding (IPCC 2021). Climate change, profoundly driven by anthropogenic activities (Abbass et al., 2022), is changing the whole earth system and yielding remarkable global and local consequences on ecosystems worldwide, such as biodiversity loss, species distribution shift and altered biogeochemical cycles (Díaz et al., 2019; Maaroufi & De Long, 2020; Weiskopf et al., 2020). Despite overwhelming evidence revealing substantial impacts of climate change on non-vascular communities globally (see Porada et al., 2023), there is still a need for a deeper understanding of the mechanisms underlying the interplay between nonvascular communities and climate change. This knowledge is crucial to elucidate and predict how climate change affects community composition,

diversity, and ecosystem functions provided by NVV both now and in the future. Knowledge of community assembly processes can provide new insights, as climate change may act as environmental filters, directly affecting the fitness of individual NVV organisms, or indirectly affecting communities via impacting community-level interactions.

4.4.1 Direct impact of climate change

Climate change affects the fitness of individual NVV organisms and thereby the NVV communities by altering their responses to varied climates. The results from Chapter 2 provide insights into the impacts of several climatic factors on the individual lichen- and moss-dominated biocrusts across various climate zones by assessing the direction and magnitude of change in their annual carbon balance with the varied climatic factor. Nevertheless, it is important to note the limitations of this study in implying the impacts of climate change, as changes in these climatic factors are often coupled, which results in complex consequences. For example, the impact of elevated CO_2 concentration may be offset by decreasing levels of relative humidity, and the effects of combined climatic variables are non-additive (Baldauf et al., 2021).

Atmospheric CO_2 concentration

My study supports a substantial positive impact of the elevated atmospheric CO_2 concentration on the carbon balance (CO_2 fertilization) of biocrusts growing in all climatic zones (Fig. 2.6), but the magnitude of this CO_2 fertilization effect may vary under resource-limited conditions (e.g., nitrogen; Reich et al., 2006). While this CO_2 fertilization impact on vascular plants has been extensively investigated through experiments and models (e.g., Ainsworth & Long, 2005; Kolby Smith et al., 2016; Matthews, 2007; Terrer et al., 2019), it may be uncertain for NVV particularly under climate change scenarios in which multiple climatic factors interact. For instance, when elevated CO_2 concentrations and more frequent droughts are expected to occur simultaneously, the effect of elevated CO_2 concentrations may play a reduced role in the net productivity of NVV. This is attributed to longer periods of inactivity of NVV caused by frequent droughts, and consequently eliminates the effect of the improved CO_2 level.

Global warming

Experimental warming showed a substantial impact on the cover and diversity of lichen and moss communities (Ladrón de Guevara et al., 2018; Maestre et al., 2015). However, the impact direction of warming on moss cover was observed to be inconsistent in drylands: a shift from late successional stage (moss) to early stage (cyanobacteria) and thus a decline in moss cover was observed with experimental warming in Colorado Plateau (Ferrenberg et al., 2015), whereas other studies conducted in drylands (Escolar et al., 2012; Ladrón de Guevara et al., 2018) reported a slight increase in moss cover. Furthermore, warming may also hinder the recovery and succession of mosses after precipitation disturbance (Phillips et al., 2022), which has large consequences on the NVV community structure.

My study suggested a large negative impact of warming on the carbon balance of biocrusts in all climatic zones (Fig. 2.6). On the one hand, the effect of warming on NVV depends on the physiological characteristics of the organisms (i.e., optimum temperature for net photosynthesis). The typically low optimum temperature of organisms in alpine regions may account for the notably negative effect of increased temperature on these organisms (Fig. 2.6). Nevertheless, my study neglected the acclimation process of the physiology of NVV, which has been confirmed for various lichen and bryophyte species (Colesie et al., 2018; Hurtado et al., 2020; Lange & Green, 2005; Minami et al., 2005) and has large impact on the annual carbon balance (Fig. 2.8). The respiration rate of lichens, for example, acclimated to seasonal varied temperature (Lange & Green, 2005) while an increased freezing tolerance of bryophyte species was observed when exposed to lower temperature (Minami et al., 2005). However, the thermal acclimation is highly uncertain for NVV species as a species-specific acclimation process of net photosynthesis in lichens was observed (Colesie et al., 2018). This leads to uncertainty regarding the extent to which warming impacts the carbon balance and, consequently, the community structure of NVV.

On the other hand, the effect of warming is usually associated with a decreased humidity in many regions, attributed to higher evapotranspiration rates under warming conditions (Cook et al., 2014; Dai, 2011). For instance, warming reduced lichen cover, while the isolated impact of warming, distinct from the associated

decreased humidity, increased the lichen cover (Baldauf et al., 2021). The reduced humidity may reduce the water status of organisms, which largely affects the productivity of NVVs by altering the trade-off between CO_2 diffusivity and metabolic activity (Lange et al., 1994, 1996).

In addition to mean annual temperature, the diurnal temperature pattern might play an essential role in shaping the NVV communities. This could be attributed to the fact that temperature during the dark night affects the dark respiration rate, which directly influences carbon loss and, consequently, community assembly. The mean diurnal temperature range, for instance, has been identified as an essential factor impacting the composition of lichenised fungi and their global distribution (Liu et al., 2021).

Precipitation

Precipitation patterns, frequently altered due to climate change, was also identified as an important factor for the distribution of lichenised fungi (Liu et al., 2021). This finding aligns with other studies that highlight the crucial role of precipitation timing and seasonality in shaping the biocrust community diversity and composition (e.g., Bowker et al., 2016; Coe et al., 2012). The increased summertime precipitation frequency, for instance, leads to a shift from moss to cyanobacteria-dominated biocrusts (Zelikova et al., 2012). The variation in annual precipitation patterns between the two drylands in my study (D1 and D2) could potentially explain the contrasting impacts of decreased precipitation amount on the carbon balance of biocrusts in these areas (Fig. 2.6): the annual carbon balance decreases at site D1 while increases at site D2.

4.4.2 Indirect impact of climate change

In addition to the direct impact of climate change on NVV communities through affecting the productivity and growth of individual NVV organisms, climate change may also influence the NVV community by altering interactions within NVV as well as between NVV and vascular plants. NVV have higher tolerance to harsh environments, including drought, extreme heat, and freezing temperatures, compared to vascular plants. This indicates that in such challenging environments, vascular plants are less competitive for resources than NVV. Thereby, NVV tend to be more abundant in harsh climate conditions (Asplund et al., 2022). However, there

is a vital "tipping point" beyond which NVV cannot adapt and eventually die. For instance, NVV may die during prolonged drought periods, as they may expend energy on protective measures against desiccation damage (Hu et al., 2016; Oliver et al., 2000). Additionally, slow and incomplete recovery upon rehydration after prolonged desiccation may cause substantial carbon loss and thus mortality as well (Proctor, 2001). Moreover, the interactions between NVV species also depend on climate change: varied climatic factors may shift the position of NVV organisms along the continuum of competitive and facilitative interactions between NVV species (Maestre et al., 2010), and consequently affect the community composition and diversity.

Despite many studies that have shown how climate change has a substantial impact on NVV community composition and diversity, the extent to which climate change affects ecosystem functioning remains largely unknown. Hence, further investigations are warranted to understand the role of climate change in influencing functional community structure (e.g., trait distribution), directly related to ecosystem functioning. My study in Chapter 2 hints at how changes in various climatic factors affect NVV carbon balance and communities, but not functional trait distribution; Chapter 3, examines the effects of competition on the distribution of functional traits, yet lacks a relationship with different climatic conditions. Variation in traits were observed in response to different climatic factors. For example, the traits related to water uptake of lichen communities were found to change along aridity gradients in Mediterranean drylands (Matos et al., 2015). However, the underlying mechanisms require further research. The mechanistic process-based model LiBry, simulating the dynamics of functional strategies (trait combinations) in response to climatic factors, can provide possibilities to quantify and predict trait distribution as well as functional diversity of NVV communities in the climate change scenarios.

However, several uncertainties persist in the model, including the absence of key processes related to community assembly, such as dispersal limitation. Additionally, the model does not consider nutrient limitation on carbon assimilation, trait acclimation to varied climates, and the feedback of community change to climate, primarily due to limited knowledge. The shifted trait distribution of NVV communities can regulate the climate largely. For example, the biocrusts can strongly alter the

land-surface energy balance via decreasing soil surface albedo (Xiao & Bowker, 2020); the community weighted mean value of maximum water content increased under conditions of more light exposure (Gauslaa & Coxson, 2011), which may exert an increased evaporative cooling effect due to more water supply for evapotranspiration, and thus have impact on the climate in return.

4.5 Final remarks

In conclusion, my research aims to provide systematic and quantitative insights into the community assembly processes of non-vascular vegetation, with a particular focus on environmental filtering and competition. The study presented in Chapter 2 is one of the first to explore the relative importance of climatic factors in community assembly via impacting the carbon balance of NVV across various climatic zones. Moreover, the carbon balance of NVV under certain environmental conditions can be largely regulated by respiration-related physiological parameters, which may acclimate rapidly in different seasons (Lange & Green, 2005) and usually neglected in process-based models. Therefore, interpreting seasonal acclimation of traits in the model is essential to improve the simulations on community assembly for the future. The study presented in Chapter 3 is also one of the few studies to investigate the impact of competition on the assembly of nonvascular communities, with a particular focus on the functional composition. This study can be improved and extended by relating competition to a high-dimensional trait space and applying these insights to other ecosystems in diverse climatic zones.

Still, the community assembly of NVV is mostly studied using empirical approaches, making it challenging to uncover underlying mechanisms. The mechanistic process-based model LiBry applied in my research can explicitly simulate assembly processes based on biochemical and ecophysiological processes. Although there are still conceptual uncertainties in the model, and further development of other key community assembly processes is essential, such as dispersal limitation, all findings in the research are reliable. As a result, the research findings improve our mechanistic understanding of the nonvascular community assembly at local scale. The acquired knowledge of community assembly processes offers great potential for explaining the global diversity pattern of NVV and predicting its changes under climate change through the application of the model at a global scale.

References

Abbass, K., Qasim, M. Z., Song, H., Murshed, M., Mahmood, H., & Younis, I. (2022). A review of the global climate change impacts, adaptation, and sustainable mitigation measures. *Environmental Science and Pollution Research*, *29*, 42539–42559. https://doi.org/10.1007/s11356-022-19718-6

Aiba, M., Katabuchi, M., Takafumi, H., Matsuzaki, S. S., Sasaki, T., & Hiura, T. (2013). Robustness of trait distribution metrics for community assembly studies under the uncertainties of assembly processes. *Ecology*, *94*, 2873–2885. https://doi.org/10.1890/13-0269.1

Ainsworth, E. A., & Long, S. P. (2005). What have we learned from 15 years of free-air CO_2 enrichment (FACE)? A meta-analytic review of the responses of photosynthesis, canopy properties and plant production to rising CO_2. *New Phytologist*, *165*, 351–372. https://doi.org/10.1111/j.1469-8137.2004.01224.x

Antonelli, A., Zizka, A., Silvestro, D., Scharn, R., Cascales-Miñana, B., & Bacon, C. D. (2015). An engine for global plant diversity: Highest evolutionary turnover and emigration in the American tropics. *Frontiers in Genetics*, *6*. https://www.frontiersin.org/articles/10.3389/fgene.2015.00130

Asplund, J., van Zuijlen, K., Roos, R. E., Birkemoe, T., Klanderud, K., Lang, S. I., & Wardle, D. A. (2022). Divergent responses of functional diversity to an elevational gradient for vascular plants, bryophytes and lichens. *Journal of Vegetation Science*, *33*, e13105. https://doi.org/10.1111/jvs.13105

Bader, M. Y., Zotz, G., & Lange, O. L. (2010). How to minimize the sampling effort for obtaining reliable estimates of diel and annual CO_2 budgets in lichens. *Lichenologist, 42*, 97–111, https://doi.org/10.1017/S0024282909990338.

Baldauf, S., Guevara, M. L. de, Maestre, F. T., & Tietjen, B. (2018). Soil moisture dynamics under two rainfall frequency treatments drive early spring CO_2 gas exchange of lichen-dominated biocrusts in central Spain. *PeerJ*, *6*, e5904. https://doi.org/10.7717/peerj.5904

Baldauf, S., Porada, P., Raggio, J., Maestre, F. T., & Tietjen, B. (2021). Relative humidity predominantly determines long-term biocrust-forming lichen cover in

drylands under climate change. *Journal of Ecology*, *109*, 1370–1385. https://doi.org/10.1111/1365-2745.13563

Belnap, J., Büdel, B., & Lange, O. L. (2003). Biological Soil Crusts: Characteristics and Distribution. In J. Belnap & O. L. Lange (Eds.), *Biological Soil Crusts: Structure, Function, and Management* (pp. 3–30). Springer. https://doi.org/10.1007/978-3-642-56475-8_1

Belnap, J., Phillips, S. L., and Miller, M. E. (2004). Response of desert biological soil crusts to alterations in precipitation frequency, *Oecologia, 141*, 306–316, https://doi.org/10.1007/s00442-003-1438-6.

Belnap, J., Weber, B., & Büdel, B. (2016). Biological Soil Crusts as an Organizing Principle in Drylands. In B. Weber, B. Büdel, & J. Belnap (Eds.), *Biological Soil Crusts: An Organizing Principle in Drylands, Ecological Studies 226* (pp. 3–13). Springer International Publishing. https://doi.org/10.1007/978-3-319-30214-0_1

Beltrán-Sanz, N., Raggio, J., Pintado, A., Dal Grande, F., & García Sancho, L. (2023). Physiological Plasticity as a Strategy to Cope with Harsh Climatic Conditions: Ecophysiological Meta-Analysis of the Cosmopolitan Moss *Ceratodon purpureus* in the Southern Hemisphere. *Plants*, *12*, 499. https://doi.org/10.3390/plants12030499

Berzaghi, F., Wright, I. J., Kramer, K., Oddou-Muratorio, S., Bohn, F. J., Reyer, C. P. O., Sabaté, S., Sanders, T. G. M., & Hartig, F. (2020). Towards a New Generation of Trait-Flexible Vegetation Models. *Trends in Ecology & Evolution*, *35*, 191–205. https://doi.org/10.1016/j.tree.2019.11.006

Bittebiere, A.-K., Saiz, H., & Mony, C. (2019). New insights from multidimensional trait space responses to competition in two clonal plant species. *Functional Ecology*, *33*, 297–307. https://doi.org/10.1111/1365-2435.13220

Bjorkman, A. D., Myers-Smith, I. H., Elmendorf, S. C., Normand, S., Rüger, N., Beck, P. S. A., Blach-Overgaard, A., Blok, D., Cornelissen, J. H. C., Forbes, B. C., Georges, D., Goetz, S. J., Guay, K. C., Henry, G. H. R., HilleRisLambers, J., Hollister, R. D., Karger, D. N., Kattge, J., Manning, P., … Weiher, E. (2018). Plant functional trait change across a warming tundra biome. *Nature*, *562*, 57-62. https://doi.org/10.1038/s41586-018-0563-7

Bonan, G. (2015). *Ecological Climatology: Concepts and Applications*. Cambridge University Press.

Botta‑Dukát, Z. (2005). Rao's quadratic entropy as a measure of functional diversity based on multiple traits. *Journal of Vegetation Science*, *16*, 533–540. https://doi.org/10.1111/j.1654-1103.2005.tb02393.x

Bowker, M. A., Belnap, J., Büdel, B., Sannier, C., Pietrasiak, N., Eldridge, D. J., & Rivera-Aguilar, V. (2016). Controls on Distribution Patterns of Biological Soil Crusts at Micro- to Global Scales. In B. Weber, B. Büdel, & J. Belnap (Eds.), *Biological Soil Crusts: An Organizing Principle in Drylands* (pp. 173–197). Springer International Publishing. https://doi.org/10.1007/978-3-319-30214-0_10

Brooker, R. W., Maestre, F. T., Callaway, R. M., Lortie, C. L., Cavieres, L. A., Kunstler, G., Liancourt, P., Tielbörger, K., Travis, J. M. J., Anthelme, F., Armas, C., Coll, L., Corcket, E., Delzon, S., Forey, E., Kikvidze, Z., Olofsson, J., Pugnaire, F., Quiroz, C. L., … Michalet, R. (2008). Facilitation in Plant Communities: The Past, the Present, and the Future. *Journal of Ecology*, *96*, 18–34.

Bowker, M. A., Maestre, F. T., & Escolar, C. (2010). Biological crusts as a model system for examining the biodiversity–ecosystem function relationship in soils. *Soil Biology and Biochemistry, 42*, 405–417. https://doi.org/10.1016/j.soilbio.2009.10.025

Brostoff, W. N., Sharifi, M. R., & Rundel, P. W. (2005). Photosynthesis of cryptobiotic soil crusts in a seasonally inundated system of pans and dunes in the western Mojave Desert, CA: Field studies, *Flora: Morphology, Distribution, Functional Ecology of Plants, 200*, 592–600, https://doi.org/10.1016/j.flora.2005.06.008.

Bruelheide, H., Dengler, J., Purschke, O., Lenoir, J., Jiménez-Alfaro, B., Hennekens, S. M., Botta-Dukát, Z., Chytrý, M., Field, R., Jansen, F., Kattge, J., Pillar, V. D., Schrodt, F., Mahecha, M. D., Peet, R. K., Sandel, B., van Bodegom, P., Altman, J., Alvarez-Dávila, E., … Jandt, U. (2018). Global trait–environment relationships of plant communities. *Nature Ecology & Evolution*, *2*, 1906–1917. https://doi.org/10.1038/s41559-018-0699-8

Butler, E. E., Wythers, K. R., Flores-Moreno, H., Chen, M., Datta, A., Ricciuto, D. M., Atkin, O. K., Kattge, J., Thornton, P. E., Banerjee, A., & Reich, P. B. (2021). Updated respiration routines alter spatio-temporal patterns of carbon cycling in a global land surface model. *Environmental Research Letters*, *16*, 104015. https://doi.org/10.1088/1748-9326/ac2528

Büdel, B., Colesie, C., Green, T. G. A., Grube, M., Lázaro Suau, R., Loewen-Schnei der, K., Maier, S., Peer, T., Pintado, A., Raggio, J., Ruprecht, U., Sancho, L. G., Schroeter, B., Türk, R., Weber, B., Wedin, M., Westberg, M., Williams, L., & Zheng, L. (2014). Improved appreciation of the functioning and importance of biological soil crusts in Europe: The Soil Crust International Project (SCIN), *Biodiversity and Conservation, 23,* 1639–1658, https://doi.org/10.1007/s10531-014-0645-2.

Büdel, B., Williams, W. J., & Reichenberger, H. (2018). Annual net primary productivity of a cyanobacteria-dominated biological soil crust in the Gulf Savannah, Queensland, Australia, *Biogeosciences, 15*, 491–505, https://doi.org/10.5194/bg-15-491-2018.

Cahill, J. F., Kembel, S. W., Lamb, E. G., & Keddy, P. A. (2008). Does phylogenetic relatedness influence the strength of competition among vascular plants? *Perspectives in Plant Ecology, Evolution and Systematics*, *10*, 41–50. https://doi.org/10.1016/j.ppees.2007.10.001

Chalmandrier, L., Stouffer, D. B., Purcell, A. S. T., Lee, W. G., Tanentzap, A. J., & Laughlin, D. C. (2022). Predictions of biodiversity are improved by integrating trait‑based competition with abiotic filtering. *Ecology Letters, 25*, 1277–1289. https://doi.org/10.1111/ele.13980

Chamizo, S., Cantón, Y., Miralles, I., & Domingo, F. (2012). Biological soil crust development affects physicochemical characteristics of soil surface in semiarid ecosystems. *Soil Biology and Biochemistry*, *49*, 96–105. https://doi.org/10.1016/j.soilbio.2012.02.017

Chamizo, S., Rodríguez-Caballero, E., Moro, M. J., & Cantón, Y. (2021). Non-rainfall water inputs: A key water source for biocrust carbon fixation. *Science of The*

Total Environment, *792*, 148299.
https://doi.org/10.1016/j.scitotenv.2021.148299

Chen, N., Yu, K., Jia, R., Teng, J., & Zhao, C. (2020). Biocrust as one of multiple stable states in global drylands. *Science Advances*, *6*, eaay3763. https://doi.org/10.1126/sciadv.aay3763

Chesson, P. (2000). Mechanisms of Maintenance of Species Diversity. *Annual Review of Ecology and Systematics*, *31*, 343–366. https://doi.org/10.1146/annurev.ecolsys.31.1.343

Chesson, P. (2020). Chapter 2: Species coexistence. In K. S. McCann & G. Gellner (Eds.), *Theoretical ecology: concepts and applications* (pp. 5–27). Oxford University Press.

Coe, K. K., Belnap, J., Grote, E. E., & Sparks, J. P. (2012). Physiological ecology of desert biocrust moss following 10 years exposure to elevated CO_2: Evidence for enhanced photosynthetic thermotolerance. *Physiologia Plantarum, 144*, 346–356, https://doi.org/10.1111/j.1399-3054.2012.01566.x.

Coe, K. K., Belnap, J., & Sparks, J. P. (2012). Precipitation‐driven carbon balance controls survivorship of desert biocrust mosses. *Ecology*, *93*, 1626–1636. https://doi.org/10.1890/11-2247.1

Coe, K. K., Sparks, J. P., & Belnap, J. (2014). Physiological Ecology of Dryland Biocrust Mosses. In D. T. Hanson & S. K. Rice (Eds.), *Photosynthesis in Bryophytes and Early Land Plants* (pp. 291–308). Springer Netherlands. https://doi.org/10.1007/978-94-007-6988-5_16

Colesie, C., Allan Green, T. G., Haferkamp, I., & Büdel, B. (2014). Habitat stress initiates changes in composition, CO_2 gas exchange and C-allocation as life traits in biological soil crusts. *The ISME Journal*, *8*, 2104–2115. https://doi.org/10.1038/ismej.2014.47

Colesie, C., Green, T. G. A., Raggio, J., & Büdel, B. (2016). Summer Activity Patterns of Antarctic and High Alpine Lichendominated Biological Soil Crusts – Similar But Different? *Arctic, Antarctic, and Alpine Research, 48,* 449–460, https://doi.org/10.1657/AAAR0015-047.

Colesie, C., Büdel, B., Hurry, V., & Green, T. G. A. (2018). Can Antarctic lichens acclimatize to changes in temperature? *Global Change Biology*, *24*, 1123–1135. https://doi.org/10.1111/gcb.13984

Colesie, C., Scheu, S., Green, T. G. A., Weber, B., Wirth, R., & Büdel, B. (2012). The advantage of growing on moss: Facilitative effects on photosynthetic performance and growth in the cyanobacterial lichen *Peltigera rufescens*. *Oecologia*, *169*, 599–607. https://doi.org/10.1007/s00442-011-2224-5

Concostrina‑Zubiri, L., Valencia, E., Ochoa, V., Gozalo, B., Mendoza, B. J., & Maestre, F. T. (2021). Species-specific effects of biocrust-forming lichens on soil properties under simulated climate change are driven by functional traits. *New Phytologist, 230*, 101–115. https://doi.org/10.1111/nph.17143

Conti, G., & Díaz, S. (2013). Plant functional diversity and carbon storage—An empirical test in semi-arid forest ecosystems. *Journal of Ecology*, *101*, 18–28. https://doi.org/10.1111/1365-2745.12012

Cook, B. I., Smerdon, J. E., Seager, R., & Coats, S. (2014). Global warming and 21st century drying. *Climate Dynamics*, *43*, 2607–2627. https://doi.org/10.1007/s00382-014-2075-y

Cornwell, W. K., & Ackerly, D. D. (2009). Community assembly and shifts in plant trait distributions across an environmental gradient in coastal California. *Ecological Monographs*, *79*(1), 109–126. https://doi.org/10.1890/07-1134.1

Cornwell, W. K., Schwilk, D. W., & Ackerly, D. D. (2006). A Trait-Based Test for Habitat Filtering: Convex Hull Volume. *Ecology*, *87*, 1465–1471. https://doi.org/10.1890/0012-9658(2006)87[1465:ATTFHF]2.0.CO;2

Cowan, I. R., Lange, O. L., & Green, T. G. A. (1992). Carbon-dioxide exchange in lichens: Determination of transport and carboxylation characteristics. *Planta*, *187*, 282–294. https://doi.org/10.1007/BF00201952

Coyle, J. R. (2017). Intraspecific variation in epiphyte functional traits reveals limited effects of microclimate on community assembly in temperate deciduous oak canopies. *Oikos, 126*, 111–120. https://doi.org/10.1111/oik.03239

Cramer, W., Bondeau, A., Woodward, F. I., Prentice, I. C., Betts, R. A., Brovkin, V., Cox, P. M., Fisher, V., Foley, J. A., Friend, A. D., Kucharik, C., Lomas, M. R.,

Ramankutty, N., Sitch, S., Smith, B., White, A., & Young-Molling, C. (2001). Global response of terrestrial ecosystem structure and function to CO_2 and climate change: Results from six dynamic global vegetation models. *Global Change Biology*, *7*, 357–373. https://doi.org/10.1046/j.1365-2486.2001.00383.x

Crous, K. Y., Uddling, J., & De Kauwe, M. G. (2022). Temperature responses of photosynthesis and respiration in evergreen trees from boreal to tropical latitudes. *New Phytologist*, *234*(2), 353–374. https://doi.org/10.1111/nph.17951

Currie, D. J., Mittelbach, G. G., Cornell, H. V., Field, R., Guégan, J.-F., Hawkins, B. A., Kaufman, D. M., Kerr, J. T., Oberdorff, T., O'Brien, E., & Turner, J. R. G. (2004). Predictions and tests of climate-based hypotheses of broad-scale variation in taxonomic richness. *Ecology Letters*, *7*, 1121–1134. https://doi.org/10.1111/j.1461-0248.2004.00671.x

Dai, A. (2011). Drought under global warming: a review. *WIREs Climate Change*, *2*(1), 45–65. https://doi.org/10.1002/wcc.81

Darrouzet-Nardi, A., Reed, S. C., Grote, E. E., & Belnap, J. (2015). Observations of net soil exchange of CO_2 in a dryland show experimental warming increases carbon losses in biocrust soils. *Biogeochemistry, 126*, 363–378, https://doi.org/10.1007/s10533-015-0163-7.

Díaz, F. P., Latorre, C., Carrasco-Puga, G., Wood, J. R., Wilmshurst, J. M., Soto, D. C., Cole, T. L., & Gutiérrez, R. A. (2019). Multiscale climate change impacts on plant diversity in the Atacama Desert. *Global Change Biology*, *25*, 1733–1745. https://doi.org/10.1111/gcb.14583

Díaz, S., & Cabido, M. (2001). Vive la différence: Plant functional diversity matters to ecosystem processes. *Trends in Ecology & Evolution, 16*(11), 646–655. https://doi.org/10.1016/S0169-5347(01)02283-2

Díaz, S., Lavorel, S., de Bello, F., Quétier, F., Grigulis, K., & Robson, T. M. (2007). Incorporating plant functional diversity effects in ecosystem service assessments. *Proceedings of the National Academy of Sciences*, *104*, 20684–20689. https://doi.org/10.1073/pnas.0704716104

Diez, M., Schmitt, D., Küppers, M., Wachendorf, M., Stefan, T., Gypser, S., & Veste, M. (2019). Modelling photosynthesis and carbon fluxes of moss-and lichen-dominated biological soil crusts in temperate dry acid grasslands in Branden-burg, *49th Annual Meeting of the Ecological Society of Germany, Austria and Switzerland, Münster, Germany*, 9–13 September 2019. https://doi.org/10.13140/RG.2.2.27244.51849.

Di Nuzzo, L., Canali, G., Giordani, P., Nascimbene, J., Benesperi, R., Papini, A., Bianchi, E., & Porada, P. (2022). Life-stage dependent response of the epiphytic lichen *Lobaria pulmonaria* to climate. *Frontiers in Forests and Global Change, 5*. https://doi.org/10.3389/ffgc.2022.903607

Dilks, T. J. K., & Proctor, M. C. F. (1979). Photosynthesis, Respiration and Water Content in Bryophytes. *New Phytologist, 82*, 97–114. https://doi.org/10.1111/j.1469-8137.1979.tb07564.x

Doebeli, M., & Ispolatov, I. (2010). Complexity and Diversity. *Science, 328*, 494–497. https://doi.org/10.1126/science.1187468

During H.J. & Ter Horst B (1987). Diversity and dynamics in bryophyte communities on earth banks in a Dutch forest. *Symposia Biological Hungarica 35,* 447–455

During, H. J., & Tooren, B. F. V. (1990). Bryophyte interactions with other plants. *Botanical Journal of the Linnean Society, 104*, 79–98. https://doi.org/10.1111/j.1095-8339.1990.tb02212.x

Dümig, A., Veste, M., Hagedorn, F., Fischer, T., Lange, P., Spröte, R., & Kögel-Knabner, I. (2014). Organic matter from biological soil crusts induces the initial formation of sandy temperate soils, *Catena, 122,* 196–208, https://doi.org/10.1016/j.catena.2014.06.011.

Drake, J. E., Tjoelker, M. G., Aspinwall, M. J., Reich, P. B., Barton, C. V. M., Medlyn, B. E., & Duursma, R. A. (2016). Does physiological acclimation to climate warming stabilize the ratio of canopy respiration to photosynthesis? *New Phytologist*, *211*, 850–863. https://doi.org/10.1111/nph.13978

Eiserhardt, W. L., Borchsenius, F., Sandel, B., Kissling, W. D., & Svenning, J.-C. (2015). Late Cenozoic climate and the phylogenetic structure of regional conifer floras world-wide. *Global Ecology and Biogeography*, *24*, 1136–1148. https://doi.org/10.1111/geb.12350

Elbert, W., Weber, B., Burrows, S., Steinkamp, J., Büdel, B., Andreae, M. O., & Pöschl, U. (2012). Contribution of cryptogamic covers to the global cycles of carbon and nitrogen, *Nature Geoscience, 5,* 459–462, https://doi.org/10.1038/ngeo1486.

Escolar, C., Martínez, I., Bowker, M. A., & Maestre, F. T. (2012). Warming reduces the growth and diversity of biological soil crusts in a semi-arid environment: Implications for ecosystem structure and functioning. *Philosophical Transactions of the Royal Society B: Biological Sciences*, *367*, 3087–3099. https://doi.org/10.1098/rstb.2011.0344

Ewel, J. J., Mazzarino, M. J., & Berish, C. W. (1991). Tropical Soil Fertility Changes Under Monocultures and Successional Communities of Different Structure. *Ecological Applications*, *1*, 289–302. https://doi.org/10.2307/1941758

Falster, D. S., Brännström, Å., Westoby, M., & Dieckmann, U. (2017). Multitrait successional forest dynamics enable diverse competitive coexistence. *Proceedings of the National Academy of Sciences, 114*, E2719–E2728. https://doi.org/10.1073/pnas.1610206114

Falster, D. S., Kunstler, G., FitzJohn, R. G., & Westoby, M. (2021). Emergent Shapes of Trait-Based Competition Functions from Resource-Based Models: A Gaussian Is Not Normal in Plant Communities. *The American Naturalist, 198*, 253–267. https://doi.org/10.1086/714868

Farquhar, G. D., & von Caemmerer, S. (1982). Modelling of Photosynthetic Response to Environmental Conditions. In Lange O. L., Nobel, P. S., Osmond, C. B., and Ziegler, H. (Eds.), *Physiological Plant Ecology II* (pp. 549–587). Springer. https://doi.org/10.1007/978-3-642-68150-9_17

Färber, L., Solhaug, K. A., Esseen, P.-A., Bilger, W., & Gauslaa, Y. (2014). Sunscreening fungal pigments influence the vertical gradient of pendulous lichens in boreal forest canopies. *Ecology*, *95*, 1464–1471. https://doi.org/10.1890/13-2319.1

Feng, W., Zhang, Y., Wu, B., Qin, S., & Lai, Z. (2014). Influence of Environmental Factors on Carbon Dioxide Exchange in Biological Soil Crusts in Desert Areas,

Arid Land Research and Management, *28*, 186–196, https://doi.org/ 10.1080/15324982.2013.835006.

Fenton, N. J., & Bergeron, Y. (2013). Stochastic processes dominate during boreal bryophyte community assembly. *Ecology*, *94*, 1993–2006. https://doi.org/10.1890/12-1944.1

Ferrenberg, S., Faist, A. M., Howell, A., & Reed, S. C. (2018). Biocrusts enhance soil fertility and *Bromus tectorum* growth, and interact with warming to influence germination, *Plant and Soil*, 429, 77–90, https://doi.org/10.1007/s11104-017-3525-1.

Ferrenberg, S., Reed, S. C., & Belnap, J. (2015). Climate change and physical disturbance cause similar community shifts in biological soil crusts. *Proceedings of the National Academy of Sciences*, *112*, 12116–12121. https://doi.org/10.1073/pnas.1509150112

Fukami, T. (2015). Historical Contingency in Community Assembly: Integrating Niches, Species Pools, and Priority Effects. *Annual Review of Ecology, Evolution, and Systematics*, *46*, 1–23. https://doi.org/10.1146/annurev-ecolsys-110411-160340

Fukami, T., Dickie, I. A., Paula Wilkie, J., Paulus, B. C., Park, D., Roberts, A., Buchanan, P. K., & Allen, R. B. (2010). Assembly history dictates ecosystem functioning: Evidence from wood decomposer communities. *Ecology Letters*, *13*, 675–684. https://doi.org/10.1111/j.1461-0248.2010.01465.x

Gauslaa, Y., & Coxson, D. (2011). Interspecific and intraspecific variations in water storage in epiphytic old forest foliose lichens. *Botany*, *89*, 787–798. https://doi.org/10.1139/b11-070

Gauslaa, Y., Lie, M., Solhaug, K. A., & Ohlson, M. (2006). Growth and ecophysiological acclimation of the foliose lichen *Lobaria pulmonaria* in forests with contrasting light climates, *Oecologia, 147,* 406–416, https://doi.org/10.1007/ s00442-005-0283-1.

Geffert, J. L., Frahm, J.-P., Barthlott, W., & Mutke, J. (2013). Global moss diversity: spatial and taxonomic patterns of species richness. *Journal of Bryology*, *35*, 1–11. https://doi.org/10.1179/1743282012Y.0000000038

Gheza, G., Di Nuzzo, L., Vallese, C., Barcella, M., Benesperi, R., Giordani, P., Nascimbene, J., & Assini, S. (2021). Morphological and Chemical Traits of Cladonia Respond to Multiple Environmental Factors in Acidic Dry Grasslands. *Microorganisms, 9*, 453. https://doi.org/10.3390/microorganisms9020453

Gong, J., Roulet, N., Frolking, S., Peltola, H., Laine, A. M., Kokkonen, N., & Tuittila, E.-S. (2020). Modelling the habitat preference of two key *Sphagnum* species in a poor fen as controlled by capitulum water content. *Biogeosciences, 17*, 5693–5719. https://doi.org/10.5194/bg-17-5693-2020

Green, T. G. A. & Lange, O. L. (1991). Ecophysiological adaptations of the lichen genera *pseudocyphellaria* and *sticta* to south temperate rainforests, *Lichenologist, 23*, 267–282, https://doi.org/10.1017/S0024282991000427.

Green, T. G. A., Sancho, L. G., & Pintado, A. (2011). Ecophysiology of Desiccation/Rehydration Cycles in Mosses and Lichens. In U. Lüttge, E. Beck, & D. Bartels (Eds.), *Plant Desiccation Tolerance* (pp. 89–120). Springer. https://doi.org/10.1007/978-3-642-19106-0_6

Groenendijk, M., Dolman, A. J., van der Molen, M. K., Leuning, R., Arneth, A., Delpierre, N., Gash, J. H. C., Lindroth, A., Richardson, A. D., Verbeeck, H., & Wohlfahrt, G. (2011). Assessing parameter variability in a photosynthesis model within and between plant functional types using global Fluxnet eddy covariance data. *Agricultural and Forest Meteorology*, *151*, 22–38. https://doi.org/10.1016/j.agrformet.2010.08.013

Groner, V. P., Raddatz, T., Reick, C. H., & Claussen, M. (2018). Plant functional diversity affects climate–vegetation interaction. *Biogeosciences*, *15*, 1947–1968. https://doi.org/10.5194/bg-15-1947-2018

Gross, N., Le Bagousse‑Pinguet, Y., Liancourt, P., Saiz, H., Violle, C., & Munoz, F. (2021). Unveiling ecological assembly rules from commonalities in trait distributions. *Ecology Letters*, *24*, 1668–1680. https://doi.org/10.1111/ele.13789

Gross, N., Liancourt, P., Butters, R., Duncan, R. P., & Hulme, P. E. (2015). Functional equivalence, competitive hierarchy and facilitation determine species

coexistence in highly invaded grasslands. *New Phytologist*, *206*, 175–186. https://doi.org/10.1111/nph.13168

Grote, E. E., Belnap, J., Housman, D. C., & Sparks, J. P. (2010). Carbon exchange in biological soil crust communities under differential temperatures and soil water contents: Implications for global change. *Global Change Biology*, *16*, 2763–2774. https://doi.org/10.1111/j.1365-2486.2010.02201.x

Haarmeyer, D. H., Luther-Mosebach, J., Dengler, J., Schmiedel, U., Finckh, M., Berger, K., Deckert, J., … Jürgens, N. (2010). The BIOTA Observatories. In Jürgens N., Haarmeyer D. H., Luther-Mosebach, J., Dengler, J., Finckh, M., & Schmiedel U. (Eds.), *Biodiversity in southern Africa. Volume I: Patterns at local scale - the BIOTA Observatories* (pp. 6–801). Klaus Hess Publisher, Göttingen & Windhoek. ISBN 978-3-933117-45- 8 (Germany), ISBN 978-99916-57-31-8 (Namibia).

Hanson, D. T., & Rice, S. K. (Eds.) (2014). *Photosynthesis in Bryophytes and Early Land Plants* (Vol. 37). Springer. https://doi.org/10.1007/978-94-007-6988-5

Harrison, S. P., Cramer, W., Franklin, O., Prentice, I. C., Wang, H., Brännström, Å., Boer, H., Dieckmann, U., Joshi, J., Keenan, T. F., Lavergne, A., Manzoni, S., Mengoli, G., Morfopoulos, C., Peñuelas, J., Pietsch, S., Rebel, K. T., Ryu, Y., Smith, N. G., … Wright, I. J. (2021). Eco-evolutionary optimality as a means to improve vegetation and land-surface models. *New Phytologist, 231*, 2125–2141. https://doi.org/10.1111/nph.17558

Haverd, V., Smith, B., Nieradzik, L., Briggs, P. R., Woodgate, W., Trudinger, C. M., Canadell, J. G., & Cuntz, M. (2018). A new version of the CABLE land surface model (Subversion revision r4601) incorporating land use and land cover change, woody vegetation demography, and a novel optimisation-based approach to plant coordination of photosynthesis. *Geoscientific Model Development*, *11*, 2995–3026. https://doi.org/10.5194/gmd-11-2995-2018

Hazelwood, K., Paine, C. E. T., Cornejo Valverde, F. H., Pringle, E. G., Beck, H., & Terborgh, J. (2020). Changes in tree community structure in defaunated forests are not driven only by dispersal limitation. *Ecology and Evolution*, *10*, 3392–3401. https://doi.org/10.1002/ece3.6133

Heitman, J. L., & Horton, R. (2011). Coupled Heat and Water Transfer in Soil. In J. Gliński, J. Horabik, & J. Lipiec (Eds.), *Encyclopedia of Agrophysics* (pp. 155–162). Springer. https://doi.org/10.1007/978-90-481-3585-1_33

Herben, T., & Goldberg, D. E. (2014). Community assembly by limiting similarity vs. competitive hierarchies: Testing the consequences of dispersion of individual traits. *Journal of Ecology*, *102*, 156–166. https://doi.org/10.1111/1365-2745.12181

Higgins, S. I., Larcombe, M. J., Beeton, N. J., Conradi, T., & Nottebrock, H. (2020). Predictive ability of a process‐based versus a correlative species distribution model. *Ecology and Evolution, 10,* 11043–11054. https://doi.org/10.1002/ece3.6712

Hillebrand, H. (2004). On the Generality of the Latitudinal Diversity Gradient. *The American Naturalist*, *163*(2), 192–211. https://doi.org/10.1086/381004

Holmgren, M., Hirota, M., van Nes, E. H., & Scheffer, M. (2013). Effects of interannual climate variability on tropical tree cover. *Nature Climate Change*, *3*, 755-758. https://doi.org/10.1038/nclimate1906

Hu, R., Xiao, L., Bao, F., Li, X., & He, Y. (2016). Dehydration-responsive features of Atrichum undulatum. *Journal of Plant Research*, *129*, 945–954. https://doi.org/10.1007/s10265-016-0836-x

Hubbell, S. P. (2001). *The Unified Neutral Theory of Biodiversity and Biogeography (MPB-32)*. Princeton University Press. ISBN 9780691021287

Hurtado, P., Prieto, M., Martínez-Vilalta, J., Giordani, P., Aragón, G., López-Angulo, J., Košuthová, A., Merinero, S., Díaz-Peña, E. M., Rosas, T., Benesperi, R., Bianchi, E., Grube, M., Mayrhofer, H., Nascimbene, J., Wedin, M., Westberg, M., & Martínez, I. (2020). Disentangling functional trait variation and covariation in epiphytic lichens along a continent-wide latitudinal gradient. *Proceedings of the Royal Society B: Biological Sciences*, *287*, 20192862. https://doi.org/10.1098/rspb.2019.2862

IPCC, 2021: *Climate Change 2021 - The Physical Science Basis: Contribution of Working Group I to the Sixth Assessment Report of the Intergovernmental*

Panel on Climate Change. Cambridge University Press, https://doi.org/10.1017/9781009157896.

Jeffries, D. L., Link, S. O., & Klopatek, J. M. (1993). CO_2 fluxes of cryptogamic crusts: I. Response to resaturation, *New Phytologist, 125*, 163–173, https://doi.org/https://doi.org/10.1111/j.1469-8137.1993.tb03874.x.

Jiao, S., Yang, Y., Xu, Y., Zhang, J., & Lu, Y. (2020). Balance between community assembly processes mediates species coexistence in agricultural soil microbiomes across eastern China. *The ISME Journal*, *14*, 202-216. https://doi.org/10.1038/s41396-019-0522-9

Jones, V. A. S., & Dolan, L. (2012). The evolution of root hairs and rhizoids. *Annals of Botany*, *110*, 205–212. https://doi.org/10.1093/aob/mcs136

Kattge, J., Díaz, S., Lavorel, S., Prentice, I. C., Leadley, P., Bönisch, G., Garnier, E., Westoby, M., Reich, P. B., Wright, I. J., Cornelissen, J. H. C., Violle, C., Harrison, S. P., Van Bodegom, P. M., Reichstein, M., Enquist, B. J., Soudzilovskaia, N. A., Ackerly, D. D., Anand, M., … Wirth, C. (2011). TRY – a global database of plant traits. *Global Change Biology*, *17*, 2905–2935. https://doi.org/10.1111/j.1365-2486.2011.02451.x

Keddy, P. A. (1989) Competition. Chapman and Hall, London.

Keddy, P. A. (1992). Assembly and response rules: Two goals for predictive community ecology. *Journal of Vegetation Science*, *3*, 157–164. https://doi.org/10.2307/3235676

Kershaw, K. A., & Webber, M. R. (1986). Seasonal changes in the chlorophyll content and quantum efficiency of the moss *Brachythecium rutabulum*. *Journal of Bryology, 14*, 151–158. https://doi.org/10.1179/jbr.1986.14.1.151

Kleinhesselink, A. R., Kraft, N. J. B., Pacala, S. W., & Levine, J. M. (2022). Detecting and interpreting higher-order interactions in ecological communities. *Ecology Letters, 25*, 1604–1617. https://doi.org/10.1111/ele.14022

Kisel, Y., & Barraclough, T. G. (2010). Speciation Has a Spatial Scale That Depends on Levels of Gene Flow. *The American Naturalist*, *175*, 316–334. https://doi.org/10.1086/650369

Kolby Smith, W., Reed, S. C., Cleveland, C. C., Ballantyne, A. P., Anderegg, W. R. L., Wieder, W. R., Liu, Y. Y., & Running, S. W. (2016). Large divergence of satellite and Earth system model estimates of global terrestrial CO_2 fertilization. *Nature Climate Change*, *6*, 306-310. https://doi.org/10.1038/nclimate2879

Kraft, N. J. B., & Ackerly, D. D. (2010). Functional trait and phylogenetic tests of community assembly across spatial scales in an Amazonian Forest. *Ecological Monographs*, *80*, 401–422. https://doi.org/10.1890/09-1672.1

Kraft, N. J. B., Adler, P. B., Godoy, O., James, E. C., Fuller, S., & Levine, J. M. (2015). Community assembly, coexistence and the environmental filtering metaphor. *Functional Ecology*, *29*, 592–599. https://doi.org/10.1111/1365-2435.12345

Kraft, N. J. B., Godoy, O., & Levine, J. M. (2015). Plant functional traits and the multidimensional nature of species coexistence. *Proceedings of the National Academy of Sciences*, *112*, 797–802. https://doi.org/10.1073/pnas.1413650112

Kunstler, G., Lavergne, S., Courbaud, B., Thuiller, W., Vieilledent, G., Zimmermann, N. E., Kattge, J., & Coomes, D. A. (2012). Competitive interactions between forest trees are driven by species' trait hierarchy, not phylogenetic or functional similarity: Implications for forest community assembly. *Ecology Letters*, *15*, 831–840. https://doi.org/10.1111/j.1461-0248.2012.01803.x

Ladrón de Guevara, M., Lázaro, R., Quero, J. L., Ochoa, V., Gozalo, B., Berdugo, M., Uclés, O., Escolar, C., & Maestre, F. T. (2014). Simulated climate change reduced the capacity of lichen-dominated biocrusts to act as carbon sinks in two semi-arid Mediterranean ecosystems, *Biodiversity and Conservation, 23*, 1787–1807, https://doi.org/10.1007/s10531-014-0681-y.

Ladrón de Guevara, M., Gozalo, B., Raggio, J., Lafuente, A., Prieto, M., & Maestre, F. T. (2018). Warming reduces the cover, richness and evenness of lichen-dominated biocrusts but promotes moss growth: Insights from an 8 yr experiment. *New Phytologist*, *220*, 811–823. https://doi.org/10.1111/nph.15000

Lakatos, M., Rascher, U., & Büdel, B. (2006). Functional characteristics of corticolous lichens in the understory of a tropical lowland rain forest. *New Phytologist*, *172*, 679–695. https://doi.org/10.1111/j.1469-8137.2006.01871.x

Lange, O. L. (1980). Moisture content and CO_2 exchange of lichens – I. Influence of temperature on moisture-dependent net photosynthesis and dark respiration in *Ramalina maciformis, Oecologia, 45*, 82–87, https://doi.org/10.1007/BF00346710.

Lange, O. L. (2002). Photosynthetic productivity of the epilithic lichen *Lecanora muralis*: Long-term field monitoring of CO_2 exchange and its physiological interpretation. I. Dependence of photosynthesis on water content, light, temperature, and CO_2 concentration from laboratory measurements. *Flora - Morphology, Distribution, Functional Ecology of Plants*, *197*, 233–249. https://doi.org/10.1078/0367-2530-00038

Lange, O. L. (2003). Photosynthetic productivity of the epilithic lichen *Lecanora muralis*: Long-term field monitoring of CO_2 exchange and its physiological interpretation. III. Diel, seasonal, and annual carbon budgets, *Flora - Morphology, Distribution, Functional Ecology of Plants*, *198*, 277–292, https://doi.org/10.1078/0367-2530-00100.

Lange, O. L., Belnap, J., Reichenberger, H., & Meyer, A. (1997). Photosynthesis of green algal soil crust lichens from arid lands in southern Utah, USA: Role of water content on light and temperature responses of CO_2 exchange, *Flora, 192*, 1–15, https://doi.org/10.1016/S0367-2530(17)30749-1.

Lange, O. L., Belnap, J., & Reichenberger, H. (1998). Photosynthesis of the cyanobacterial soil-crust lichen *Collema tenax* from arid lands in southern Utah, USA: Role of water content on light and temperature responses of CO_2 exchange: Photosynthesis of the cyanobacterial soil-crust lichen *Collema tenax*. *Functional Ecology*, *12*, 195–202. https://doi.org/10.1046/j.1365-2435.1998.00192.x

Lange, O. L., Büdel, B., Heber, U., Meyer, A., Zellner, H., & Green, T. G. A. (1993). Temperate rainforest lichens in New Zealand: High thallus water content can severely limit photosynthetic CO_2 exchange. *Oecologia, 95*, 303–313. https://doi.org/10.1007/BF00320981

Lange, O. L., & Green, T. G. A. (2005). Lichens show that fungi can acclimate their respiration to seasonal changes in temperature. *Oecologia*, *142,* 11–19. https://doi.org/10.1007/s00442-004-1697-x

Lange, O. L., Green, T. G. A., & Heber, U. (2001). Hydration‑dependent photosynthetic production of lichens: What do laboratory studies tell us about field performance? *Journal of Experimental Botany*, *52*, 2033–2042. https://doi.org/10.1093/jexbot/52.363.2033

Lange, O. L., Green, T. G. A., Melzer, B., Meyer, A., & Zellner, H. (2006). Water relations and CO_2 exchange of the terrestrial lichen *Teloschistes capensis* in the Namib fog desert: Measurements during two seasons in the field and under controlled conditions, *Flora - Morphology, Distribution, Functional Ecology of Plants, 201,* 268–280, https://doi.org/10.1016/j.flora.2005.08.003.

Lange, O. L., Green, T. G. A., & Reichenberger, H. (1999). The Response of Lichen Photosynthesis to External CO_2 Concentration and its Interaction with Thallus Water-status. *Journal of Plant Physiology*, *154*, 157–166. https://doi.org/10.1016/S0176-1617(99)80204-1

Lange, O. L., Green, T. G. A., Reichenberger, H., & Meyer, A. (1996). Photosynthetic Depression at High Thallus Water Contents in Lichens: Concurrent Use of Gas Exchange and Fluorescence Techniques with a Cyanobacterial and a Green Algal *Peltigera* Species. *Botanica Acta*, *109*, 43–50. https://doi.org/10.1111/j.1438-8677.1996.tb00868.x

Lange, O. L., Meyer, A., Zellner, H., & Heber, U. (1994). Photosynthesis and Water Relations of Lichen Soil Crusts: Field Measurements in the Coastal Fog Zone of the Namib Desert. *Functional Ecology*, *8*, 253. https://doi.org/10.2307/2389909

Lange, O. L., Reichenberger, H., & Meyer, A. (1995). High thallus water content and photosynthetic CO_2 exchange of lichens. Laboratory experiments with soil crust species from local xerothermic steppe formations in Franconia, Germany. In Daniels, F., Schulz, M., Peine, J. (Eds.), *Flechten Follmann: contributions to lichenology in honour of Gerhard Follmann, Geobotanical and Phyto‑taxonomical Study Group, University of Cologne*, 139–153, ISBN 3 87429 380 7.

Lavorel, S., & Garnier, E. (2002). Predicting changes in community composition and ecosystem functioning from plant traits: Revisiting the Holy Grail. *Functional Ecology, 16*, 545–556. https://doi.org/10.1046/j.1365-2435.2002.00664.x

LeBauer, D. S., & Treseder, K. K. (2008). Nitrogen Limitation of Net Primary Productivity in Terrestrial Ecosystems Is Globally Distributed. *Ecology*, *89*, 371–379. https://doi.org/10.1890/06-2057.1

Li, H., Colica, G., Wu, P., Li, D., Rossi, F., De Philippis, R., & Liu, Y. (2013). Shifting Species Interaction in Soil Microbial Community and Its Influence on Ecosystem Functions Modulating. *Microbial Ecology*, *65*, 700–708. https://doi.org/10.1007/s00248-012-0171-2

Li, H., Li, R., Rossi, F., Li, D., De Philippis, R., Hu, C., & Liu, Y. (2016). Differentiation of microbial activity and functional diversity between various biocrust elements in a heterogeneous crustal community. *CATENA*, *147*, 138–145. https://doi.org/10.1016/j.catena.2016.07.008

Li, X., Hui, R., Tan, H., Zhao, Y., Liu, R., & Song, N. (2021). Biocrust Research in China: Recent Progress and Application in Land Degradation Control. *Frontiers in Plant Science*, *12*. https://www.frontiersin.org/articles/10.3389/fpls.2021.751521

Li, X., Hui, R., Zhang, P., & Song, N. (2021). Divergent responses of moss- and lichen-dominated biocrusts to warming and increased drought in arid desert regions, *Agricultural and Forest Meteorology, 303*, 108387, https://doi.org/10.1016/j.agrformet.2021.108387.

Liu, Y.-R., Eldridge, D. J., Zeng, X.-M., Wang, J., Singh, B. K., & Delgado-Baquerizo, M. (2021). Global diversity and ecological drivers of lichenised soil fungi. *New Phytologist*, *231*, 1210–1219. https://doi.org/10.1111/nph.17433

Ma, Y. (2023). Ma_et_al: Carbon balance Modelling, *Zenodo*, https://doi.org/10.5281/zenodo.7756960.

Ma, Y & Porada. P (2024). Dataset associated to "Quantifying the effect of competition on the functional assembly of bryophyte and lichen communities: A process-based model analysis". *Zenodo*. https://doi.org/10.5281/zenodo.8199734

Ma, Y., Weber, B., Kratz, A., Raggio, J., Colesie, C., Veste, M., Bader, M. Y., & Porada, P. (2023). Exploring environmental and physiological drivers of the annual carbon budget of biocrusts from various climatic zones with a mechanistic data-driven model. *Biogeosciences, 20*, 2553–2572. https://doi.org/10.5194/bg-20-2553-2023

Maaroufi, N. I., & De Long, J. R. (2020). Global Change Impacts on Forest Soils: Linkage Between Soil Biota and Carbon-Nitrogen-Phosphorus Stoichiometry. *Frontiers in Forests and Global Change*, *3*. https://www.frontiersin.org/articles/10.3389/ffgc.2020.00016

MacArthur, R., & Levins, R. (1967). The Limiting Similarity, Convergence, and Divergence of Coexisting Species. *The American Naturalist*, *101*, 377–385.

Maestre, F. T., Bowker, M. A., Escolar, C., Puche, M. D., Soliveres, S., Maltez-Mouro, S., García-Palacios, P., Castillo-Monroy, A. P., Martínez, I., & Escudero, A. (2010). Do biotic interactions modulate ecosystem functioning along stress gradients? Insights from semi-arid plant and biological soil crust communities. *Philosophical Transactions of the Royal Society B: Biological Sciences*, *365*, 2057–2070. https://doi.org/10.1098/rstb.2010.0016

Maestre, F. T., Escolar, C., Bardgett, R. D., Dungait, J. A. J., Gozalo, B., & Ochoa, V. (2015). Warming reduces the cover and diversity of biocrust-forming mosses and lichens, and increases the physiological stress of soil microbial communities in a semi-arid Pinus halepensis plantation. *Frontiers in Microbiology, 6*. https://www.frontiersin.org/articles/10.3389/fmicb.2015.00865

Maestre, F. T., Escolar, C., Ladrón de Guevara, M., Quero, J. L., Lázaro, R., Delgado-Baquerizo, M., Ochoa, V., Berdugo, M., Gozalo, B., & Gallardo, A. (2013). Changes in biocrust cover drive carbon cycle responses to climate change in drylands, *Global Change Biology, 19*, 3835–3847, https://doi.org/10.1111/gcb.12306.

Maestre, F. T., Escolar, C., Martínez, I., & Escudero, A. (2008). Are soil lichen communities structured by biotic interactions? A null model analysis. *Journal of Vegetation Science, 19*, 261–266. https://doi.org/10.3170/2007-8-18366

Maestre, F. T., Martínez, I., Escolar, C., & Escudero, A. (2009). On the relationship between abiotic stress and co-occurrence patterns: An assessment at the

community level using soil lichen communities and multiple stress gradients. *Oikos*, *118*, 1015–1022. https://doi.org/10.1111/j.1600-0706.2009.17362.x

Mälson, K., & Rydin, H. (2009). Competitive hierarchy, but no competitive exclusions in experiments with rich fen bryophytes. *Journal of Bryology*, *31*, 41–45. https://doi.org/10.1179/174328209X404916

Matos, P., Pinho, P., Aragón, G., Martínez, I., Nunes, A., Soares, A. M. V. M., & Branquinho, C. (2015). Lichen traits responding to aridity. *Journal of Ecology*, *103*, 451–458. https://doi.org/10.1111/1365-2745.12364

Matthews, H. D. (2007). Implications of CO_2 fertilization for future climate change in a coupled climate–carbon model. *Global Change Biology*, *13*, 1068–1078. https://doi.org/10.1111/j.1365-2486.2007.01343.x

Maréchaux, I., Langerwisch, F., Huth, A., Bugmann, H., Morin, X., Reyer, C. P. O., Seidl, R., Collalti, A., Dantas de Paula, M., Fischer, R., Gutsch, M., Lexer, M. J., Lischke, H., Rammig, A., Rödig, E., Sakschewski, B., Taubert, F., Thonicke, K., Vacchiano, G., & Bohn, F. J. (2021). Tackling unresolved questions in forest ecology: The past and future role of simulation models. *Ecology and Evolution, 11*, 3746–3770.

Metcalfe, D. B., & Ahlstrand, J. C. M. (2019). Effects of moisture dynamics on bryophyte carbon fluxes in a tropical cloud forest. *New Phytologist*, *222*, 1766–1777. https://doi.org/10.1111/nph.15727

Minami, A., Nagao, M., Ikegami, K., Koshiba, T., Arakawa, K., Fujikawa, S., & Takezawa, D. (2005). Cold acclimation in bryophytes: Low-temperature-induced freezing tolerance in *Physcomitrella patens* is associated with increases in expression levels of stress-related genes but not with increase in level of endogenous abscisic acid. *Planta*, *220*, 414–423. https://doi.org/10.1007/s00425-004-1361-z

Mittelbach, G. G., Schemske, D. W., Cornell, H. V., Allen, A. P., Brown, J. M., Bush, M. B., Harrison, S. P., Hurlbert, A. H., Knowlton, N., Lessios, H. A., McCain, C. M., McCune, A. R., McDade, L. A., McPeek, M. A., Near, T. J., Price, T. D., Ricklefs, R. E., Roy, K., Sax, D. F., … Turelli, M. (2007). Evolution and the latitudinal diversity gradient: Speciation, extinction and biogeography. *Ecology Letters*, *10*, 315–331. https://doi.org/10.1111/j.1461-0248.2007.01020.x

Monteiro, J., Vieira, C., & Branquinho, C. (2023). Bryophyte assembly rules across scales. *Journal of Ecology, 111*, 1531–1544. https://doi.org/10.1111/1365-2745.14117

Mouillot, D., Graham, N. A. J., Villéger, S., Mason, N. W. H., & Bellwood, D. R. (2013). A functional approach reveals community responses to disturbances. *Trends in Ecology & Evolution, 28*, 167–177. https://doi.org/10.1016/j.tree.2012.10.004

Moura, M. R., Villalobos, F., Costa, G. C., & Garcia, P. C. A. (2016). Disentangling the Role of Climate, Topography and Vegetation in Species Richness Gradients. *PLoS ONE, 11*, e0152468. https://doi.org/10.1371/journal.pone.0152468

Munoz, F., & Huneman, P. (2016). From the Neutral Theory to a Comprehensive and Multiscale Theory of Ecological Equivalence. *The Quarterly Review of Biology, 91*, 321–342. https://doi.org/10.1086/688098

Neuhauser, C., & Fargione, J. E. (2004). A mutualism–parasitism continuum model and its application to plant–mycorrhizae interactions. *Ecological Modelling, 177*, 337–352. https://doi.org/10.1016/j.ecolmodel.2004.02.010

Nock, C. A., Vogt, R. J., & Beisner, B. E. (2016). Functional Traits. In John Wiley & Sons, Ltd (Ed.), *eLS* (pp. 1–8). Wiley. https://doi.org/10.1002/9780470015902.a0026282

Oke, T. A., & Turetsky, M. R. (2020). Evaluating *Sphagnum* traits in the context of resource economics and optimal partitioning theories. *Oikos, 129*, 1204–1215. https://doi.org/10.1111/oik.07195

Oliver, M. J., Velten, J., & Wood, A. J. (2000). Bryophytes as experimental models for the study of environmental stress tolerance: Tortula ruralis and desiccation-tolerance in mosses. *Plant Ecology, 151*, 73–84. https://doi.org/10.1023/A:1026598724487

Ouborg, N. J. (1993). Isolation, Population Size and Extinction: The Classical and Metapopulation Approaches Applied to Vascular Plants along the Dutch Rhine-System. *Oikos, 66*, 298–308. https://doi.org/10.2307/3544818

Ouyang, H., Lan, S., Yang, H., & Hu, C. (2017). Mechanism of biocrusts boosting and utilizing non-rainfall water in Hobq Desert of China, *Applied Soil Ecology, 120*, 70–80, https://doi.org/10.1016/j.apsoil.2017.07.024.

Pavlick, R., Drewry, D. T., Bohn, K., Reu, B., & Kleidon, A. (2013). The Jena Diversity-Dynamic Global Vegetation Model (JeDi-DGVM): A diverse approach to representing terrestrial biogeography and biogeochemistry based on plant functional trade-offs. *Biogeosciences*, *10*, 4137–4177. https://doi.org/10.5194/bg-10-4137-2013

Perera-Castro, A. V., Waterman, M. J., Turnbull, J. D., Ashcroft, M. B., McKinley, E., Watling, J. R., Bramley-Alves, J., Casanova-Katny, A., Zuniga, G., Flexas, J., & Robinson, S. A. (2020). It Is Hot in the Sun: Antarctic Mosses Have High Temperature Optima for Photosynthesis Despite Cold Climate. *Frontiers in Plant Science*, *11*. https://www.frontiersin.org/articles/10.3389/fpls.2020.01178

Phillips, M. L., McNellis, B. E., Howell, A., Lauria, C. M., Belnap, J., & Reed, S. C. (2022). Biocrusts mediate a new mechanism for land degradation under a changing climate. *Nature Climate Change*, *12*, 71–76. https://doi.org/10.1038/s41558-021-01249-6

Phinney, N. H., Gauslaa, Y., Palmqvist, K., & Esseen, P. A. (2021). Macroclimate drives growth of hair lichens in boreal forest canopies, *Journal of Ecology, 109*, 478–490, https://doi.org/10.1111/1365-2745.13522.

Piao, S., Ciais, P., Friedlingstein, P., Peylin, P., Reichstein, M., Luyssaert, S., Margolis, H., Fang, J., Barr, A., Chen, A., Grelle, A., Hollinger, D. Y., Laurila, T., Lindroth, A., Richardson, A. D., & Vesala, T. (2008). Net carbon dioxide losses of northern ecosystems in response to autumn warming. *Nature*, *451*, 49-52. https://doi.org/10.1038/nature06444

Porada, P., Bader, M. Y., Berdugo, M. B., Colesie, C., Ellis, C. J., Giordani, P., Herzschuh, U., Ma, Y., Launiainen, S., Nascimbene, J., Petersen, I., Raggio Quílez, J., Rodríguez-Caballero, E., Rousk, K., Sancho, L. G., Scheidegger, C., Seitz, S., Van Stan II, J. T., Veste, M., … Weston, D. J. (2023). A research agenda for nonvascular photoautotrophs under climate change. *New Phytologist*, *237*, 1495–1504. https://doi.org/10.1111/nph.18631

Porada, P., & Paolo, G. (2021). Bark Water Storage Plays Key Role for Growth of Mediterranean Epiphytic Bark Water Storage Plays Key Role for Growth of

Mediterranean Epiphytic Lichens. *Frontiers in Forests and Global Change, 4*, 30. https://doi.org/10.3389/ffgc.2021.668682

Porada, P., Pöschl, U., Kleidon, A., Beer, C., & Weber, B. (2017). Estimating global nitrous oxide emissions by lichens and bryophytes with a process-based productivity model. *Biogeosciences, 14*, 1593–1602. https://doi.org/10.5194/bg-14-1593-2017

Porada, P., Van Stan, J. T., & Kleidon, A. (2018). Significant contribution of non-vascular vegetation to global rainfall interception. *Nature Geoscience*, *11*, 563–567. https://doi.org/10.1038/s41561-018-0176-7

Porada, P., Weber, B., Elbert, W., Pöschl, U., & Kleidon, A. (2013). Estimating global carbon uptake by lichens and bryophytes with a process-based model. *Biogeosciences*, *10*, 6989–7033. https://doi.org/10.5194/bg-10-6989-2013

Porada, P., Weber, B., Elbert, W., Pöschl, U., & Kleidon, A. (2014). Estimating impacts of lichens and bryophytes on global biogeochemical cycles. *Global Biogeochemical Cycles, 28*, 71–85. https://doi.org/10.1002/2013GB004705

Porada, P., Tamm, A., Raggio, J., Cheng, Y., Kleidon, A., Pöschl, U., & Weber, B. (2019). Global NO and HONO emissions of biological soil crusts estimated by a process-based non-vascular vegetation model. *Biogeosciences, 16*, 2003–2031. https://doi.org/10.5194/bg-16-2003-2019

Prentice, I. C., Bondeau, A., Cramer, W., Harrison, S. P., Hickler, T., Lucht, W., Sitch, S., Smith, B., & Sykes, M. T. (2007). Dynamic Global Vegetation Modeling: Quantifying Terrestrial Ecosystem Responses to Large-Scale Environmental Change. In J. G. Canadell, D. E. Pataki, & L. F. Pitelka (Eds.), *Terrestrial Ecosystems in a Changing World* (pp. 175–192). Springer. https://doi.org/10.1007/978-3-540-32730-1_15

Proctor, M. (2001). Patterns of desiccation tolerance and recovery in bryophytes. *Plant Growth Regulation*, *35*, 147–156. https://doi.org/10.1023/A:1014429720821

Raggio, J., Pintado, A., Vivas, M., Sancho, L. G., Büdel, B., Colesie, C., Weber, B., Schroeter, B., Lázaro, R., & Green, T. G. A. (2014). Continuous chlorophyll fluorescence, gas exchange and microclimate monitoring in a natural soil crust habitat in Tabernas badlands, Almería, Spain: Progressing towards a model to

understand productivity, *Biodiversity and Conservation, 23*, 1809–1826, https://doi.org/10.1007/s10531-014-0692-8.

Raggio, J., Green, T. G. A., Sancho, L. G., Pintado, A., Colesie, C., Weber, B., & Büdel, B. (2017). Metabolic activity duration can be effectively predicted from macroclimatic data for biological soil crust habitats across Europe, *Geoderma, 306*, 10–17, https://doi.org/10.1016/j.geoderma.2017.07.001.

Raggio, J., Green, T. G. A., Pintado, A., Sancho, L. G., & Büdel, B. (2018). Environmental determinants of biocrust carbon fluxes across Europe: possibilities for a functional type approach, *Plant and Soil, 429*, 147–157, https://doi.org/10.1007/s11104-018-3646-1.

Rastorfer, J. R., & Higinbotham, N. (1968). Rates of Photosynthesis and Respiration of the Moss Bryum Sandbergii as Influenced by Light Intensity and Temperature. *American Journal of Botany, 55*, 1225–1229. https://doi.org/10.1002/j.1537-2197.1968.tb07488.x

Reed, S. C., Coe, K. K., Sparks, J. P., Housman, D. C., Zelikova, T. J., & Belnap, J. (2012). Changes to dryland rainfall result in rapid moss mortality and altered soil fertility. *Nature Climate Change, 2,* 752-755. https://doi.org/10.1038/nclimate1596

Reich, P. B., Hobbie, S. E., Lee, T., Ellsworth, D. S., West, J. B., Tilman, D., Knops, J. M. H., Naeem, S., & Trost, J. (2006). Nitrogen limitation constrains sustainability of ecosystem response to CO_2. *Nature, 440, 922-925*. https://doi.org/10.1038/nature04486

Reu, B., Proulx, R., Bohn, K., Dyke, J. G., Kleidon, A., Pavlick, R., & Schmidtlein, S. (2011). The role of climate and plant functional trade-offs in shaping global biome and biodiversity patterns: Climate, biome and biodiversity patterns. *Global Ecology and Biogeography, 20*, 570–581. https://doi.org/10.1111/j.1466-8238.2010.00621.x

Rice, S. K. (2012). The cost of capillary integration for bryophyte canopy water and carbon dynamics. *Lindbergia, 35*, 53–62.

Rodriguez-Caballero, E., Belnap, J., Büdel, B., Crutzen, P. J., Andreae, M. O., Pöschl, U., & Weber, B. (2018). Dryland photoautotrophic soil surface

communities endangered by global change. *Nature Geoscience*, *11*, 185–189. https://doi.org/10.1038/s41561-018-0072-1

Roos, R. E., Zuijlen, K., Birkemoe, T., Klanderud, K., Lang, S. I., Bokhorst, S., Wardle, D. A., & Asplund, J. (2019). Contrasting drivers of community‐level trait variation for vascular plants, lichens and bryophytes across an elevational gradient. *Functional Ecology*, *33*, 2430–2446. https://doi.org/10.1111/1365-2435.13454

Rousk, K. (2022). Biotic and abiotic controls of nitrogen fixation in cyanobacteria–moss associations. *New Phytologist*, *235*, 1330–1335. https://doi.org/10.1111/nph.18264

Rousk, K., Sorensen, P. L., & Michelsen, A. (2017). Nitrogen fixation in the High Arctic: A source of 'new' nitrogen? *Biogeochemistry*, *136*, 213–222. https://doi.org/10.1007/s10533-017-0393-y

Rydin, H. (1997). Competition among bryophytes. *Advances in Bryology, 6*, 135–168.

Sakschewski, B., von Bloh, W., Boit, A., Rammig, A., Kattge, J., Poorter, L., Peñuelas, J., & Thonicke, K. (2015). Leaf and stem economics spectra drive diversity of functional plant traits in a dynamic global vegetation model. *Global Change Biology, 21*, 2711–2725. https://doi.org/10.1111/gcb.12870

Samolov, E., Baumann, K., Büdel, B., Jung, P., Leinweber, P., Mikhailyuk, T., Karsten, U., & Glaser, K. (2020). Biodiversity of Algae and Cyanobacteria in Biological Soil Crusts Collected Along a Climatic Gradient in Chile Using an Integrative Approach. *Microorganisms*, *8*, 1047. https://doi.org/10.3390/microorganisms8071047

Scheiter, S., Langan, L., & Higgins, S. I. (2013). Next‐generation dynamic global vegetation models: Learning from community ecology. *New Phytologist*, *198*, 957–969. https://doi.org/10.1111/nph.12210

Schmitz, D., Schaefer, C. E. R. G., Putzke, J., Francelino, M. R., Ferrari, F. R., Corrêa, G. R., & Villa, P. M. (2020). How does the pedoenvironmental gradient shape non-vascular species assemblages and community structures in

Maritime Antarctica? *Ecological Indicators*, *108*, 105726. https://doi.org/10.1016/j.ecolind.2019.105726

Schofield, W. B. (2024). bryophyte. *Encyclopedia Britannica*. https://www.britannica.com/plant/bryophyte

Schulze, E.-D., & Mooney, H. A. (1994). Ecosystem Function of Biodiversity: A Summary. In E.-D. Schulze & H. A. Mooney (Eds.), *Biodiversity and Ecosystem Function* (pp. 497–510). Springer. https://doi.org/10.1007/978-3-642-58001-7_24

Schuur, E. A. G., Crummer, K. G., Vogel, J. G., & Mack, M. C. (2007). Plant species composition and productivity following permafrost thaw and thermokarst in Alaskan tundra, *Ecosystems, 10*, 280–292, https://doi.org/10.1007/s10021-007-9024-0.

Schwinning, S., & Ehleringer, J. R. (2001). Water use trade-offs and optimal adaptations to pulse-driven arid ecosystems. *Journal of Ecology*, *89*, 464–480. https://doi.org/10.1046/j.1365-2745.2001.00576.x

Shaw, A. J., Cox, C. J., & Goffinet, B. (2005). Global patterns of moss diversity: Taxonomic and molecular inferences. *TAXON*, *54*, 337–352. https://doi.org/10.2307/25065362

Shehawy, R. M., & Kleiner, D. (2001). Nitrogen Limitation. In L. C. Rai & J. P. Gaur (Eds.), *Algal Adaptation to Environmental Stresses: Physiological, Biochemical and Molecular Mechanisms* (pp. 45–64). Springer. https://doi.org/10.1007/978-3-642-59491-5_3

Silvertown, J., & Dale, P. (1991). Competitive Hierarchies and the Structure of Herbaceous Plant Communities. *Oikos*, *61*, 441-444. https://doi.org/10.2307/3545253

Smith, N. G., & Dukes, J. S. (2013). Plant respiration and photosynthesis in global-scale models: Incorporating acclimation to temperature and CO_2. *Global Change Biology*, *19*, 45–63. https://doi.org/10.1111/j.1365-2486.2012.02797.x

Soliveres, S., & Eldridge, D. J. (2020). Dual community assembly processes in dryland biocrust communities. *Functional Ecology, 34*, 877–887. https://doi.org/10.1111/1365-2435.13521

Spasojevic, M. J., & Suding, K. N. (2012). Inferring community assembly mechanisms from functional diversity patterns: The importance of multiple assembly processes. *Journal of Ecology*, *100*, 652–661. https://doi.org/10.1111/j.1365-2745.2011.01945.x

Spencer, S. (2001). Effects of coal dust on species composition of mosses and lichens in an arid environment. *Journal of Arid Environments, 49*, 843–853. https://doi.org/10.1006/jare.2001.0816

Spitale, D. (2009). Switch between competition and facilitation within a seasonal scale at colony level in bryophytes. *Oecologia*, *160*, 471–482. https://doi.org/10.1007/s00442-009-1324-y

Stitt, M., & Schulze, D. (1994). Does Rubisco control the rate of photosynthesis and plant growth? An exercise in molecular ecophysiology. *Plant, Cell & Environment*, *17*, 465–487. https://doi.org/10.1111/j.1365-3040.1994.tb00144.x

Sun, J., Li, X., Jia, R., Chen, N., & Zhang, T. (2021). Null-model analysis and changes in species interactions in biocrusts along a successional gradient in the Tengger Desert, northern China. *Journal of Vegetation Science*, *32*. https://doi.org/10.1111/jvs.13037

Svenning, J.-C., Eiserhardt, W. L., Normand, S., Ordonez, A., & Sandel, B. (2015). The Influence of Paleoclimate on Present-Day Patterns in Biodiversity and Ecosystems. *Annual Review of Ecology, Evolution, and Systematics*, *46*, 551–572. https://doi.org/10.1146/annurev-ecolsys-112414-054314

Syers, J. K., & Iskandar, I. K. (1973). Chapter 7—PEDOGENETIC SIGNIFICANCE OF LICHENS. In V. Ahmadjian & M. E. Hale (Eds.), *The Lichens* (pp. 225–248). Academic Press. https://doi.org/10.1016/B978-0-12-044950-7.50012-X

Tamm, A., Caesar, J., Kunz, N., Colesie, C., Reichenberger, H., & Weber, B. (2018). Ecophysiological properties of three biological soil crust types and their photoautotrophs from the Succulent Karoo, South Africa, *Plant and Soil, 429*, 127–146, https://doi.org/10.1007/s11104-018-3635-4.

Tao, F., & Zhang, Z. (2010). Dynamic responses of terrestrial ecosystems structure and function to climate change in China. *Journal of Geophysical Research: Biogeosciences*, *115*. https://doi.org/10.1029/2009JG001062

Terrer, C., Jackson, R. B., Prentice, I. C., Keenan, T. F., Kaiser, C., Vicca, S., Fisher, J. B., Reich, P. B., Stocker, B. D., Hungate, B. A., Peñuelas, J., McCallum, I., Soudzilovskaia, N. A., Cernusak, L. A., Talhelm, A. F., Van Sundert, K., Piao, S., Newton, P. C. D., Hovenden, M. J., … Franklin, O. (2019). Nitrogen and phosphorus constrain the CO_2 fertilization of global plant biomass. *Nature Climate Change*, *9,* 684-689. https://doi.org/10.1038/s41558-019-0545-2

Thuiller, W., Midgley, G. F., Hughes, G. O., Bomhard, B., Drew, G., Rutherford, M. C., & Woodward, F. I. (2006). Endemic species and ecosystem sensitivity to climate change in Namibia. *Global Change Biology*, *12*, 759–776. https://doi.org/10.1111/j.1365-2486.2006.01140.x

Tilman, D., Isbell, F., & Cowles, J. M. (2014). Biodiversity and Ecosystem Functioning. *Annual Review of Ecology, Evolution, and Systematics*, *45*, 471–493. https://doi.org/10.1146/annurev-ecolsys-120213-091917

Tjoelker, M.G., Oleksyn, J. & Reich, P.B. (2001). Modelling respiration of vegetation: evidence for a general temperature-dependent Q_{10}. *Global Change Biology, 7*, 223–230.

Turner, P. A. M., & Pharo, E. J. (2005). Influence of Substrate Type and Forest Age on Bryophyte Species Distribution in Tasmanian Mixed Forest. *The Bryologist*, *108*, 67–85. https://doi.org/10.1639/0007-2745(2005)108[67:IOSTAF]2.0.CO;2

Usinowicz, J., Chang-Yang, C.-H., Chen, Y.-Y., Clark, J. S., Fletcher, C., Garwood, N. C., Hao, Z., Johnstone, J., Lin, Y., Metz, M. R., Masaki, T., Nakashizuka, T., Sun, I.-F., Valencia, R., Wang, Y., Zimmerman, J. K., Ives, A. R., & Wright, S. J. (2017). Temporal coexistence mechanisms contribute to the latitudinal gradient in forest diversity. *Nature, 550*, 105-108. https://doi.org/10.1038/nature24038

van der Plas, F., Janzen, T., Ordonez, A., Fokkema, W., Reinders, J., Etienne, R. S., & Olff, H. (2015). A new modeling approach estimates the relative importance of different community assembly processes. *Ecology*, *96*, 1502–1515. https://doi.org/10.1890/14-0454.1

Vellend, M. (2010). Conceptual Synthesis in Community Ecology. *The Quarterly Review of Biology*, *85*, 183–206. https://doi.org/10.1086/652373

Verheijen, L. M., Aerts, R., Brovkin, V., Cavender-Bares, J., Cornelissen, J. H. C., Kattge, J., & van Bodegom, P. M. (2015). Inclusion of ecologically based trait variation in plant functional types reduces the projected land carbon sink in an earth system model. *Global Change Biology, 21*, 3074–3086. https://doi.org/10.1111/gcb.12871

Verheijen, L. M., Brovkin, V., Aerts, R., Bönisch, G., Cornelissen, J. H. C., Kattge, J., Reich, P. B., Wright, I. J., & van Bodegom, P. M. (2013). Impacts of trait variation through observed trait–climate relationships on performance of an Earth system model: A conceptual analysis. *Biogeosciences*, *10*, 5497–5515. https://doi.org/10.5194/bg-10-5497-2013

Veste, M. & Littmann, T. (2006). Dewfall and its Geo-ecological Implication for Biological Surface Crusts in Desert Sand Dunes (Northwestern Negev, Israel), *Journal of Arid Land Studies, 16*, 139–147.

Veste, M., Heusinkveld, B. G., Berkowicz, S. M., Breckle, S.-W., Littmann, T., & Jacobs, A. F. G. (2008). Dew Formation and Activity of Biological Soil Crusts. In S.-W. Breckle, A. Yair, & M. Veste (Eds.), *Arid Dune Ecosystems: The Nizzana Sands in the Negev Desert* (pp. 305–318). Springer. https://doi.org/10.1007/978-3-540-75498-5_21

Violle, C., Navas, M.-L., Vile, D., Kazakou, E., Fortunel, C., Hummel, I., & Garnier, E. (2007). Let the concept of trait be functional! *Oikos*, *116*, 882–892. https://doi.org/10.1111/j.0030-1299.2007.15559.x

Vitousek, P. M., & Hooper, D. U. (1994). Biological Diversity and Terrestrial Ecosystem Biogeochemistry. In E.-D. Schulze & H. A. Mooney (Eds.), *Biodiversity and Ecosystem Function* (pp. 3–14). Springer. https://doi.org/10.1007/978-3-642-58001-7_1

Vitousek, P. M., & Howarth, R. W. (1991). Nitrogen limitation on land and in the sea: How can it occur? *Biogeochemistry*, *13*, 87–115. https://doi.org/10.1007/BF00002772

Vivas, M., Pérez-Ortega, S., Pintado, A., & Sancho, L. G. (2017). Fv/Fm acclimation to the Mediterranean summer drought in two sympatric Lasallia species from

the Iberian mountains, *Lichenologist,* *49,* 157–165, https://doi.org/10.1017/S0024282917000032.

Wagner, S., Zotz, G., & Bader, M. Y. (2014). The temperature acclimation potential of tropical bryophytes, *Plant* *Biology.,* *16,* 117–124, https://doi.org/10.1111/plb.12037.

Walker, A. P., Beckerman, A. P., Gu, L., Kattge, J., Cernusak, L. A., Domingues, T. F., Scales, J. C., Wohlfahrt, G., Wullschleger, S. D., & Woodward, F. I. (2014). The relationship of leaf photosynthetic traits – Vcmax and Jmax – to leaf nitrogen, leaf phosphorus, and specific leaf area: a meta-analysis and modeling study*, Ecology and Evolution, 4,* 3218–3235, https://doi.org/10.1002/ece3.1173.

Wang, Z., Liu, X., Bader, M. Y., Feng, D., & Bao, W. (2017). The 'plant economic spectrum' in bryophytes, a comparative study in subalpine forest. *American Journal of Botany, 104*, 261–270. https://doi.org/10.3732/ajb.1600335

Weber, B., Graf, T., & Bass, M. (2012). Ecophysiological analysis of moss-dominated biological soil crusts and their separate components from the Succulent Karoo, South Africa, *Planta, 236,* 129–139, https://doi.org/10.1007/s00425-012-1595-0.

Weber, B., Berkemeier, T., Ruckteschler, N., Caesar, J., Heintz, H., Ritter, H., & Braß, H. (2016). Development and calibration of a novel sensor to quantify the water content of surface soils and biological soil crusts, *Methods in Ecology and Evolution, 7*, 14–22, https://doi.org/10.1111/2041-210X.12459.

Weiher, E., Clarke, G. D. P., & Keddy, P. A. (1998). Community Assembly Rules, Morphological Dispersion, and the Coexistence of Plant Species. *Oikos, 81*, 309–322. https://doi.org/10.2307/3547051

Weiskopf, S. R., Rubenstein, M. A., Crozier, L. G., Gaichas, S., Griffis, R., Halofsky, J. E., Hyde, K. J. W., Morelli, T. L., Morisette, J. T., Muñoz, R. C., Pershing, A. J., Peterson, D. L., Poudel, R., Staudinger, M. D., Sutton-Grier, A. E., Thompson, L., Vose, J., Weltzin, J. F., & Whyte, K. P. (2020). Climate change effects on biodiversity, ecosystems, ecosystem services, and natural resource management in the United States. *Science of The Total Environment*, *733*, 137782. https://doi.org/10.1016/j.scitotenv.2020.137782

Welch, D. (1984). Studies in the Grazing of Heather Moorland in North-East Scotland. III. Floristics. *Journal of Applied Ecology*, *21*, 209–225. https://doi.org/10.2307/2403048

Whitton, J. (2013). Plant Biodiversity, Overview. In S. A. Levin (Eds.), *Encyclopedia of Biodiversity (Second Edition)* (pp. 56–64). Academic Press. https://doi.org/10.1016/B978-0-12-384719-5.00110-6

Wolf, J. H. D. (1994). Factors controlling the distribution of vascular and non-vascular epiphytes in the northern Andes. *Vegetatio*, *112*, 15–28. https://doi.org/10.1007/BF00045096

Xiao, B., & Bowker, M. A. (2020). Moss-biocrusts strongly decrease soil surface albedo, altering land-surface energy balance in a dryland ecosystem. *Science of The Total Environment*, *741*, 140425. https://doi.org/10.1016/j.scitotenv.2020.140425

Xiao, B., Zhao, Y., Wang, Q., & Li, C. (2015). Development of artificial moss-dominated biological soil crusts and their effects on runoff and soil water content in a semi-arid environment. *Journal of Arid Environments*, *117*, 75–83. https://doi.org/10.1016/j.jaridenv.2015.02.017

Xu, M., Zheng, L.-T., He, D., Chen, H. Y. H., & Yan, E.-R. (2021). Microenvironment filtering and plant competition jointly structure trait distributions across co-occurring individuals. *Ecological Indicators*, *129*, 107893. https://doi.org/10.1016/j.ecolind.2021.107893

Zhao, Y., Zhang, Z., Hu, Y., & Chen, Y. (2016). The seasonal and successional variations of carbon release from biological soil crust-covered soil, *Journal of Arid Environments,* *127,* 148–153, https://doi.org/10.1016/j.jaridenv.2015.11.012.

Zelikova, T. J., Housman, D. C., Grote, E. E., Neher, D. A., & Belnap, J. (2012). Warming and increased precipitation frequency on the Colorado Plateau: Implications for biological soil crusts and soil processes. *Plant and Soil*, *355*, 265–282. https://doi.org/10.1007/s11104-011-1097-z

Zotz, G., Schultz, S., & Rottenberger, S. (2003). Are tropical lowlands a marginal habitat for macrolichens? Evidence from a field study with *Parmotrema*

endosulphureum in Panama, *Flora - Morphology, Distribution, Functional Ecology of Plants*, *198*, 71–77, https://doi.org/10.1078/0367-2530-00077.

Zraik, M., Booth, T., & Piercey-Normore, M. D. (2018). Relationship between lichen species composition, secondary metabolites and soil pH, organic matter, and grain characteristics in Manitoba. *Botany, 96*, 267–279. https://doi.org/10.1139/cjb-2017-0176

Summary

Non-vascular vegetation, such as mosses, lichens and biological soil crusts, are widely distributed across the globe, providing essential ecosystem functions in various regions worldwide. Therefore, understanding the community assembly processes of non-vascular vegetation and their impact on shaping community structure are important. Environmental filtering and competition are two fundamental processes driving community assembly. However, the relative importance of different climatic factors and the role of competition in non-vascular community assembly are largely unknown. Hence, this thesis focuses on quantifying their roles in driving non-vascular community assembly using a process-based model, with critical implications for understanding the global diversity pattern and responses to climate change. Four chapters are included in this thesis: **Chapter 1** presents a general introduction to the topic, **Chapter 2** and **Chapter 3** are two manuscripts as the main part to the topic, **Chapter 4** is a general discussion, which discussed the findings of the main chapters (2 and 3) and explores their implications for future investigations into the mechanisms underlying the global diversity pattern and the impacts of climate change on the structure of non-vascular communities.

Chapter 2 investigates the relative importance of climatic factors and physiological parameters in the carbon balance of biocrusts across different climatic regions using a mechanistic data-driven model. The results indicate that all examined climatic factors play a crucial role, with CO_2 concentration and air temperature being of primary importance in all climatic zones. Additionally, respiration-related physiological parameters have a substantial effect on the annual carbon balance of biocrusts. Nevertheless, the relative importance of the climatic factors varies across different climatic zones. This study suggests that the uncertainties introduced by these most important factors, together with the missing seasonal acclimation of physiological traits, may result in unrealistic simulated carbon balance values of biocrusts in humid regions, which may lead to biases in predicted community assemblages.

Chapter 3 disentangles the roles of environmental filtering and competition in driving the community composition in terms of trait distributions based on a process-based model incorporating a trait-based competition process and a field transplantation experiment. The results show that environmental filtering plays a critical role, while

weak competition rather than strong drives the functional community assembly. Furthermore, this study suggests caution when associating competition with a single trait while analyzing the community functional assembly, as no single-trait competition scheme consistently explains the observed trait distributions of non-vascular communities.

My works show that environmental filtering can play an important role in the community assembly of non-vascular vegetation by strongly affecting their carbon balance. Additionally, their carbon balance is largely regulated by respiration-related physiological parameters. However, the relative importance of various climatic factors is different across climatic zones, with important implications for understanding the impacts of climate change. Besides, environmental filtering might be more important than competition in nonvascular community assembly under temperate climatic conditions. In conclusion, this thesis applies a process-based model to elucidate the community assembly of non-vascular vegetation by examining not only their biochemical and physiological responses to climatic factors, but also the ecological process (i.e., competition), thereby enhancing the understanding of the assembly processes of non-vascular communities.

Zusammenfassung

Non-vaskuläre Vegetation wie Moose, Flechten und biologische Bodenkrusten sind weltweit verbreitet und leisten in verschiedenen Regionen der Welt wichtige ökologische Funktionen. Daher ist es wichtig, die Prozesse zu verstehen, welche die Gemeinschaftsbildung von nicht-vaskulären Pflanzen beeinflussen. Zwei grundlegende Prozesse, die die Gemeinschaftsbildung beeinflussen, sind Umweltfilter und Konkurrenz. Allerdings ist die relative Bedeutung verschiedener klimatischer Faktoren und die Rolle der Konkurrenz bei der Gemeinschaftsbildung von nicht-vaskulären Pflanzen weitestgehend unbekannt. Daher konzentriert sich diese Dissertation darauf, den Einfluss dieser Faktoren auf die Gemeinschaftsbildung von nicht-vaskulären Pflanzen mithilfe eines prozessbasierten Modells zu quantifizieren, was ein zentraler Bestandteil für das Verständnis des globalen Diversitätsmusters und dessen Reaktionen auf den Klimawandel darstellt. Die Dissertation umfasst vier Kapitel: **Kapitel 1** stellt eine allgemeine Einführung in das Thema dar, **Kapitel 2** und **Kapitel 3** sind zwei Manuskripte, die den Hauptteil des Themas bilden, **Kapitel 4** diskutiert die Ergebnisse der Hauptkapitel (2 und 3) und beleuchtet ihre Bedeutung für zukünftige Studien, die sich mit den bestimmenden Mechanismen von globalen Diversitätsmustern befassen und die Auswirkungen des Klimawandels auf die Struktur von nicht-vaskulären Gemeinschaften untersuchen.

In **Kapitel 2** wird die relative Bedeutung von klimatischen Faktoren und physiologischen Parametern im Kohlenstoffhaushalt von Biokrusten in verschiedenen klimatischen Regionen mithilfe eines mechanistischen datengesteuerten Modells untersucht. Die Ergebnisse zeigen, dass alle untersuchten klimatischen Faktoren dabei eine entscheidende Rolle spielen, wobei die CO_2-Konzentration und die Umgebungstemperatur in allen klimatischen Zonen von vorrangiger Bedeutung sind. Zudem haben respirationsbezogene physiologische Parameter einen signifikanten Einfluss auf den jährlichen Kohlenstoffhaushalt der Biokrusten. Die relative Bedeutung der klimatischen Faktoren variiert jedoch zwischen den verschiedenen klimatischen Zonen. Diese Studie deutet darauf hin, dass in Folge der faktoriellen Unsicherheiten zusammen mit der fehlenden saisonalen Anpassung physiologischer Merkmale es zu unrealistisch simulierten Kohlenstoffbilanzen von Biokrusten in feuchten Regionen kom-

men könnte, was wiederum zu einer Verzerrung bei den vorhergesagten Gemeinschaften führen könnte.

In **Kapitel 3** wird die Rolle von Umweltfiltern und Konkurrenz auf die Zusammensetzung der Artgemeinschaft in Bezug auf die Merkmalsverteilung anhand eines prozessbasierten Modells, das einen auf Merkmalen basierenden Konkurrenzprozess beinhaltet, und eines Feldverpflanzungsexperiment entschlüsselt. Diese Studie zeigt, dass Umweltfilter eine entscheidende Rolle spielen, während schwache Konkurrenz anstelle von starker die funktionale Gemeinschaftszusammensetzung vorantreibt. Darüber hinaus mahnt diese Studie zur Vorsicht, wenn man bei der Analyse der funktionalen Zusammensetzung von Gemeinschaften die Konkurrenz mit nur einem einzigen Merkmal in Verbindung bringt, da kein einziges dieser Merkmale die beobachteten Merkmalsverteilungen von nicht-vaskulären Gemeinschaften alleinstehend konsistent erklärt.

Meine Arbeiten zeigen, dass Umweltfilter eine wichtige Rolle bei der Gemeinschaftszusammensetzung von nicht-vaskulären Pflanzen spielen, indem sie ihren Kohlenstoffhaushalt stark beeinflussen. Zusätzlich wird ihr Kohlenstoffhaushalt weitestgehend von respirationsbezogenen physiologischen Parametern reguliert. Die relative Bedeutung verschiedener klimatischer Faktoren variiert jedoch in verschiedenen klimatischen Zonen, was wichtige Auswirkungen auf das Verständnis der Folgen des Klimawandels hat. Außerdem könnten Umweltfilter unter gemäßigten klimatischen Bedingungen wichtiger sein als die Konkurrenz bei der Gemeinschaftszusammensetzung nicht-vaskulärer Pflanzen. Zusammenfassend verwendet diese Dissertation ein prozessbasiertes Modell, um die Gemeinschaftszusammensetzung nicht-vaskulärer Pflanzen zu erklären. Dabei wird nicht nur ihre biochemischen und physiologischen Reaktionen auf klimatische Faktoren untersucht, sondern auch der ökologische Prozess der Konkurrenz. Auf diese Weise wird das Verständnis der Zusammensetzungsprozesse nicht-vaskulärer Gemeinschaften vertieft.

Co-Author affiliations

Philipp Porada and Imke Petersen: Institute of Plant Science and Microbiology, Universität Hamburg, 22609 Hamburg, Germany

Maaike Y. Bader: Faculty of Geography, University of Marburg, 35032 Marburg, Germany

Bettina Weber: Institute of Plant Sciences, Department of Biology, University of Graz, 8010 Graz, Austria; Department of Multiphase Chemistry, Max Planck Institute for Chemistry, 55128 Mainz, Germany

Alexandra Kratz: Department of Multiphase Chemistry, Max Planck Institute for Chemistry, 55128 Mainz, Germany

José Raggio: Departamento de Farmacología, Farmacognosia y Botánica, Complutense University of Madrid, 28040 Madrid, Spain

Claudia Colesie: School of Geosciences, University of Edinburgh, EH9 3FF Edinburgh, United Kingdom

Maik Veste: Institute of Environmental Sciences, Brandenburg University of Technology Cottbus-Senftenberg, 03046 Cottbus, Germany; CEBra – Centre for Energy Technology Brandenburg e.V., 03042 Cottbus, Germany

Acknowledgments/Danksagung

At the beginning of my study, I was so optimistic and confident in my ability to perform well. As the project progressed, I realized it was not at all what I had imagined. Even seemingly straightforward tasks were filled with countless unknowns and details that have led to unexpected results. I was struggling and had no idea at that time how to advance my own research. Especially during the process of drafting and refining my first manuscript, I encountered unexpected challenges. Those moments of thinking, rewriting, deleting – a cycle playing out day and night – still stand out in my memory. I even doubted myself during that period. However, it got published, and eventually, I reached the point of completing my PhD studies. This achievement was impossible without my supervisor Philipp Porada, who guided me through every challenge with patient discussions, and shared his experiences, not only in scientific work but also in navigating the journey of PhD life and future planning. Furthermore, I would thank my co-supervisor Maaike Bader and panel chair Christian Beer for their valuable guidance, comments and questions to pull me to think of and advance my research. I would also like to thank all my colleagues in the Ecological Modelling working group for the discussions on my PhD project and their valuable input, especially the lovely PhDs: Suman Halder, Imke Petersen, Youssef Saadaoui, Mikita Maslouski and Panunporn Tutiyasarn (a.k.a. Elly). Thank you for the calls for lunches and many great chats making fun of our PhD. It has certainly made my PhD life more relaxed and enjoyable. I also want to thank my colleague Monica Wilson and Robin Pelchen for their help with the language check of my thesis. Furthermore, I want to express my gratitude to the SICSS graduate school and especially Dr. Berit Hachfeld for offering and organizing many helpful courses and interesting retreats.

My PhD journey is unique and unforgettable, marked by the once-in-a-century pandemic. Those days spent alone in a small rented room, in front of the computer every day, enduring the terrible winter weather in Hamburg, added extra stress to my mental well-being and my PhD study. I am very thankful to my many friends to take me out of the stressful study, share the colorful life with me, accompany me in venting, listen to my complaints and cheer me up.

I also want to thank my parents, who selflessly supported and encouraged me, accompanying me on this journey. Despite the prolonged physical separation caused by the pandemic, they never complained, always being by my side through video calls. They are my pillars of strength and my warm harbor during the four-year long challenging period.

Lastly, I sincerely want to appreciate myself: You have done a great job! These last four years have been challenging, and I sincerely acknowledge your hard work!

Eidesstattliche Versicherung | Declaration on Oath

Hiermit erkläre ich an Eides statt, dass ich die vorliegende Dissertationsschrift selbst verfasst und keine anderen als die angegebenen Quellen und Hilfsmittel benutzt habe.

I hereby declare upon oath that I have written the present dissertation independently and have not used further resources and aids than those stated in the dissertation.

Hamburg, den 9. Februar 2024

Unterschrift (Yunyao Ma)